Dissertation

Maternal Obesity in Early Human Pregnancy: Placental DNA Integrity and Stress Response

submitted by

Denise HOCH, BSc. MSc.

for the Academic Degree of

Doctor of Philosophy (PhD)

at the

Medical University of Graz

Department of Obstetrics and Gynecology

under supervision of

Ao.Univ.-Prof. Dr.phil. Gernot DESOYE

2020

Declaration

I hereby declare that this thesis is my own original work and that I have fully acknowledged by name all of those individuals and organisations that have contributed to the research for this thesis. Due acknowledgement has been made in the text to all other material used. Throughout this thesis and in all related publications I followed the "Guidelines of the Medical University of Graz on Good Scientific Practice".

Denise Hoch, MSc.

Graz, December 2020

Disclosures

This thesis has been published in the following original papers and all co-authors agreed to the re-use of the data in this dissertation:

- *Hoch, D***.** et al. (2018) '**Diabesity-associated oxidative and inflammatory stress signalling in the early human placenta**', Molecular aspects of medicine. doi: 10.1016/j.mam.2018.11.002.

- *Hoch, D*., Bachbauer, M., et al. (2020) '**Maternal Obesity Alters Placental Cell Cycle Regulators in the First Trimester of Human Pregnancy: New Insights for BRCA1**', International journal of molecular sciences, 21(2), pp. 1–18. doi: 10.3390/ijms21020468.

- *Hoch, D.,* Novakovic, B., et al. (2020) '**Sex matters: XIST and DDX3Y gene expression as a tool to determine fetal sex in human first trimester placenta**', Placenta. Elsevier Ltd, 97, pp. 68–70. doi: 10.1016/j.placenta.2020.06.016.

Doctoral candidate Denise Hoch was trained within the frame of the **PhD Program "Molecular Fundamentals of Inflammation"** (DK-MOLIN, W1241) at the Medical University of Graz, was financial support by the **Medical University of Graz** and was recipient of the **EASD Albert Renold Travel Fellowship**.

The following researchers have actively contributed to results reported in this thesis:

- **Alejandro Majali-Martinez** (Department of Obstetrics and Gynecology, Medical University of Graz)
- **Caroline Pöchlauer** (Department of Obstetrics and Gynecology, Medical University of Graz)
- **Martina Bachbauer** (Department of Obstetrics and Gynecology, Medical University of Graz)
- **Theresa-Maria Kaudela** (Department of Obstetrics and Gynecology, Medical University of Graz)
- **Ezgi Eylül Bankoglu** (Institute of Pharmacology and Toxicology, Julius-Maximilians-Universität Würzburg)
- **Boris Novakovic** (Murdoch Children's Research Institute, Royal Children's Hospital, Melbourne)
- **Francisco Algaba-Chueca** (Department of Endocrinology and Nutrition, and research unit, Joan XXIII University Hospital of Tarragona)

All of the above mentioned have explicitly agreed to the use of their data in this thesis.

Acknowledgements

It is done! I want to take the time to say thank you to all those, who accompanied me throughout the past 4 years.

First and foremost, I would like to thank my dear supervisor and mentor **Gernot** who believed in me from the start and gave me the freedom to develop this study according to my own ideas. His motivation, guidance and great enthusiasm helped to overcome also the demanding times of my doctorate. I would sign up for this PhD again at any time!

I would like to thank my thesis committee members, **Sylvie Hauguel-de Mouzon** and **Martin Gauster**, who followed my scientific development throughout this thesis. My warmest thanks go to **all my dear colleagues from the Forschungslabor**, for their continuous help and support, for becoming more than colleagues and friends, and being a family in Graz to me. In particular I want to thank **Alejandro** who always had an open ear for my academic and non-academic problems. He is not only the nicest person on this planet but also a good example of a scientist. Many thanks go to **Ate, Moni, Jasmin, Ilaria, Caro, Michi, Waltraud, Elisa, Julia, Ursi, Evelyn, Birgit, Bettina** and **Babsi.** Thank you for your friendship, steady support and for sharing all the heights and depths of my PhD. Special thanks go to my Master students **Sebastian, Veronika, Theresa, Caroline** and **Martina** for their tremendous work and effort.

Moreover, I want to thank **Sonja, Daniel, Tommaso** and **Paul** for always supporting me and making Graz the best place to live in. Thank you, **Anja, Ele** and **Julia** for always giving me a reason to return to Weiden for coffee dates.

I also want to thank **Richard Saffery** and **Boris Novakovic** for hosting me in their lab in Melbourne. I learned so much and had the best time of my life during this research stay. I want to thank everybody in the **epigenetics team** for the great teamwork we had and also for the fun outside the lab. Here, I also want to say thank you to my dear flatmate **Inna**. She made this stay unforgettable and I hope we will see each other very soon.

I further want to thank **Francisco** and **Lutz**; both were part of my PhD journey for just a short period of time but their impact on this thesis is unmeasurable.

Finally, I want to thank my dear family, especially my parents **Verena** and **Bernd** as well as my siblings **Vanessa, Michael, Lara** and **Leni** for their infinite support and love.

Table of Contents

Abbreviations

8-OHdG	8-hydroxy-2' -deoxyguanosine
APE1	Apurinic/Apyrimidinic Endodeoxyribonuclease 1
ATM	Ataxia Telangiectasia Mutated
ATR	Ataxia Telangiectasia And Rad3-Related
BCA	Bicinchoninic acid assay
BER	Base excision repair
BMI	Body mass index
BRCA1	Breast Cancer 1 gene
CK18	Caspase-cleaved cytokeratin 18
CTB	Cytotrophoblasts
DAPI	4′,6-diamidino-2-phenylindole
DIN	DNA Integrity Number
DMEM	Dulbecco's Modified Eagle Medium
DNA	Desoxyribonucleic acid
DSB	Double strand break
ELISA	Enzyme-linked immunosorbent assay
evCTB	Extravillous cytotrophoblasts
FCS	Fetal calf serum
FFPE	formalin-fixed paraffin-embedded
FPG	Formamidopyrimidine DNA glycosylase
FT	First trimester
GA	Gestational age
GADD45a	Growth Arrest and DNA Damage Inducible Alpha
GDM	Gestational diabetes
HBSS	Hanks' Balanced Salt solution
hCG	Human chorionic gonadotropin
HNE	4-Hydroxynonenal
HO-1	Heme oxygenase 1
HOMA	Homeostatic model assessment
HR	Homologous recombination

HSP70	Heat shock protein 70
IF	Immunofluorescence
IgG	Immunoglobulin G
IL	Interleukin
IS	Insulin sensitivity
LCM	Laser capture microdissection
M	Molar
µl	Microliter
µm	Micrometer
ng/ml	Nanograms/mililiter
MMR	DNA mismatch repair
mRNA	Messenger ribonucleic acid
MVLR	Multivariate linear regression model
NBS1	Ninbrin
NEIL3	Nei Like DNA Glycosylase 3
NER	Nucleotide excision repair
NHJR	Non-homologous end joining
O_2	Oxygen
PFA	Paraformaldehyde
p53	Tumor protein p53
PBS	Phosphate buffered saline
PCNA	Proliferating Cell Nuclear Antigen
PCR	Polymerase chain reaction
p.m.	Post menstruationem
PNA	Peptide nucleic acid
Q-FISH	Quantitative fluorescent in situ hybridization
RNA	Ribonucleic acid
ROS	Reactive oxygen species
RT-qPCR	Quantitative real-time polymerase chain reaction
SD	Standard deviation
SSB	Single strand break
STB	Syncytiotrophoblasts

T1DM	Type 1 diabetes mellitus
T2DM	Type 2 diabetes mellitus
TBE	Tris-borate-EDTA
TNF-α	Tumor necrosis factor alpha
TUNEL	TdT-mediated dUTP-biotin nick end labeling
VEGF	Vascular endothelial growth factor

Abstract

In the first trimester (FT) of human pregnancy, the intrauterine environment directly affects development of the rapidly growing placenta. Maternal obesity - a frequent manifestation of metabolic derangements - is associated with metabolic complications, systemic low-grade inflammation and genotoxicity. Considering that the developing placenta is exposed to obesity-associated changes in the early intrauterine environment, we hypothesize that maternal obesity affects DNA integrity that triggers DNA damage responses (ATM/ATR signaling) and affects placental stress response with consequences for trophoblast turnover in early human pregnancy, respectively. The present study aimed to determine FT placental DNA damage, telomere shortening and subsequent effects on DNA damage repair and cell cycle regulation. Furthermore, we aimed to characterize FT placental stress status and final effects on trophoblast proliferation and apoptosis.

For this purpose, placental tissue (week 4-12 p.m.) was obtained from non-smoking (self-report and serum cotinine measurement) women terminating pregnancy for psycho-social reasons. DNA damage and oxygen-induced modification in total tissue were determined by COMET assay. We quantified DNA damage (γH2AX) and oxidative DNA modification (8-OHdG), proliferation (Ki67) and apoptosis (TUNEL, caspase cleaved cytokeratin 18) in villous cytotrophoblasts (CTB) using a semi-quantitative *in situ* analysis based on immunofluorescence triple-staining. Telomere length in total placental tissue and laser-capture microdissected trophoblast was quantified by RT-qPCR and confirmed by quantitative fluorescence *in situ* hybridization (Q-FISH). Pre-selected placental stress markers, cytokines, DNA damage repair and cell cycle related genes were assessed using a PCR-gene panel and Nanostring assay, while proteins were quantified by a cell cycle-specific protein array or immunoblotting. Data was analyzed using a multivariate linear regression model with adjustments for gestational age and tissue processing time.

The key findings of this study were:

i. Maternal obesity in early pregnancy was not associated with oxidative DNA modifications (8-OHdG) in total tissue and CTB. Other indicators of oxidative stress such as products of lipid peroxidation and protein nitration as well as the classical stress marker HSP70 were unaltered by maternal obesity in early pregnancy.

Furthermore, gene expression of placental antioxidants (*MGST3, SOD3, GSTP1, GLRX, TXNRD1*) and heme oxygenase 1 (*HO-1*) was lower in obese pregnant women, while placental *Nrf2* expression and HO-1 protein levels were not altered in samples from obese pregnant women.

ii. Maternal obesity affected placental inflammatory cytokine expression (*IL1A, IL6*) and stress signaling genes (*ASK2, MAPK11, MAPK12, MAPK13, JNK1*) in FT placentas.

iii. Maternal obesity induced placental DNA damage specifically in CTBs. CTB telomeres *in situ* were shorter in maternal obesity. Shortening was associated with high C-peptide levels, low insulin sensitivity or high BMI. Despite higher ATM/ATR protein levels and increased substrate phosphorylation in FT placentas of obese pregnant women, selected downstream proteins remained unaffected, while central DNA damage repair transducers (*HDAC1, HDAC8, PARP1, FEN1, ku70, BLM*) were downregulated in FT placentas from obese pregnant women. This dysregulated damage repair was also accompanied by an induction of cell cycle arrest.

iv. Finally, we found decreased CTB proliferation and an increase in apoptosis in FT placentas from obese pregnant women, while senescence was unaltered.

Altogether, these results argue for absence of oxidative stress in first trimester placentas of obese women. They also suggest that maternal obesity in the first trimester affects CTB turnover and therefore alter placental development, potentially ensuing adverse consequences for maternal and fetal health.

Zusammenfassung

Die intrauterine Umgebung beeinflusst die Entwicklung der schnell wachsenden Plazenta im ersten Trimester maßgeblich. Adipositas ist im Allgemeinen mit Stoffwechselkomplikationen, niedrig-gradiger systemischer Entzündung und Genotoxizität assoziiert. Die frühe Plazenta ist demnach der durch mütterliches Übergewicht veränderten intrauterinen Umgebung ausgesetzt. Die molekularen und zellulären Folgen für die Plazenta im ersten Trimester sind bisher unklar. Wir stellen die Hypothese auf, dass maternale Adipositas im ersten Trimester sowohl eine plazentare Stressreaktion auslöst als auch die DNA-Integrität beeinflusst. Diese Stressadaptionen haben ebenso Auswirkungen auf die Entwicklung der Trophoblasten sowie auch auf die, durch DNA-Schäden hervorgerufenen, Reparaturprozesse und veränderte Zellzyklusregulation. Diese Studie zielte darauf ab, plazentare DNA-Schäden (Strangbrüche und oxidative Modifikationen), Telomerlänge und nachfolgende Auswirkungen auf die Reparatur von Plazenta-DNA-Schäden und Zellzyklusregulation zu bestimmen. Darüber hinaus wurde oxidativer Stress als potentieller Auslöser dieser Schäden an der Plazenta im ersten Trimester charakterisiert.

Zu diesem Zweck wurde Plazentagewebe (Gestationswoche 4 - 12) von Nichtraucherinnen gesammelt, die die Schwangerschaft aus psychosozialen Gründen beendeten. DNA-Schäden im Gesamtgewebe wurden durch COMET-Assay bestimmt. Außerdem wurde γH2AX, 8-OHdG, Ki67 und TUNEL/ Caspase-gespaltenes Cytokeratin 18 in villösen Cytotrophoblasten (CTB) unter Verwendung einer selbst entwickelten, semi-quantitativen, *in situ* Analyse bestimmt. Telomerlängen wurden mittesl qPCR und Q-FISH bestimmt. Stressmarker, Zytokine, sowie DNA-Reparatur- und zellzyklusregulierende Gene in der Plazenta wurden unter Verwendung eines PCR-Gen-Panels und Nanostring. gemessen. Zudem wurden ausgewählte Proteine mittels Proteinarray oder Immunoblot quantifiziert. Die Daten wurden unter Verwendung eines multivariaten linearen Regressionsmodells mit Korrekturen für Gestationsalter und Verarbeitungszeit analysiert.

Die Ergebnisse dieser Studie waren:

i. 8-OHdG-Modifikationen waren im Gesamtgewebe und in CTB von normalgewichtigen und adipösen Frauen nicht unterschiedlich. Sowohl Lipidperoxidation und Protein-nitrierung als auch der Stressmarker HS70 wurden in der frühen Schwangerschaft nicht

durch mütterliche Adipositas beeinflusst. Die Expression vonAntioxidantien und anti-oxidative wirkender Hämoxygenase 1 (HO-1) bei adipösen schwangeren Frauen geringer, während Nrf2 Expression und HO-1-Proteinlevel nicht verändert wurden.

ii. Maternale Adipositas beeinflusste die Expression plazentarer Zytokine und stress assoziierten Genen in der frühen Schwangerschaft.

iii. Maternale Adipositas war mit mehr plazentaren DNA-Schäden, spezifisch im CTB, assoziiert. CTB-Telomere *in situ* waren bei adipösen Müttern kürzer. Eine Verkürzung war mit hohen C-Peptidspiegeln, geringer Insulinsensitivität oder hohem BMI verbunden.

iv. Trotz höherer ATM/ATR-Proteinlevel und erhöhter Substratphosphorylierung durch diese beiden Kinasen in Plazenten adipöser Frauen, blieben ausgewählte nachgeschaltete Proteine unverändert. Zentrale Gene für die Reparatur von DNA-Schäden waren bei Adipositas in verminderter Menge vorhanden. Diese dysregulierte Schadensreparatur ging mit einer Induktion eines Zellzyklusstillstands einher.

v. Schließlich fanden wir bei adipösen schwangeren Frauen im ersten Trimester verminderte CTB-Proliferation und eine Zunahme der CTB-Apoptose, während Seneszenz unverändert blieb.

Die Resultate dieser Studie sprechen gegen Adipositas-induzierten oxidativen Stress der Plazenta im ersten Trimester. Außerdem kann maternale Adipositas im ersten Trimester den CTB-Umsatz charakterisiert durch Proliferation und Apoptose beeinflussen und somit die Plazentaentwicklung verändern. Dies mag zu nachteiligen Folgen für die Gesundheit von Mutter und Kind führen, die oft mit mütterlicher Adipositas verbunden sind.

1. Introduction

Parts of this chapter are already published in adapted form in Hoch, Bachbauer *et al.* (2018) and Hoch, Novakovic *et al.* (2020).

1.1. The human placenta

The human placenta is a highly specialized and rapidly developing villous organ located at the interface between mother and fetus. It fulfils an extensive range of functions that are essential for growth and proper development of the fetus (Forbes and Westwood, 2010). Among these, the placenta is involved in oxygen and nutrient transport to the fetus. It also removes metabolic waste products and carbon dioxide while acting as a barrier in the defense against xenobiotics and pathogens. Together with its protective and metabolic role, the human placenta also synthesizes and secretes a broad range of cytokines, hormones and growth factors that are essential to facilitate maternal adaptation to pregnancy (Rama and Rao, 2003). Failures in placental development and impairment of proper function can lead to early abortions or result in pregnancy disorders (Jauniaux, Greenwold, *et al.*, 2003). Although the human placenta is a plastic organ that develops to accommodate fetal demands during pregnancy, the first trimester (FT) is a critical time period not only for placental, but also for fetal development (Gude *et al.*, 2004).

1.2. Early human pregnancy: Placental development and cell types

1.2.1. Early placental development

As the placenta, extraembryonic membranes and the fetus are derived from the zygote, they share genetic composition (Burton and Fowden, 2015). The zygote develops into the morula, a solid cell mass, and transitions into the blastocyst. The surface of the blastocyst consists of the trophectoderm that differentiates into the trophoblast, while the extraembryonic mesoderm will develop into the stromal core (Red-Horse *et al.*, 2004). The blastocyst enters the uterine cavity at approximately day 5 – 6 post conception and attaches to the uterine epithelium prior to implantation into the decidua (Benirschke *et al.*, 2000). At the embryonic pole, mononucleated trophoblast cells - that surround the inner cell mass - differentiate into the invasive multinucleated syncytiotrophoblast (STB) which penetrate the uterine epithelium (Huppertz, 2008). The blastocyst is entirely embedded in the endometrium at day 10 post conception

(Norwitz, Schust and Fisher, 2001). The STB forms the outer layer and is in direct contact with maternal tissue, whereas the layer beneath consists of the mononucleated cytotrophoblasts (CTB) that continuously divide and fuse to expand the STB (Huppertz, 2008).

1.2.2. Formation of chorionic villi

During the lacunar stage, fluid-filled spaces (lacunae) appear within the syncytial mass that enlarge and merge, forming a system of trabeculae (Hertig, Rock and Adams, 1956). CTB cells start to invade into the trabeculae and they arrive at the maternal side where they develop into trophoblastic cell columns at day 15 after conception. Meanwhile, the trabeculae form side branches – so called primary villi – consisting of only STB or STB and CTB. The basal side of the CTB is in contact with the basement membrane that separates the trophoblast from the stromal core. Together, the trophoblast layer and the mesenchymal core are referred to as the chorion. The stromal core is derived from extraembryonic mesodermal cells penetrating the trabeculae and primary villi. The latter are transformed into secondary villi in which the development and differentiation of haematopoietic progenitor cells occur. Continuously, placental endothelial cells develop and form placental vessels which leads to the final transformation to tertiary villi (Huppertz, 2008).

At the end of the third week post conception the whole chorionic sac is surrounded by villi - the structural unit of the FT placenta - that can be floating in the IVS or be attached to the uterine wall by cytotrophoblast cell columns at the tip (Burton, Jauniaux and Sephen Charnock-Jones, 2010). The latter are named anchoring villi and play an essential role in elaborating the maternal blood flow into the placenta (Red-Horse *et al.*, 2004).

1.2.3. Placental cell types and function in early pregnancy

During the first trimester of pregnancy, proper placental development relies predominantly on trophoblast cell proliferation, fusion and differentiation. These specialized trophoblasts differentiate following two pathways that are essential for placental function: extravillous cytotrophoblasts (evCTB), and villous cytotrophoblasts (CTB). Figure 1 shows a representative FT placenta obtained after pregnancy termination at gestational week 9, p.m., a schematic representation and histological cross-section of a placental villus in early gestational age.

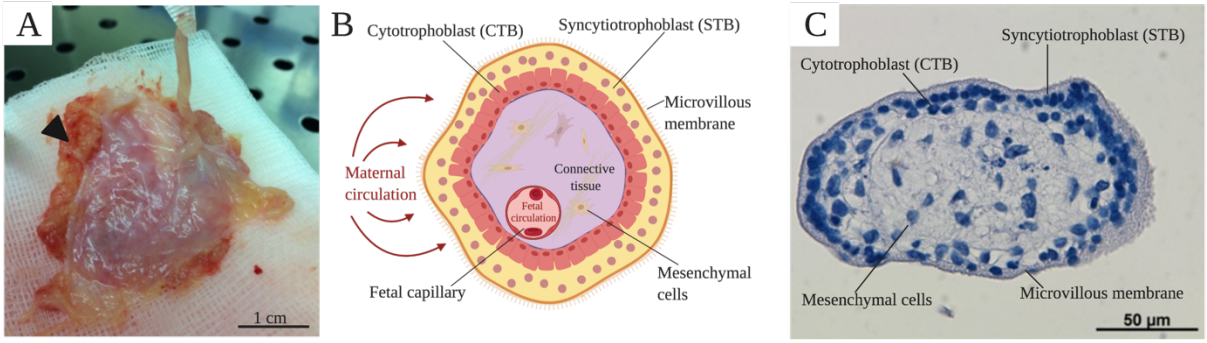

Figure 1: The human first trimester placenta and its structural units. (**A)** Macroscopic structure of the human first trimester placenta. The black arrow points towards the villous tissue that is covered by the amnion that contacts the amniotic fluid, the fetus and the umbilical cord *in vivo*. The placenta can be broken down into structural units called villi. **(B)** Schematic representation of a chorionic villus cross section in the first trimester of pregnancy. Each villus is surrounded by a fused multi-nucleated syncytiotrophblast (STB) layer which is in direct contact with maternal blood. Mitotic cytotrophoblasts differentiate and fuse to give rise to STB. (**C)** Immunoshistochemistry of a normal placental villus in gestational week 9. Scheme created with BioRender.com.

As described in 1.2.2., in villi in contact with the uterine basement membrane, i.e., anchoring villi, CTB proliferate and form cell columns. They differentiate into evCTB at the tip of the cell columns, where the cells acquire an invasive phenotype to migrate and invade into the decidua. This results in anchoring of the feto-placental unit to the uterus (Knöfler and Pollheimer, 2013). EvCTB also reach the uterine spiral arteries where they remodel them into wide, low resistance vessels. This is essential for establishment of an adequate supply of fully oxygenated blood to the fetus (Whitley and Cartwright, 2010).

Nutrient transport as well as endocrine and metabolic functions of the placenta reside mainly in the floating villi making up the villus tree. The villus tree is covered by a terminally differentiated multinucleated layer, i.e., the syncytium, that represents the feto-maternal barrier. This layer is involved in transport of maternal nutrients to the fetal circulation and in the secretion of essential pregnancy hormones (Knöfler, 2010). Due to its location, STB are in direct contact with maternal blood after the onset of arterial circulation (Burton and Fowden, 2015). STB are only found in a post-mitotic state protecting the mother from chimaerism as their shed nuclear material is mitotically incompetent (Chan, Lao and Cheung, 1999; Kar, Ghosh and Sengupta, 2007). Korgun *et al.* showed that mitotic cyclins as well as PCNA and Ki67 are absent in STB , while high levels of p21 might additionally contribute to an arrest at G1 phase (Korgun *et al.*, 2006).

CTB are the proliferating trophoblast stem cell population that undergo cell division, differentiation and that further fuse in order to give rise to the STB (Benirschke *et al.*, 2000; Aplin, 2010). DNA is synthesized exclusively in CTB reflected by a mitotic index of roughly 1.5 - 2.9% between gestational weeks six and nine that decreases with gestation (Chan, Lao and Cheung, 1999; Kar, Ghosh and Sengupta, 2007). As CTB undergo asymmetric cell divisions, each cycle results in a progenitor cell, maintaining the pool, and another cell that differentiates into an intermediate CTB form, prior to fusion with the overlying syncytium. Before cell fusion, transitional cells - that are already differentiated and in preparation for fusion – may undergo up to four symmetrical transit-amplifying divisions (Mayhew, 2001). Within this heterogeneous villous trophoblast population, intermediate and transitional cells can be clearly identified by transmission electron microscopy (Jones and Fox, 1991; Kar, Ghosh and Sengupta, 2007) and separated by expression of molecular markers, such as transcription factor *GCM-1* (Baczyk *et al.*, 2004), FGFR2 (Baczyk *et al.*, 2006), caspases 8 and 10 (Huppertz *et al.*, 1999; Black *et al.*, 2004) and the α subunit of chorionic gonadotropin (Hoshina, Boothby and Boime, 1982). After gestational week 10, the cytotrophoblast pool increases with placental growth while its volume fraction decreases. Therefore, as tissue surface area expands, the CTB layer changes from relatively closely-packed in late first trimester to being sparse at term (Jones and Fox, 1991; Mayhew, 2001).

Syncytiotrophoblast renewal and CTB proliferation are highly regulated both in a spatial and a time-dependent manner to ensure proper placental surface expansion and replacement of cellular material (Gude *et al.*, 2004; Redman and Sargent, 2007). Figure 2 shows normal CTB turnover and consequences of reduced proliferation on syncytialization. Next to autocrine regulation mediated by placental-derived signals (Gude *et al.*, 2004), the maternal intrauterine environment also plays a pivotal role in placental regulation (Burton, Jauniaux and Sephen Charnock-Jones, 2010). Changes in intraplacental oxygen tension and immune modulators are further described in the following chapter.

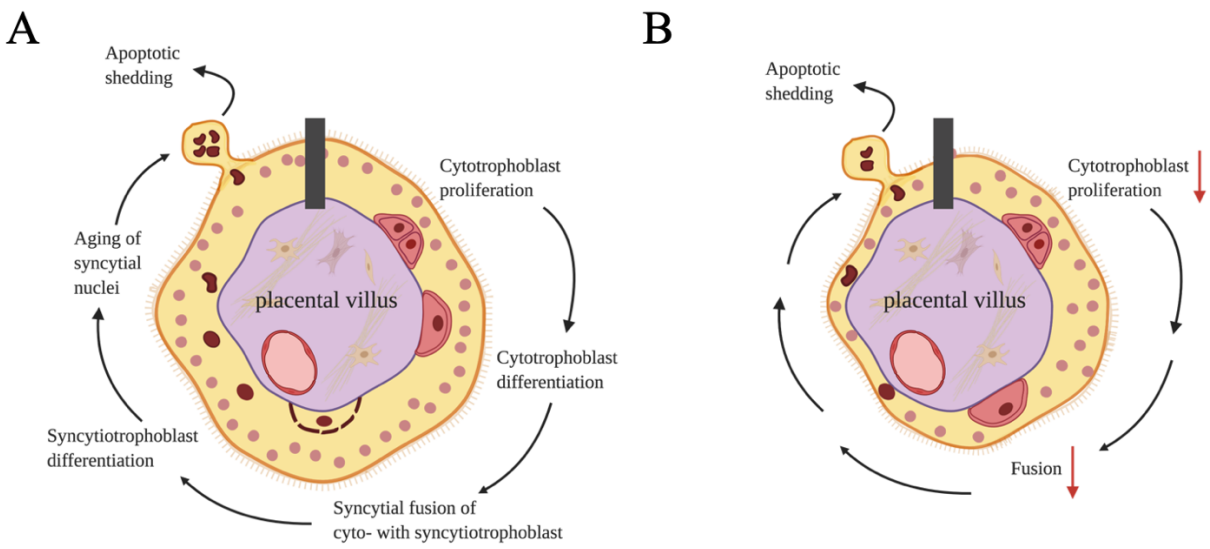

Figure 2: Villous cytotrophoblast (CTB) turnover. Turnover events are arranged in a clockwise manner around the placental villus starting on top. (**A)** Normal CTB proliferation followed by differentiation, syncytial fusion and syncytiotrophoblast. (**B)** Decreased CTB proliferation alters the CTB turnover impairing the maintenance of the syncytiotrophoblast. Modified from Huppertz, Kaufmann and Kingdom (2002). Created with BioRender.com.

1.3. Oxygen tension, immune mediators and inflammation in uncomplicated early pregnancies

1.3.1. Oxygen tension and antioxidant defenses in the early placenta

At the time of implantation a wide variation in oxygen levels in the human uterus between women is reported in literature averaging from 15 mmHg (Yedwab *et al.*, 1976) to 18.9 mmHg (Ottosen *et al.*, 2006). This generally low oxygen condition may protect from teratogenesis and favors optimal preimplantation embryo development by minimizing reactive oxygen species (ROS) production as oxidative metabolism is slowed down (Leese, 2002).

Based on several morphological and Doppler ultrasound studies, early placental development occurs under a similar low oxygen condition as the uteroplacental circulation is not fully established prior to approximately 10 weeks of gestation (Hustin and Schaaps, 1987; Jaffe and Woods, 1993). Here, the early human embryo is supported by secretions from endometrial glands (Hempstock et al., 2004; Burton et al., 2015). In gestational weeks 7 - 10 the partial oxygen pressure measured in the human placenta *in vivo* is less than 20 mmHg (Rodesch *et al.*, 1992; Jauniaux *et al.*, 2000). During the embryonic period, maintaining a low

oxygen concentration appears to protect from damaging effects of free radicals and favors normal cell differentiation (Burton, Hempstock and Jauniaux, 2003).

With the onset of oxygenated maternal blood flow at the end of the first trimester, the environment, in which the early embryo develops changes drastically to an intraplacental oxygen tension greater than 50 mmHg after the circulation is fully established (Rodesch *et al.*, 1992; Jauniaux *et al.*, 2000). Despite the rise in placental oxygen concentration, values remain low within the fetus as placental oxygen diffusion is limited at this gestational stage (Jauniaux, Gulbis and Burton, 2003). At week 13 to 16, mean fetal blood oxygen tension (24 mmHg) and saturation was found to be significantly lower than the values of the placenta and decidua (60 mmHg). However, in the second half of pregnancy umbilical vein oxygen level ranges between 35 and 55 mmHg (Jauniaux, Watson and Burton, 2001), suggesting an oxygen gradient between maternal and fetal tissues throughout pregnancy.

As the intervillous circulation is gradually established, maternal blood flow is mostly initiated in the peripheral regions of the early placenta (Jauniaux, Hempstock, *et al.*, 2003). This peripheral flow may be associated with regional differences of trophoblast capacity to plug spiral arteries. Pijnenborg *et al.* determined trophoblast migration through the endometrium by morphometric analyses and showed that invasion of endometrial arteries occurs most extensively at the center of the implantation site and, subsequently, extends centrifugally (Pijnenborg *et al.*, 1980, 1981). This suggests that the trophoblast plugs are more extensive in the central region and supports the concept of an initial onset of peripheral blood flow that gradually expands to the rest of the placenta. It has been suggested that this oxygen gradient within the placenta might lead to the formation of placental membranes or ‘chorion laeve’ by regulating regression of villi in the periphery. Indeed, Jauniaux *et al.* observed increased activation of the apoptotic cascade and lower proliferation of CTB in the peripheral villi (Jauniaux, Hempstock, *et al.*, 2003). Moreover, this first trimester oxygen gradient may play a major role in cytotrophoblast differentiation and proliferation, therefore, directly affecting placental tissue function and development (Genbacev, 1997; Jauniaux, Hempstock, *et al.*, 2003).

In parallel with drastic changes in oxygen concentration at the end of the first trimester of pregnancy, antioxidant enzyme expression correlates with the onset of maternal blood flow after the trophoblast plugs dissipate. A complex system of enzymatic and non-enzymatic

antioxidant defense mechanisms has evolved to protect cells from harmful oxidant attacks of ROS. Superoxide dismutases (SODs), catalase and peroxidases are the most important enzymes to inhibit the built up of ROS intermediates and detoxify the species completely. In STB of the early placenta, mRNA levels and activity of copper/zinc superoxide dismutase and catalase are very low suggesting a limited requirement in accordance with the concept of physiologically low oxygen environment in early pregnancy. As pregnancy progresses, the sharp increase in placental oxygen tension is accompanied by a rise in the activity of these principal intracellular antioxidant enzymes (Watson *et al.*, 1997, 1998).

Rapid increase of heat shock protein 70 (HSP70) levels, formation of nitrotyrosine residues, and derangement of the mitochondrial cristae within the STB coincides with changes in the uterine arteries and indicates a burst of oxidative stress as soon as the maternal circulation is established (Jauniaux *et al.*, 2000). Lipid soluble Vitamin E protects membranes and lipoproteins against lipid peroxidation and is located in the STB brush border where it may play an essential role in protecting early pregnancy (Qanungo, Sen and Mukherjea, 1999). The reducing agent vitamin C is water soluble and an essential antioxidant in the plasma. The synergistic interaction between vitamin C and vitamin E at the aqueous-lipid interface reduces tocopheryl free radical to α-tocopherol-OH which is then excreted as dehydroascorbate (Buettner, 1993; Chan, 1993). Throughout pregnancy vitamin C levels decrease progressively and FT villous explant culture demonstrates that at early gestation the STB are highly sensitive to oxygen-mediated damage. Specifically, the STB brush border membrane, which is in direct contact with maternal blood, is most susceptible to lipid peroxidation (Watson *et al.*, 1998).

1.3.2. Effects of altered oxygen tension in early pregnancy

Rise in oxygen tension at the end of the first trimester of human pregnancy is not solely associated with harmful oxidative damage but may also play a physiological role by influencing a number of cellular functions, such as angiogenesis, cytotrophoblast proliferation and migration, and cytotrophoblast fusion.

The physiological burst of oxidative stress may trigger normal placental differentiation and development as several angiogenic factors are regulated by oxygen. Indeed, it has been convincingly shown in tumors and vascular smooth muscle cells that a decrease in oxygen tension regulates vascular endothelial growth factor (VEGF) transcriptionally by stabilizing its mRNA (Stavri *et al.*, 1995; Levy, Levy and Goldberg, 1996). In the endometrium, VEGF is

physiologically regulated in a similar way and VEGF production by placental fibroblasts is correspondingly oxygen-sensitive (Wheeler, Elcock and Anthony, 1995). In contrast, placenta growth factor (PlGF) levels appear to be suppressed by low oxygen (Ahmed *et al.*, 2000). Furthermore, *in vitro* studies showed that levels and the ratio of angiopoietin 1 (ANG1) and angiopoietin 2 (ANG2) are regulated by hypoxia. ANG1 is regulated by alterations in RNA stability, whereas ANG2 is transcriptionally regulated (Zhang *et al.*, 2001). Thus, the ratio between ANG1 and ANG2 shifts under low oxygen towards ANG2, thereby promoting angiogenesis and vessel remodeling. As VEGFA, PlGF and the angiopoietins can all be regulated by the local oxygen concentration, oxygen serves as a main controller of placental development.

Studies showed that oxygen also modulates trophoblast differentiation and suggested an association between exposure to increasing oxygen and enhanced trophoblast invasion (Genbacev, 1997). In human FT villous explants, an increase in trophoblast outgrowth was observed after exposure to physiologically low oxygen tension (3% O_2). This increased outgrowth from the distal end of the villous tips was associated with increased cell proliferation, whereas under higher oxygen tensions CTB adopt an invasive phenotype (Genbacev, 1997; Caniggia *et al.*, 2000). Furthermore, there is evidence for almost complete absence of apoptosis in the STB indicating CTB fusion is used for growth instead of maintaining a steady-state (Smith, Baker and Symonds, 1997; Smith *et al.*, 2000).

1.3.3. Immune mediators and inflammation in early pregnancy

A well-controlled synergistic crosstalk of immune-modulating and inflammatory factors is essential to allow tolerance of the semi-allogeneic embryo, while sustaining maternal immune functions to fight infections in early pregnancy (Hoch *et al.*, 2019). Already during implantation, endometrial damage and replacement of endothelium and smooth muscle cells by trophoblasts during blood vessel remodeling require a strong inflammatory response to secure adequate repair and removal of debris (Abrahams *et al.*, 2004; Dekel *et al.*, 2010). While the immunological profile is dynamic and adapts to each stage of pregnancy, the first trimester is regarded as a pro-inflammatory phase. Later in the second trimester, when the fetus rapidly grows and develops, an Th2 anti-inflammatory environment prevails. (Mor *et al.*, 2011).

In early stages during implantation and placentation, a helper 1 (Th1) cytokine profile is observed, while also concentrations of Leukemia inhibitory factor, interleukins IL1, IL6, IL8,

and tumor necrosis factor (TNF-α) increase gradually. At the site of implantation, maternal leukocytes, including natural killer cells, macrophages and dendritic cells infiltrate as response to trophoblast invasion (Mor *et al.*, 2011). Furthermore, invading trophoblasts are capable of triggering immune responses at the implantation site by secretion of various immunomodulatory factors (PrabhuDas *et al.*, 2015). Those factors secreted by trophoblasts may induce the differentiation of peripheral blood monocytes into macrophages and lead to recruitment and differentiation of inducible regulatory T cells (Ramhorst *et al.*, 2012; Aldo *et al.*, 2014).

The early human placenta secretes several inflammatory and immune factors, including IL6, IL8 and chemokine ligand 2 (CCL2), into the intervillous space facilitating maternal leukocyte infiltration (Siwetz *et al.*, 2016). In addition to their inflammatory functions, IL8 and CCL2 also exert angiogenic functions by modulation endothelial cell migration, proliferation and tube formation (Chen *et al.*, 2010; Du, Wang and Li, 2014). Another immunomodulatory factor secreted by the FT placenta is Granulocyte-macrophage colony-stimulating factor (GM-CSF) that also functions in an autocrine manner by binding to the GM-CSF receptor subunit GM-Rα expressed on the cell surface of CTB and STB (Jokhi *et al.*, 1994; Siwetz *et al.*, 2016). Next to other factors, GM-CSF induces villous trophoblast differentiation and stimulates secretion of human chorionic gonadotropin (hCG) (Garcia-Lloret *et al.*, 1994) and IL10 (Bennett *et al.*, 1997). This may result in suppression of pro-inflammatory Th1 cytokines and trigger peripheral T-cell differentiation inhibiting functions of other T-cells (Blaschitz *et al.*, 2015).

In general, pregnancy pathologies may affect this shift in the FT placental inflammatory secretion profile, as well as changes in utero-placental oxygen concentration with subsequent adverse consequences for the pregnancy. One condition that has gained enormous interested is maternal obesity (c.f. below). Understanding its impact of the metabolic derangements in the mother on FT trophoblast biology might help unravelling the molecular mechanisms underlying some of the obesity-associated pregnancy complications (Hoch *et al.*, 2019).

1.4. Obesity and its prevalence

Over the last two decades obesity has become a major public health problem not only in western countries but also in developing nations. Obesity is a complex condition defined by excessive fat accumulation that is associated with multiple risk factors and impairs the normal state of the

human organism (Keaney *et al.*, 2003). As obesity prevalence nearly tripled between 1975 and 2016, nowadays worldwide more people are obese than underweight except for Asia and sub-Saharan Africa (Chou, Grossman and Saffer, 2004). In Europe, the number of overweight or obese people rose drastically, with highest numbers in the United Kingdom where 63.7% and 27.8% of all adults are categorized as overweight and obese, respectively. In comparison to the United Kingdom, the proportion of overweight adults in Austria is 54.3%, while 20.1% of the population are obese (Berghöfer *et al.*, 2008; Mendis, Davis and Norrving, 2015). This general increase in non-communicable diseases is a societal burden and leads to major economic costs.

Body mass index (BMI) is calculated by kilograms per squared body length (kg/m^2). A BMI between 19 and 25 kilograms per squared body length (kg/m^2) is defined as lean, i.e., normal weight, while overweight is defined as BMI higher than 25 kg/m^2 but lower than 30 kg/m^2. Obesity is defined as a BMI higher than 30 kg/m^2. Obesity is further categorized by BMI into class 1 (BMI 30.0 to 34.9 kg/m^2), class 2 (BMI 35.0 to 39.9 kg/m^2) and class 3 (BMI $\geq$ 40 kg/m^2). Classification into BMI groups is a robust method to assess large populations as it is easy to calculate and measurements do not require any specialized equipment (James, 2004). However, for a more precise assessment of body fatness, anthropomorphic data, such as waist circumference, waist-to-hip ratio and distribution of fat mass (visceral/omental fat *vs.* subcutaneous fat) should be considered (Cox and Whichelow, 1996). While obesity is a risk factor for multiple diseases, the association with diabetes mellitus (T2DM) is profound (Kahn, Hull and Utzschneider, 2006). Obese individuals carry a 7-fold higher risk for T2DM compared to lean controls. More than 80% of people with T2DM are overweight or obese (Abdullah *et al.*, 2010).

Excessive fatness, i.e. elevated lipid deposition in adipose tissue, is accompanied by insulin resistance, increased leptin levels and systemic dyslipidemia (Jung and Choi, 2014). As obesity involves expansion of adipose tissue – which is not only a mere storage site for triglycerides, but also a highly active endocrine organ – it is highly associated with increased levels of low-grade inflammation. Already in 1993, Hotamisligil *et al.* demonstrated that mouse adipocytes actively secrete TNF-α and obese mice showed higher circulating levels of TNF-α compared to lean controls (Fernandez, Gonzalez and Subirats, 1988). This increase in circulating TNF-α functions predominately paracrine and is regarded as pro-inflammatory by downregulation of multiple anti-inflammatory pathways (Cartier *et al.*, 2008). Leptin was also

found to be released by adipocytes and the term adipokine - proteins released by adipose tissue - was introduced. Nowadays, over 50 adipokines are known that signal to distant organs and contribute profoundly to the low-grade inflammatory state of obesity (Hotamisligil, 2006). Next to others, IL6 (Maury and Brichard, 2010), IL8 (Straczkowski *et al.*, 2002), IL1B (Juge-Aubry *et al.*, 2003) and CCL2 (Bruun *et al.*, 2005) are secreted, reflected by higher circulating serum levels in obesity.

In general, the metabolic derangements and low-grade inflammation in obese women are associated with health complications. In pregnancy, this environment may not only affect the women and her health, but through the placenta also the growing fetus.

1.5. Maternal obesity in pregnancy

As obesity has become a worldwide epidemic, also numbers in overweight or obese women in reproductive age are rising. For European countries, prevalence of obesity in women ranges from 6 to 37% (Berghöfer *et al.*, 2008) and it is estimated that about 20% of pregnant women are overweight or obese (Heslehurst *et al.*, 2010).

As seen in non-pregnant women, maternal obesity during pregnancy is also characterized by low-grade inflammation (Basu *et al.*, 2011). During pregnancy, maternal BMI and TNF-α levels have been shown to correlate positively (Aye *et al.*, 2014). Furthermore, the number of CD14+ and CD68+ macrophages that release pro-inflammatory cytokines such as IL1, IL6 and TNF-α, is three times higher in the placenta derived from obese as compared to lean women (Challier *et al.*, 2008). We recently showed that maternal obesity in early human pregnancy is associated with higher C-peptide concentrations and lower insulin sensitivity, but not with changes in maternal fasting glucose levels (Bandres-Meriz *et al.*, 2020).

1.5.1. Obesity-Related Pregnancy Complications

In general, maternal obesity is a condition known to affect pregnancy outcome. Obese pregnant women have a higher prevalence of infertility, recurrent miscarriage, and intrauterine fetal death compared to normal weight (Boots and Stephenson, 2011; Gardosi *et al.*, 2013). In a study by Bellver *et al*., the implantation rate in obese pregnant women decreased by approximately 10% compared to lean controls, indicating reduced uterine receptivity (Bellver *et al.*, 2013). Obesity affects not only ovarian granulosa cells and the follicular fluid surrounding the oocyte, but also alters endometrial gene expression during luteal phase

(Bausenwein *et al.*, 2010; Bellver *et al.*, 2011; La Vignera *et al.*, 2011). This suggests that both, ovarian alterations and changes in the uterine environment, contribute to reproductive dysfunction associated with maternal obesity.

Compared to women with normal BMI, obese pregnant women have an increased risk of developing other pregnancy complications such gestational diabetes (GDM) and pregnancy-induced hypertension or preeclampsia (Bautista-Castaño *et al.*, 2013; Jeyabalan, 2013).

Due to extensive adipose tissue mass, fetal structures are more difficult to detect sonographically in obese pregnant women. Consequently, the ultrasound examinations need to be repeated more frequently in obese women. However, approximately 20% of fetal malformations remain poorly detected in obese woman compared to a lean cohort (Wolfe *et al.*, 1990). Not only rates of preterm birth and induction of labor are higher in obese women, but also the risk of cesarean section (Dempsey *et al.*, 2005). In a study with 24423 women, the Cesarean rate increased from 26.5% in lean women to 42.6% in women with a BMI over 35 (Dietz *et al.*, 2005). After delivery, obese women show increased rates of hemorrhage, genital and urinary tract infection, and wound infection (Rode *et al.*, 2005; Smith, Hulsey and Goodnight, 2008).

In addition to pre-conceptional complications and various risks for pregnancy complications, maternal obesity further leads to short term and long-term adverse consequences for the offspring.

1.5.2. Maternal obesity and perinatal outcomes

Maternal obesity and developmental overnutrition impose risks in the offspring, with both perinatal and long-term consequences. Fetal macrosomia, usually referred to a birth weight higher than 4000-4500g, is associated with high maternal BMI, while maternal pregravid weight and decreased insulin sensitivity correlate with fetal fat mass at time of delivery (Catalano, Drago and Amini, 1995). Neonatal body fat mass, in turn, correlates with maternal obesity-associated insulin resistance in the neonates. Moreover, umbilical cord leptin and interleukin 6 (IL6) concentrations are elevated in newborns of obese mothers compared to lean controls (Catalano *et al.*, 2009).

Implications of maternal obesity go beyond pregnancy and affect infancy and adulthood. Long-term fetal health outcome regarding increased risk for can be explained in part by genetic

and environmental factors (Herskind *et al.*, 1996) as well as epigenetic mechanisms (Godfrey, Inskip and Hanson, 2011). In the last decade, several studies have implicated epigenetic mechanisms in the development of metabolic diseases. There is evidence that maternal obesity contributes to higher BMI in adolescent offspring (Yu *et al.*, 2013). Epigenetics is thought to mediate these changes as there are several studies showing maternal obesity-associated changes in various DNA methylation sites (Hjort *et al.*, 2018; Martin *et al.*, 2019; Nogues *et al.*, 2019). Although DNA methylation changes are relatively modest (<5% change), this data indicate that obesity-induced changes at birth remain also postnatally. In addition to methylation changes, also telomeres are affected. In maternal obesity telomeres are shorter in the placenta at term of pregnancy and also in cord blood. This may affect cellular ageing, disease susceptibility, and molecular longevity later in life. (Martens *et al.*, 2016).

1.5.3. The influence of obesity on term placenta

As the placenta constitutes the maternal-fetal interphase, it is directly exposed to the maternal environment. Therefore, metabolic changes in the mother directly affect placental function (Desoye, 2018). Several studies found obesity-associated changes in term placental tissue. Gene expression of placental IL1, IL6 and TNF-α as well as of MCP-1 and IL8 were increased. Data is inconsistent regarding macrophage infiltration. While Challier *et al.* showed increased histochemical staining of macrophage markers CD68 and CD14, Roberts and colleagues did not detect leukocyte infiltration in placental villi (Challier *et al.*, 2008; Roberts *et al.*, 2011).

Moreover, maternal obesity may affect placental nutrient transport reflected by placental changes in lipids and fatty acid. Placentas from obese women show a trophoblast specific increase in expression of FABP4 and in placental PLA2G2A and PLA2G5 which are, in turn, activated by adipokines leptin and TNF-α (Varastehpour *et al.*, 2006; Scifres *et al.*, 2011). Maternal obesity further affects placental insulin signaling pathways, reflected by lower expression of PI3K and GLUT4 and increased gene expression of IRS-2 in obese placentas (Colomiere *et al.*, 2009; Colomiere, Permezel and Lappas, 2010). Further studies showed reduced mTOR signaling as well as increased NFkB, but decreased AMPK, expression (Martino *et al.*, 2016). Maternal obesity also impairs total antioxidant capacity in the placenta accompanied by a switch from oxidative to a nitrative stress signaling (Roberts *et al.*, 2011; Saben *et al.*, 2014). Increased generation of ROS may lead to changes in placental gene expression and protein levels. These changes may reflect placental adaption to the adverse

metabolic environment probably to protect itself and in doing so also the fetus (Denison *et al.*, 2010; Desoye, 2018).

1.5.4. Maternal obesity and the first trimester placenta

Due to limited tissue availability and ethical issues around FT placentas, most studies on maternal obesity in pregnancy have focused on time of delivery using term placental tissue. However, assessing the effects of obesity in early pregnancy is key to understand the molecular mechanisms leading to maternal and fetal complications later in pregnancy.

Placental growth rate is highest in early pregnancy (Desoye, 2018). Thus, FT placental tissue is highly susceptible to changes in the environment, i.e., hyperglycemia, hyperinsulinemia, inflammation or changes in intervillous oxygen level, that might be associated with maternal obesity. The effects of high glucose and insulin levels on some aspects of placental function have already been studied (Fröhlich *et al.*, 2012; Lassance, Haghiac, Leahy, *et al.*, 2015; O'Tierney-Ginn *et al.*, 2015).

In FT placentas from obese women, transcriptomic analysis identified changes in main biological processes related to energy production and cell metabolism. In this analysis, several genes involved in cholesterol utilization and steroid synthesis and also genes regulating lipid metabolism and mitochondrial activity were downregulated by maternal obesity (Lassance, Haghiac, Leahy, *et al.*, 2015). This indicates an adverse effect on placental mitochondrial function in FT placentas from obese women compared to lean controls, which is concordant with findings at the end of pregnancy (Myatt and Maloyan, 2016). Moreover, mitochondrial dysfunction might contribute to obesity-induced FT placental maladaptation as extracellular hyperglycemia activates mitochondrial activity in numerous cell types enhancing ROS generation. When compared to lean controls, FT trophoblasts of obese women show downregulation of genes related to mitochondrial metabolism (Lassance, Haghiac, Minium, *et al.*, 2015). Considering the low oxygen utero-placental environment in the FT of pregnancy, the hyperoxic environment (21% oxygen) typically used in *in vitro* studies might *per se* overwhelm placental antioxidant defense systems masking potential obesity effects. A study of FT trophoblasts cultured under physiologically low oxygen tension showed that high glucose levels increased ROS levels independent of mitochondrial activity, indicating the presence of non-mitochondrial pathways for ROS generation (Fröhlich *et al.*, 2012).

Changes in oxygen tension after spiral artery remodeling are physiological drivers for normal placental development during the first trimester of pregnancy. Interestingly, in a rat model of lifelong maternal obesity, changes in trophoblast invasion accompanied by increased levels of smooth muscle actin surrounding the placental spiral arteries suggest an impairment in spiral artery remodeling in obesity (Hayes *et al.*, 2014). Furthermore, studies in humans also suggest reduction in uterine natural killer cell numbers accompanied with impaired uterine artery remodeling in maternal obesity (Perdu *et al.*, 2016; Castellana *et al.*, 2018; St-Germain *et al.*, 2020). Dysfunctional spiral arteries may result in impaired blood flow to the placenta associated with decreased intervillous oxygen levels in obese women (Berger *et al.*, 1983; Frias *et al.*, 2011). This might be associated with secretion of inflammatory cytokines (Laresgoiti-Servitje and Gomez-Lopez, 2012) and might affect trophoblast invasion (Huppertz *et al.*, 2009), thereby affecting proper placental function.

Adequate trophoblast invasion is essential for a successful pregnancy and, therefore, highly regulated. In addition to the already mentioned effect of altered oxygen tension during early pregnancy, trophoblast invasion might be disrupted by a variety of obesity-induced changes in the placental environment. Several paracrine factors have been found to modulate trophoblast invasion: TNF-α (Bauer *et al.*, 2004), transforming growth factor beta (TGF-β) (Lash *et al.*, 2005) and endothelin-1 (Majali-Martinez *et al.*, 2017).

1.6. DNA damage and damage repair in obesity

As previously described, maternal obesity is not only associated with profound metabolic changes, but also linked with elevated inflammatory and oxidative stress levels. In an oxidative stress environment, highly reactive ROS can further react with biological molecules. Therefore, a high and prolonged concentration of ROS may damage DNA, proteins and lipids. Oxidation of proteins can lead to insoluble protein aggregates that are implicated in various pathophysiological manifestations that affect placental function (Levytska *et al.*, 2013). When DNA is attacked by reactive species, its function and structure is affected severely leading to base modifications, strand breaks, crosslinks within one or both strands or between DNA and proteins (Jena, 2012). In general, DNA oxidation by ROS may lead to DNA instability, induce mutations and alter gene expression (Brieger *et al.*, 2012).

DNA damage is rapidly detected in cells by sensor proteins that activate downstream transducer proteins to transmit the signal to effectors. DNA damage results in increased

deposition of phosphorylated H2A histone family member X (γH2AX) in chromatin that activates multiple signaling pathways involved in the response to one single DNA lesion (Plesca, Mazumder and Almasan, 2008). Depending on stress level, mammalian cells can exhibit various response mechanisms to cellular stress. The activated pathways eventually lead to the induction of cell-cycle checkpoints and DNA repair, or to the activation of apoptosis (Barzilai and Yamamoto, 2004).

Oxidized pyrimidines and purines, single strand breaks (SSB) and double strand breaks (DSB) are the main types of DNA damage that are caused by ROS. Of these, 8-oxo-7,8-dihydroguanine (8-OHdG) is derived from reaction of guanine with the hydroxyl radical (Cooke *et al.*, 2000). Oxidative DNA damage is mainly repaired by the base excision pathway (Gonzalez-Hunt, Wadhwa and Sanders, 2018). Studies already showed various DNA lesions in lymphocytes of obese non-pregnant women. Obesity also correlated with oxidative DNA damage measured by serum 8-OHdG (Al-Aubaidy and Jelinek, 2011; Włodarczyk *et al.*, 2018).

Ataxia telangiectasia mutated (ATM) and ataxia telangiectasia and Rad3-related (ATR) signaling pathways are central to maintain genome integrity and are well conserved throughout evolution. ATM has serine/threonine kinase activity that is inactive in undamaged cells. It is primarily implicated in the response to double-strand breaks (DSB), which belong to the most fatal DNA lesions as one single DSB can result in apoptosis of the cell (Maréchal and Zou, 2013). ATM depends on the MRE11-RAD50-NBS1 (MRN) complex and signals through Chk2 and p53, finally leading to cell cycle arrest while DNA damage is repaired. Furthermore, ATR activation is a response to a variety of DNA lesions that induce the formation of single-strand breaks (SSB) (Cimprich and Cortez, 2008). ATR forms a heterodimer with ATR-interacting protein (ATRIP) and localizes to sites of replication stress and DNA damage (Zou, Liu and Elledge, 2003). ATR is activated by replication protein A heterotrimer (RPA) and single strand DNA nucleofilaments leading to subsequent Chk1 phosphorylation following genotoxic stress which in turn affects further cell cycle regulation (Awasthi *et al.*, 2016).

The ATM/ATR complex binds to the damaged sites and targets downstream effectors, i.e. BRCA1, Chk2, and p53 (Lavin, 2008) that are involved in multiple cellular processes like cell cycle transition, DNA repair, gene transcription, protein translation, degradation and apoptosis (Barzilai and Yamamoto, 2004) (Figure 3).

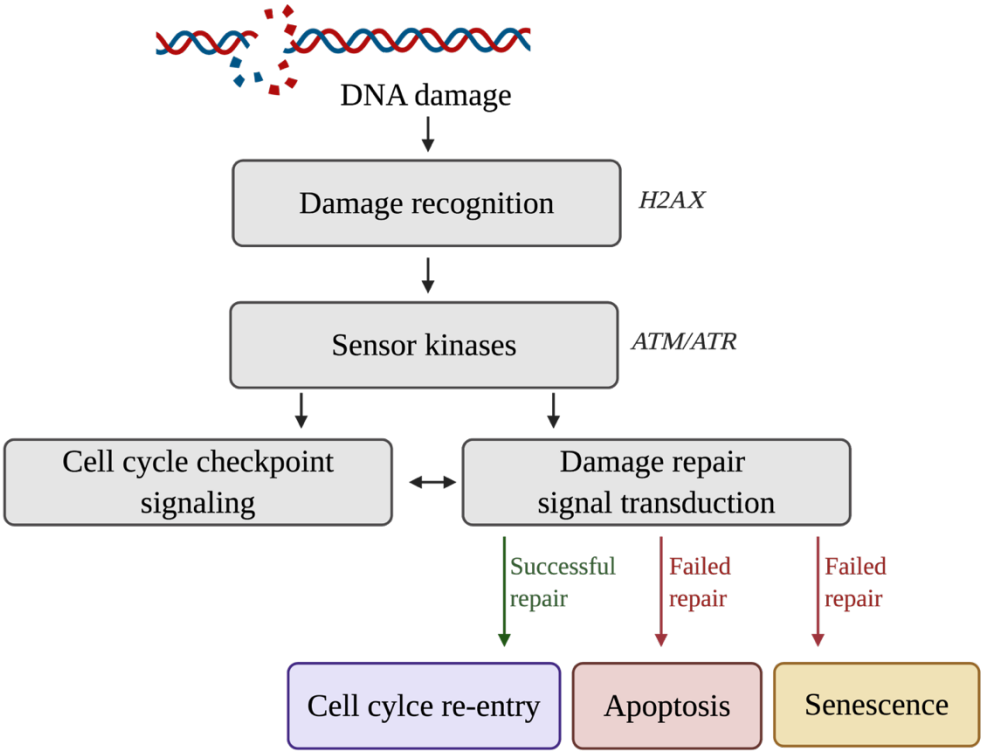

Figure 3: DNA damage response. Genomic DNA damage is recognized and activates downstream sensor kinases. A complex damage response is orchestrated including cell cycle checkpoint activation. After successful damage repair cells reenter cell cycle and resume proliferation. Unsuccessful damage repair leads to apoptosis or cellular senescence. Created with BioRender.com.

Also, critically short telomeres can be recognized as DNA breaks and thus active DNA damage response as described previously. Telomeres are dynamic nucleoprotein-DNA structures that define the physical ends of linear chromosomes and protect their ends. Maintaining telomere length is a dynamic process of lengthening and shortening. While telomere shortening results of nucleolytic degradation and incomplete DNA replication, lengthening is facilitated by the reverse transcriptase telomerase (TERT) (Greider and Blackburn, 1985).

In general, oxidative stress accelerates telomere loss (Von Zglinicki, 2002). Maternal obesity was associated with significantly shorter placental telomeres at the time of birth

(Martens *et al.*, 2016). Furthermore, ATR kinase that is involved in repair of single stranded DNA damage, also contributes to telomere maintenance leading to the activation of classical DNA damage downstream effectors (Pennarun *et al.*, 2010). A framework of telomere shortening, genome stability, damage sensing, ATM/ATR signaling and subsequent effects on cellular function is shown in Figure 4.

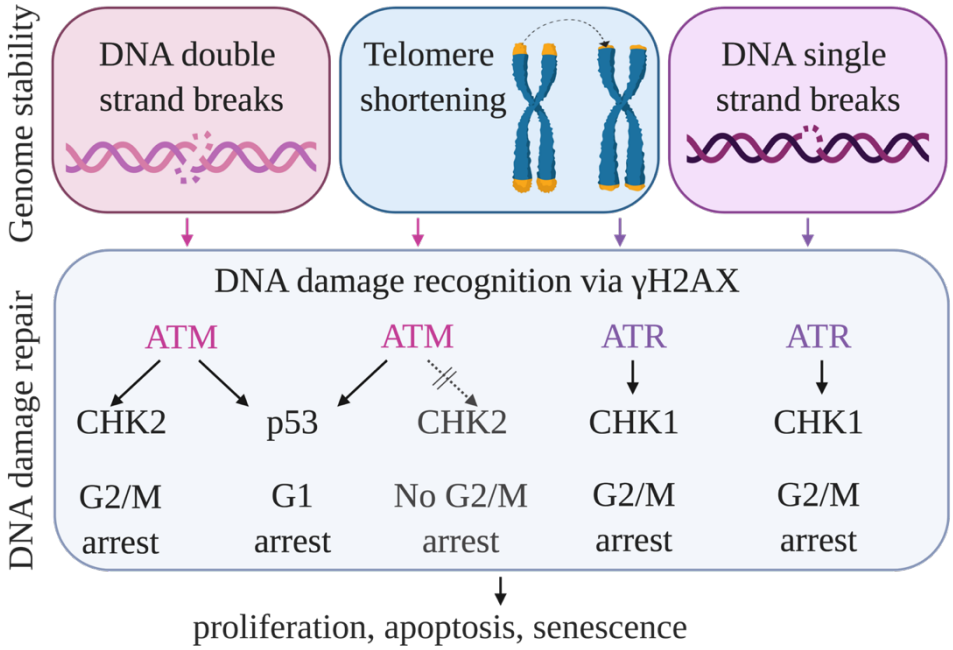

Figure 4: Genome stability is maintained by ATM/ATR signaling that alters cell cycle and finally affects cell proliferation, apoptosis and senescence. DNA damage signaling via ATM/ATR pathways induced by genomic DNA damage and critically short telomeres. Damaged sites are recognized by H2AX that gets activated by phosphorylation at serine 139. Signaling pathway activates cell cycle arrest in G1 or G2/M phase after activation of CHK1 and CHK2, respectively. Created with BioRender.com

Several studies found associations between obesity and elevated levels of maternal leucocyte DNA damage and subsequent repair signaling in the circulation in pregnant and non-pregnant women (Al-Aubaidy and Jelinek, 2011). However, the effect of maternal obesity on the placenta, that is as the feto-maternal interphase also direct in contact with potential obesity-associated DNA damage inducers, remains to be assessed. Moreover, further consequences for DNA damage associated ATM/ATR damage repair signaling and telomere length still await elucidation. Here, the first trimester is of specific interest as placental growth rate is highest, while it is the crucial time frame for fetal development and therefore affects the offspring's later life.

2. Hypothesis and Objectives

Considering obesity-associated changes in early placental intrauterine environment, we hypothesize that a maternal obese metabolic status affects first trimester placental function by

i) Oxidative stress-induced modification of macromolecules, antioxidants and activation of stress markers
ii) Activation of FT placental stress signalling and cytokine release by obesity-induced oxidative or inflammatory conditions
iii) Affecting placental and trophoblast DNA integrity, e.g., DNA damage and telomere length
iv) Induction of placental DNA damage repair with subsequent consequences for cell cycle progression
v) Finally affecting FT trophoblast viability due to failed adaption to an obesity-associated stress of the intrauterine environment

Hence, we aim to study the consequences of maternal obesity in the first trimester of human pregnancy by assessing

i) Placental oxidative and inflammatory status by oxidative DNA modification, protein nitration, lipid peroxidation, expression of antioxidants and marker proteins
ii) FT placental stress signalling transducers and cytokine expression
iii) FT placental and trophoblast specific DNA damage and telomere length
iv) Cellular DNA damage adaptation, e.g., DNA damage repair and cell cycle regulation
v) Acute consequences on first trimester trophoblast proliferation, apoptosis and placental senescence

For that purpose, we used i) human FT placental tissue, and ii) human chorionic FT explants under physiological oxygen concentrations to investigate whether inflammation-associated TNF-α or a physiological change in oxygen levels triggers obesity-associated consequences (Figure 5).

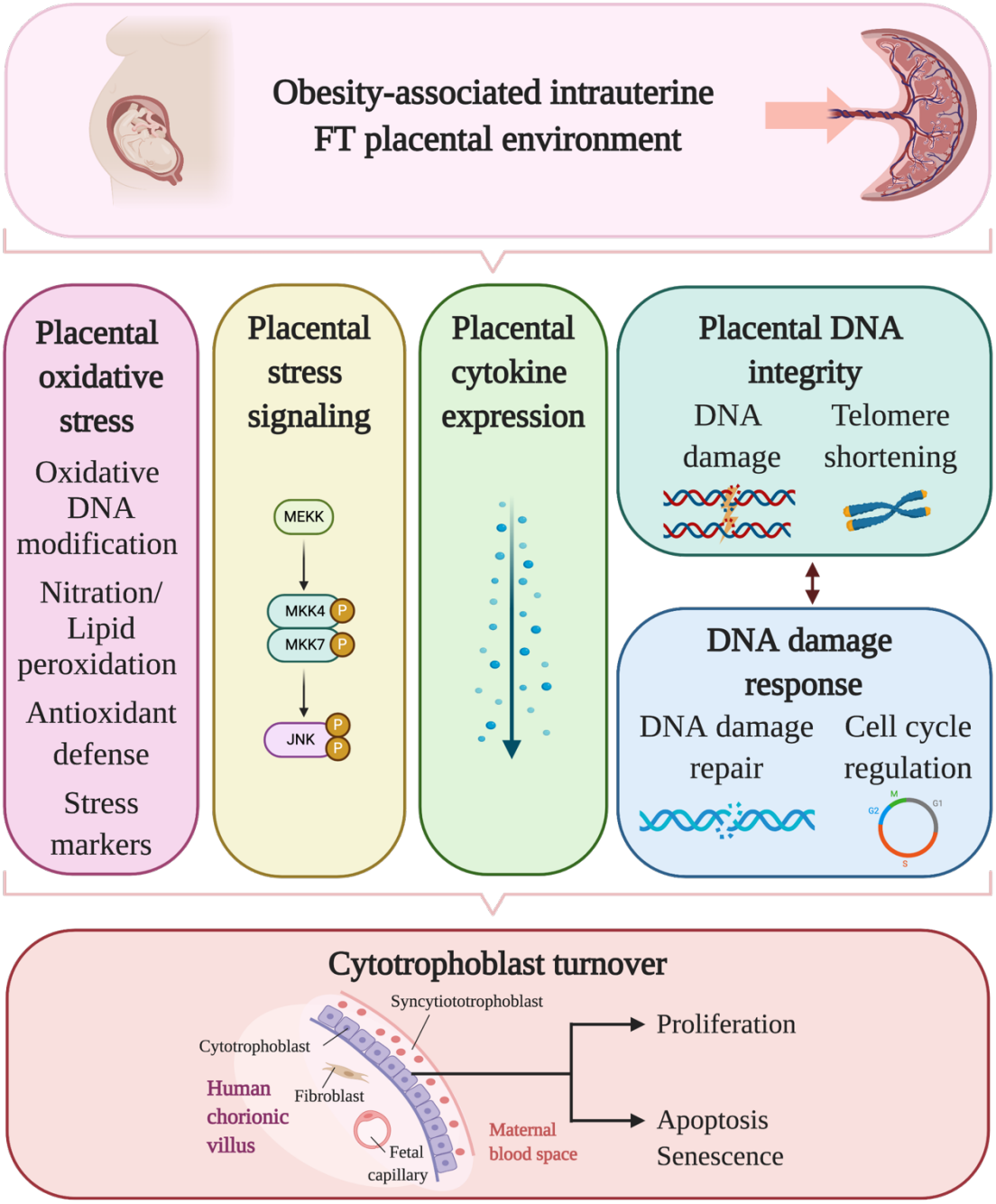

Figure 5: Graphical representation of the hypothesis and aims of the present study. FT: First trimester. Created with BioRender.com

3. Materials and Methods

Parts of this chapter are already published in adapted form in Hoch, Bachbauer *et al.* (2018) and Hoch, Novakovic *et al.* (2020).

3.1. Study subjects

The study was approved by the institutional review board and the ethical committee of the Medical University of Graz (29-095 ex16/17). Women with a singleton pregnancy scheduled for legal elective pregnancy termination were recruited upon signing a written informed consent. Exclusion criteria for all subjects were smoking (questionnaire and verified by serum cotinine), other co-morbidities and current medication. Gestational age was calculated based on the patient's last menstrual period and verified by measurement of fetal crown-rump-length.

3.2. Human placental tissue collection

First trimester placental tissue (gestational week 5-12) was obtained after surgery, washed with phosphate buffered saline (PBS, Sigma Aldrich, St. Louis, MO, USA) and cryopreserved at -80°C after snap-freezing or formalin fixed and paraffin embedded until further use. Time between surgery and tissue cryopreservation was recorded and fetal sex was assessed by gene expression analysis (c.f. 3.8). Based on the maternal pre-gravid BMI, gestational age matched samples were subsequently divided into two groups, i.e., lean (mean BMI < 25 kg/m^2) and obese (mean BMI ≥ 30 kg/m^2).

3.3. First trimester chorionic villi explant culture

Human FT chorionic villi were micro-dissected into small pieces (15-20 mg wet weight), rinsed with PBS and cultured in Dulbecco's Modified Eagle Medium (DMEM; Gibco, Invitrogen, Carlsbad, CA, USA) and Ham's F-12 medium 1:1 (v/v; Gibco) supplemented with 10% fetal calf serum (FCS, Thermo Scientific, Rockford, IL, USA) and 1% penicillin-streptomycin (Gibco). Placental explants were cultured in a hypoxic workstation (BioSpherix; Redfeld, NY, USA). After 24 hours of pre-incubation, samples were treated with TNF-α (50ng/mL, Sigma Aldrich), leptin (100ng/mL, Sigma Aldrich),IL6 (100ng/mL, Sigma Aldrich) at 2.5% O_2 for 48 hours. The effect of oxygen tension was additionally assessed at 6.5% O_2 for 48 hours.

Thereafter, explants were snap-frozen for subsequent RNA extraction or protein isolation. Culture supernatant was frozen and used for human gonadotropin (hCG) analysis.

3.4. COMET assay

FT placental tissue was minced by pressing through a sieve (2 μm pore size) with cold DMEM medium (Gibco). After washing with PBS, collected cells were centrifuged at 400 g for 5 min at 4°C. The cell pellet was re-suspended in cold DMEM medium (Gibco) and mixed with preheated 0.8 % low melting point agarose. Slides were kept on ice until solidification and then placed in lysis solution (2.5 M NaCl, 10 mM EDTA-Na_2, 10 mM Tris, 1% Triton-X 100 and 5% DMSO) for an hour. After lysis, slides for FPG comet assay were incubated with enzyme reaction buffer (40 mM Hepes, 0.1 M KCl, 0.5 mM EDTA, 0.2 mg/ml BSA, ph 8.0) and then incubated either with FPG enzyme or with enzyme reaction buffer for an hour at 37°C. The slides were placed in a horizontal electrophoresis chamber filled with cold alkaline buffer (1 mM Na_2EDTA, 300 mM NaOH, pH >13) and kept for 20 min in the dark to allow unwinding of DNA before electrophoresis (~1V/cm, on ice for 20 min).

Slides for alkaline comet assay were directly placed in electrophoresis chamber after the lysis. After electrophoresis, slides were immersed in PBS and then in bi-distilled water for 10 min for neutralization. For the *ex vivo* H_2O_2 challenge slides were immersed in a cold H_2O_2 solution (50 μM) for 5 min at 4°C and immersed in lysis solution for an hour. Except for omitting the enzyme treatment step, the rest of the assay was performed as described above. Slides were fixed in 70% and then 100% ethanol for 15 min. After air-drying, slides were stained with GelRed (Sigma Aldrich) and 100 cells were scored per subject and per time point by using Komet 6 software (Oxford Instruments, Abingdon, GBR).

3.5. Laser capture microdissection of trophoblasts and DNA extraction

To study villous trophoblasts in their native environment, we performed laser capture microdissection (LCM). This method is a useful tool for isolation of specific cell subpopulations from a diverse background via direct visualization of the cells. The basic LCM principle is the capture of selected cells onto a thermoplastic membrane from histological sections of stained formalin-fixed paraffin-embedded (FFPE) tissue. Therefore, FFPE placenta tissue was cut into sections (7 μm), deparaffinized in xylene and rehydrated with decreasing concentrations of ethanol and stained with sterile-filtered Papanicolaou′s solution 1a Harris′ hematoxylin solution (Sigma-Aldrich).

PEN-MembraneSlides (Life Technologies, Darmstadt, DEU) slides were rinsed with DEPC-water (Thermo Scientific, Waltham, CA, USA) and air-dried overnight at 37°C. The VERITAS Microdissection Instrument Arcturus (Applied Biosystems, Foster City, CA, USA) was used to cut out villous trophoblasts. First, villous tissue was centred in the device and the region of interest was defined in an overview mode. Trophoblasts were defined manually, tissue was cut using the cutting laser (power: 12.08 mW) and captured onto the thermoplastic membrane by adjusting the capturing laser to 65-100 mW for 1200-3000 µsec. Trophoblast selection, device settings and cell layer separation is shown in Figure 6.

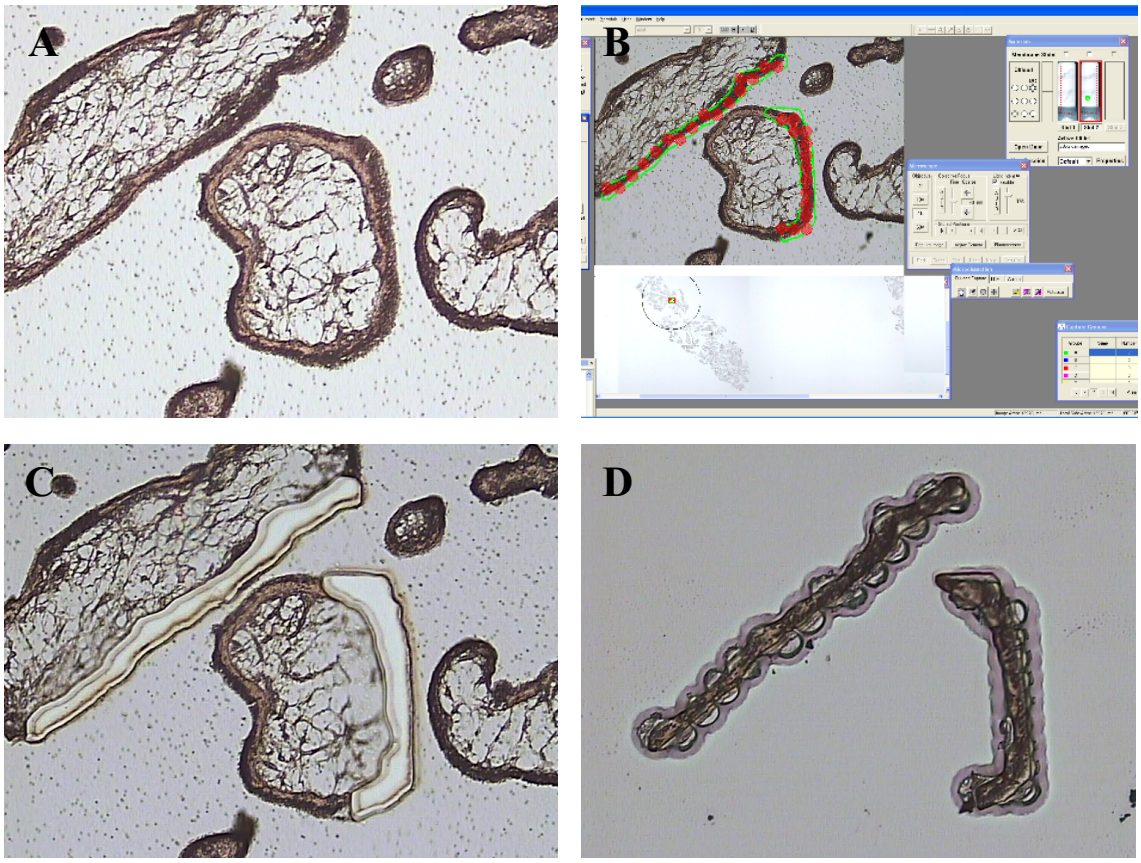

Figure 6: Laser capture microdissection workflow. (**A)** After slide and cap insertion, placental villous tissue was identified and centred on the plate. (**B**) Villous trophoblasts were selected by manually defining the region of interest (green line). Cutting laser (power: 12.08 mW) was set and capture laser (power: 65-100 mW for 1200-3000 µsec) adjusted for each section. After microdissection, stromal tissue remains on the slide (**C**) while villous trophoblasts are separated on the capture cap (**D**) and transferred into a tube for further DNA extraction.

Caps containing selected trophoblasts were immediately covered with DNA extraction buffer and the Arcturus PicoPure DNA Extraction Kit (Thermo Scientific) was used for DNA extractions according to manufacturer's guidelines. Briefly, inverted caps were incubated with extraction solution for 16 hours at 65°C in an incubator and centrifuged for one minute at 1000g.

The tube containing the extract was heated to 95°C for ten minutes to inactivate Proteinase K (Thermo Scientific), cooled to room temperature and frozen until further PCR analysis.

3.6. DNA/RNA isolation and reverse transcription

FT placental tissue was homogenized in RLT Plus Buffer (Qiagen, Hilden, DEU) with 1% β-Mercaptoethanol (v/v, Merck) using a tissue lyser (MagNa Lyser, Roche, Basel, CHE). DNA and total RNA was isolated with the AllPrep DNA/RNA/miRNA Universal Kit (Qiagen) according to the manufacturer's guidelines. After quality control using Bioanalyzer (Agilent, Santa Clara, CA, USA), mRNA was reverse transcribed using the SuperScript II Reverse Transcriptase kit (Life Technologies) as per manufacturer's protocol.

3.7. PrimePCR panel

Differential expression of 187 genes associated with DNA damage-repair and oxidative stress was analyzed using a PrimePCR Collection panel (DNA damage H384 Predesigned 384-well, Biorad, Hercules, CA, USA) according to the manufacturer´s guidelines. A complete list of the genes and controls can be found on the manufacturer's website (https://www.bio-rad.com/de-at/prime-pcr-assays/pathway/dna-damage-collection-panel). For each PCR reaction 10 ng of cDNA were used. Real-time PCR was then conducted using the CFX384 PCR detection system (Biorad) and the associated software. Ct values were normalized using hypoxanthine phosphoribosyltransferase 1 (*HPRT1*) and TATA box binding protein (*TBP*) as reference genes and results were analyzed using the $2^{-\Delta\Delta Ct}$ method (Meller *et al.*, 2005).

3.8. Real time PCR

Gene expression was determined by quantitative real-time PCR (RT-qPCR) using FAM-labeled TaqMan gene expression assays (Life Technologies, BRCA1: Hs01556193_m1). Fetal sex was determined in a multiplex PCR setup using FAM labelled DDX3Y and VIC labelled XIST expression assays (Life Technologies, DDX3Y: Hs00965254_gH, XIST: Hs01079824_m1) as previously described (Hoch, Novakovic, *et al.*, 2020). RT-qPCR was performed using TaqMan Universal PCR Master Mix (Life Technologies) using the CFX96 Thermocycler (BioRad). A calibrator sample was added onto each plate to control for inter-run variations. Ct values were generated by the CFX Manager 3.1 software (BioRad) and relative gene expression was calculated by the $2^{-\Delta\Delta Ct}$ method, with HPRT1 (Life Technologies, HPRT1: Hs02800695_m1)

and Peptidylprolyl isomerase A (Life Technologies, PPIA: Hs04194521_s1) as housekeeping genes (Hoch, Novakovic, *et al.*, 2020).

For telomere assessment, DNA quality and concentration were evaluated using the Qubit dsDNA BR Assay Kit (Thermo Fisher Scientific). We measured the average relative telomere length by a RT-qPCR protocol modified from the method by Cawthon (Cawthon, 2009). In brief, within each DNA sample a measure of the average telomere length as a ratio (T/S) of telomere repeat length (T) to copy number of a single-copy gene (S) was generated. We used β-globin (BG) as the reference single-copy gene. All measurements were performed in Triplicates in 384-well plate formats, using the LightCycler 480 Real-Time PCR System (Roche, Melbourne, VIC, AUS). Equal DNA amounts (5 ng) were used in each reaction with amplification using SensiMix SYBR Fluorescein Mastermix (Bioline, Sydney, NSW, AUS). Reactions were set up on ice to prevent premature DNA polymerase activation, non-specific amplification and primer-dimerisation. Two sets of standard oligomers (telomere TTAGGG repeat and reference gene BG) were run as a standard curve on each plate to ensure that sample Ct values were within the linear range, as well as to assess inter-run variation. Furthermore, an inter-run control was measured on all plates (placental genomic DNA sample) to account for inter-run variability. A negative (no template) control was also included on all plates. The ΔCt method was used to calculate relative average telomere length.

3.9. Nanostring analysis

Results from the PrimePCR Panel were validated using the NanoString nCounter system (Nanostring Technologies, Seattle, WA, USA) which is based on direct digital detection of mRNA molecules using target-specific, color-coded probe pairs that hybridize directly to target molecules. Housekeepers and oligonucleotides were synthesized at Integrated DNA Technologies (Leuven, BEL). Gene expression was measured by counting the barcode for each specific molecule, which is detected by a digital analyzer. In order to define the required RNA amount for hybridization. We performed titration with 20 ng, 100 ng and 200 ng according to the supplier's guidelines at the Core Facility Molecular Biology of the Center for Medical Research (Medical University of Graz). Positive normalization to the geo-mean of the top 3 positive controls and codeset normalization (Molania *et al.*, 2019) on the reference genes WD Repeat Domain 45B (WDR45L) and TBP (Meller *et al.*, 2005) was performed using the nSolver 4.0

analysis software (Nanostring Technologies). Results are expressed as gene counts of mRNA molecules in 100 ng/µl RNA.

3.10. Protein isolation, quantification and immunoblotting

Placental tissue was homogenized in RIPA buffer (Sigma Aldrich) with protease inhibitor (Roche, Basel, CH) using an ultra-turrax homogenizer. Protein amount was quantified using BCA assay (Thermo Scientific).

Protein lysates were mixed with Laemmli buffer 2x (Sigma Aldrich) and denatured at 96°C for 5 minutes. Equal amounts of total protein (10 µg/well in tissue lysates) were loaded onto 4-20% SDS-PAGE gels (BioRad) and resolved at 120 V for 1 hour. Proteins were transferred to a nitrocellulose membrane (BioRad) and nonspecific binding sites were blocked for 1 hour with 5% non-fat dry milk (BioRad) in tris-borate-EDTA (TBE) + 0.1% Tween 20 (Sigma Aldrich). After blocking, the membranes were incubated with primary antibodies overnight at 4°C. The antibodies used for immunoblotting are shown in Table 1.

Table 1: Antibodies used for immunoblotting

Antibody	Host	Dilution
4-Hydroxynonenal (Abcam, ab48506)	Mouse	1:100
3-Nitrotyrosine (Cell Signaling, #9691)	Rabbit	1:1000
APE1 (Abcam, ab137708)	Rabbit	1:1000
ATM (Cell Signaling, #2873)	Rabbit	1:1000
ATR (Merck, 09-070)	Rabbit	1:1000
p-ATM/ATR Substrate (S*Q) (Cell Signaling, #9607)	Rabbit	1:1000
GADD45α (Santa Cruz Biotechnology, sc-6850)	Mouse	1:200
BRCA1 (Sigma-Aldrich, AB-1423)	Rabbit	1:1000
HO-1 (Enzo Life Science, ADI-SPA-895)	Rabbit	1:2000
HSP70 (Invitrogen, MA3-006)	Mouse	1:1000
NEIL3 (Abcam, ab174205)	Rabbit	1:500
p$^{(Ser1423)}$BRCA1 (Merck, 07-635)	Rabbit	1:1000
p16 (Abcam, ab108349)	Rabbit	1:1000
p53 (Santa Cruz Biotechnology, sc-126)	Mouse	1:500
p$^{(Ser15)}$p53 (Cell Signaling, #9284)	Rabbit	1:1000
α-tubulin (Merck, CP06-100UG)	Mouse	1:1000

β-actin (Abcam, ab8227)	Mouse	1:10000
Anti-mouse (H + L)-HRP conjugate (Bio-Rad, #1706516)	Goat	1:2000
Anti-rabbit (H + L)-HRP conjugate (Bio-Rad, #1706515)	Goat	1:2000

Membranes were washed three times with TBE and incubated with the appropriate secondary antibody conjugated with horseradish peroxidase. After washing, protein bands were visualized using an enhanced chemiluminescent detection system (Thermo Scientific) and the Fusion device (Vilber Lourmat, Eberhardzell, DEU). We tested Beta-Actin stability and found protein level unaltered by maternal BMI and gestational age (data not shown). Therefore, I decided to use Beta-Actin as a loading control for Western Blotting. Band densitometry was determined using the EvolutionCapt software (Vilber Lourmat).

3.11. Cell cycle control protein array

Cell cycle related proteins were profiled in placental tissue lysates of women with low and high BMI women using the Cell Cycle Control Phospho-Antibody Array covering 238 immobilized antibodies (Fullmoon Biosystems, Sunnyvale, CA, USA). Each antibody has 6 replicates, which are printed on coated glass microscope slides. Briefly, the array was blocked with blocking solution (Fullmoon Biosystems) for 30 minutes at room temperature, followed by incubation with biotin-labelled cell lysates at 4°C overnight. After washing, the conjugated proteins were detected using Cy3-conjugated streptavidin (Sigma Aldrich). The slides were sent to the manufacturer and scanned using an array scanner. Image analysis was performed using GenePix Pro 7.0 software (Molecular Devices, San Jose, CA, USA). After local background subtraction, data were normalized by dividing the intensity signals of each spot with the median intensity value of all antibodies on the array (excluding empty spots and negative/positive marker). Signals were considered as true, when the signal intensity exceeded background intensity by two-fold.

3.12. Cotinine enzyme-linked immunosorbent assay (ELISA)

Serum cotinine levels were measured by solid phase competitive ELISA (Abnova, Taipei, TWN) according to manufacturer's guidelines. Briefly, 10 µl of maternal serum was pipetted in duplicates into the wells of the 96-well-plate coated with polyclonal antibody to Cotinine. H_2O was used as blank control. One hundred µl of the Enzyme Conjugate were added and incubated for 60 minutes at room temperature in the dark. After washing 3 times with 1x wash

buffer, the wells were slapped dry and Substrate reagent was added. The Stop Solution was added after an incubation of 30 minutes at room temperature in the dark. Absorbance was read at 450 nm using the spectrometer SPECTROstar Nano (BMG Labtech, Offenburg, DEU). According to literature, we used serum cotinine levels > 0.03 nmol/L as a cut-off for smoking (Benowitz *et al.*, 2009).

3.13. Oxidative DNA damage ELISA

Levels of 8-hydroxydeoxyguanosine (8-OHdG) were measured in DNA extracted from first trimester villous tissues using the commercially available OxiSelect Oxidative DNA Damage ELISA Kit (Cell Biolabs, Heidelberg, DEU) according to manufacturer's protocol. Prior to the competitive ELISA for the quantitative measurement of 8-OHdG, DNA was converted to single-stranded DNA by incubation at 95°C for 5 minutes followed by digestion to nucleosides by nuclease P1 incubation for 2 hours at 37°C. Samples were incubated with 8-OHdG antibody for 60 minutes at room temperature. Absorbance was read at 450 nm using the spectrometer SPECTROstar Nano (BMG Labtech).

3.14. Measurement of secreted human chorionic gonadotropin

Tissue supernatant was collected for all explant experiments, centrifuged at 1800x g for 10 minutes and stored at -20°C until immunoassay analysis. Human chorionic gonadotropin (hCG) levels were determined using IMMULITE 1000 Systems Immunoassay (Siemens, Munich, DEU). Supernatant (30 µl) was diluted (1:10) with 270 µl of IMMULITE 1000 Systems hCG diluent. Results were normalized to total protein content in each well quantified by BCA.

3.15. Immunohistochemistry

Paraffin embedded placental tissues were cut into sections (3 µm) and placed on Superfrost Plus slides (Thermo Fisher Scientific). Slides were deparaffinized in xylene followed by rehydration in decreasing concentrations of ethanol. Heat induced antigen-retrieval was performed in citrate buffer at pH 6 (Anstaltsapotheke, LKH Graz, AUT) in a pressure cooker (Biocare Medical, Pacheco, CA, USA) for 15 min at 120°C before TUNEL Assay, immunohistochemistry and Q-FISH. Prior to immunohistochemistry, slides were allowed to cool at room temperature for one hour. Primary antibodies used for immunohistochemistry staining are presented in Table 2.

Table 2: Primary antibodies used for immunofluorescence

Primary antibody	Host	Dilution
8-oxoguanine (Sigma-Aldrich, MAB3560)	Mouse	1:100
Caspase-cleaved cytokeratin 18 (Roche, 14533800)	Rabbit	1:25
E-Cadherin (Cell Signaling Technology, #14472)	Mouse	1:100
Ki67 (Thermo Scientific, RM-9106-S0)	Rabbit	1:100
TUNEL assay (Roche, 11684795910)	Mouse	1:10

TUNEL Assay

In situ cell death detection was performed by TUNEL (TdT-mediated dUTP-biotin nick end labeling) technology as described by the manufacturer (#11684795910, Roche Applied Science). As a positive control, we exposed FT placental tissue to X-Ray (DLP: 6889,6 mGy.cm). In brief, the slides were incubated with fluorescein conjugated TUNEL reaction mixture in a humidified chamber at 37°C for 1 hour in the dark. TUNEL reaction mixture without enzyme solution was included as negative control on the tissue sections. To identify the trophoblast layers, tissue sections were incubated with E-Cadherin Antibody (1:100, Cell Signaling Technology) diluted in Antibody Diluent (Dako, Hovestaden, DNK) followed by the corresponding Alexa Fluor 633 goat anti-mouse IgG (1:200, Molecular Probes) as secondary antibody. Negative control slides were incubated with mouse IgG fractions (1:100, Dako) as isotype controls. The slides were stored at 4°C protected from light until imaging. Images were captured within 5 days after staining, using the Zeiss LSM 510 META Axiovert 200M Zeiss confocal system (Carl Zeiss Meditec AG, Jena, DEU). Images were generated with a 40x Plan-Neofluar 1.3 DIC oil immersion objective (Carl Zeiss Meditec AG) and the ZEN 2012 software (Carl Zeiss Meditec AG).

Triple staining

For detection of DNA damage or proliferation, exclusively in both trophoblast layers i.e syncytiotrophoblast and subjacent CTB, we established a triple staining protocol for E-Cadherin (trophoblasts), γH2AX/Ki67 (DNA strand breaks/proliferation) and DAPI (total DNA). To block unspecific background staining, slides were incubated with Ultra V Block or UV Block (Dako) for 5 minutes. Sections were incubated with primary antibody at room temperature in a humidified chamber for 1 hour. Antibodies against E-cadherin and either γH2AX (1:100, Merck) or Ki67 (1:100, Novus Biologicals, Littleton, CO, USA) were diluted in antibody diluent (Dako) and mixed. Negative control slides were incubated with rabbit or

mouse IgG fractions (1:100, Dako) as isotype controls, respectively. After washing (TBE buffer containing 0.1% Tween), a mixture of appropriate coupled secondary fluorescent antibodies (Table 3) was incubated for another hour at room temperature.

Table 3: Secondary antibodies used for immunofluorescence

Anti-mouse IgG Alexa Fluor
Fluor 488 (green, 11001, Thermo Scientific)
Fluor 568 (red, 11004, Thermo Scientific)
Anti-rabbit IgG Alexa Fluor
Fluor 488 (green, 11008, Thermo Scientific)
Fluor 568 (red, 11011, Thermo Scientific)

Slides were mounted with ProLong Gold Antifade Mountant with DAPI (Thermo Fisher Scientific). Imaging was performed as described in the TUNEL Assay section.

3.16. Telomere Q-FISH

Antigen retrieved slides were washed with PBS, fixed with 4% PFA and ethanol dehydrated for 5 minutes on a rocker. Slides were incubated with SSC/Formamide mix at 71°C for 5 minutes and subsequently dehydrated in cold ethanol. After drying, 50 ul of Cy5-telomere probe ($(CCCTAA)_3$ peptide nucleic acid (PNA) probe) was added to the slides, sealed with glue and incubated over night at 37°C. After overnight incubation, slides were placed in FISH buffer 1 (10mM Tris-HCL,70% formamide) for one hour, washed and incubated with FISH buffer 2 (0.1M Tris-HCL, 0.15M NaCl, 0.08% Tween-20).

Subsequently, slides were ethanol dehydrated, stained with 4',6-diamidino-2-phenylindole (DAPI; Molecular Probes, Eugene, OR) and mounted with Vectashield (Vector Laboratories Inc., Burlingame, CA, USA). Slides were imaged by a single blinded investigator within 24 hours to avoid loss of signal intensity. Ten randomly selected areas within every placental tissue section were captured using a Zeiss LSM510 Meta microscope (Zeiss, Oberkochen, DEU). Image analysis workflow including trophoblast specific analysis is presented in Figure 7.

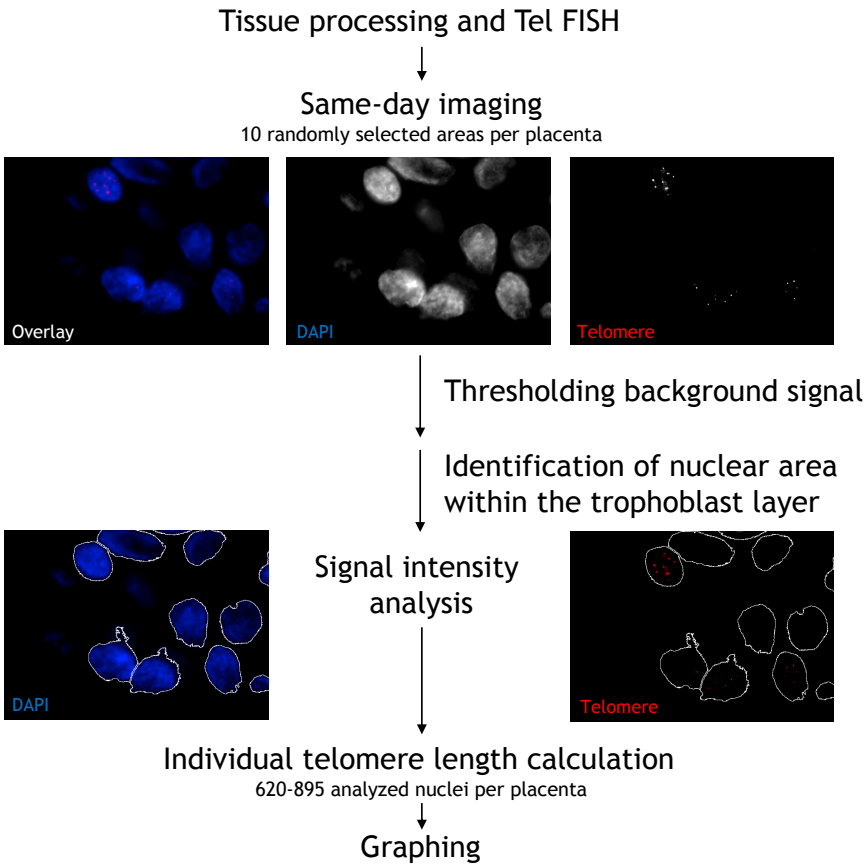

Figure 7: Image analysis workflow after telomere Q-FISH. After FT placenta tissue processing and telomere Q-FISH, color channels were separated and an automated threshold was set to binarize the image. After identification of nuclear area (DAPI staining) within the trophoblast layer, signal intensity was assessed in both channels specifically in the region of interest (defined by trophoblast nuclei mask). Finally, telomere length was assessed in individual trophoblast nuclei (620 – 895 nuclei per placenta) in the ten randomly selected areas of each FT placenta. Mean of all telomere/nuclei intensities per placenta was used for further statistics in a multivariate linear regression model.

Briefly, the DAPI (blue channel) and telomere (red channel) overlay image was color separated and a threshold was set on each individual channel to eliminate background signal. Trophoblast layer was identified manually while DAPI staining was used as a mask to identify telomeres in the region of interest. Next, telomere intensity was normalized on nuclei specific DAPI intensity in 620-895 nuclei per FT placenta.

3.17.Semi-quantitative image analysis

A mean of 1249 (range: 958 – 1755) cells were counted in ten randomly selected areas for each treatment. Results were given in percentage of apoptotic cells versus viable cells. To analyze TUNEL/Ki67 positive nuclei and γH2AX foci in trophoblast cells we developed a macro in ImageJ (National Institutes of Health, https://imagej.nih.gov/ij/). First, the color channels (green, red, blue) were separated and set a color threshold all three channels. In the red channel, we separated the trophoblast layer in the binary image through the selected threshold. As a result, the trophoblast can be used as a mask to extract the corresponding pixel in the blue (DAPI for DNA) fluorescent channels. In this way, only trophoblast nuclei remain for further processing. Next, I used trophoblast nuclei as a mask on the green channel eventually showing only the TUNEL positive trophoblast cells. To count all nuclei and the TUNEL positive nuclei, I performed a watershed step, which allowed me to separate close objects, and subsequently inverted the image.

3.18.Statistical analysis

Statistical analysis was performed with GraphPad Prism 8, IBM SPSS Statistics 25 and R 3.6.1 (Team, 2019). Normal distribution of the data was determined using the Shapiro-Wilk test. When data were normally distributed, statistical significance was determined using t-test and one-way ANOVA analysis. When appropriate, i.e., control versus treatment, paired t-test and one-way ANOVA with repeated measures were used. For non-parametric analysis, Mann Whitney or Friedman's test followed by Dunn's post hoc test was used. Correlations were determined by Pearson's correlation. A multivariate linear regression model with adjustments for gestational age was applied for gene expression, protein array and immunoblotting analysis. Here, gestational age was considered as a continuous variable and maternal BMI categorized into lean (BMI < 25 kg/m^2) and obese (BMI > 30 kg/m^2). Volcano plots were generated using the linear regression p-value (-log10) and a pre-calculated fold change (log2) and visualized using the R Bioconductor packages ggplot2 (Wickham, 2009), gridExtra (Baptiste Auguie, 2017) and plotly (Plotly Technologies Inc., 2015). $p < 0.05$ was considered statistically significant.

4. Results

Parts of this chapter are already published in adapted form in Hoch, Bachbauer *et al.* (2020). This study only includes FT placental villous tissue from non-smoking women verified by serum cotinine ELISA.

4.1. First trimester placental oxidative stress in obese pregnant women

To maintain cellular homeostasis and to counteract intrinsic and extrinsic challenges, cells have developed the capacity to set up a diversity of stress responses. These stress response pathways comprise of sensors, signaling cascades and repair modules (Xiao and Loscalzo, 2019)). In this study, we quantified placental oxidative stress, e.g., placental oxygen-induced DNA damage, levels of lipid peroxidation and protein tyrosine nitration, antioxidant responses and stress markers.

4.1.1. FT placental oxygen-induced DNA damage in obesity

To test specifically for oxygen-induced DNA damage, reflected by 8-OHdG oxidized bases, the alkaline COMET assay was modified. To this end, the DNA repair enzyme FPG – that converts damaged bases to breaks – was added to the standard COMET assay protocol. We used a multivariate linear regression model (MVLR) with adjustments for gestational age and tissue processing time.

Representative images of different stages of DNA fragmentation are shown in Figure 8A. No difference in DNA lesions resulting from reactive oxygen species in FT placental tissue from lean and obese women was observed (Figure 8B). As we could not find changes in oxidative stress-induced DNA damage in obese placental tissue, we further assessed whether the early placenta is susceptible to oxygen-induced DNA damage *per se*. We exposed FT tissue to an *in vitro* H_20_2 challenge prior to the alkaline COMET Assay. As shown in Figure 8C, FT placenta tissue from obese women is even more prone to oxygen-induced DNA damage after H_2O_2 treatment reflected by an increase in DNA fragmentation (72.6%, $p = 0.03$) compared to tissue from lean women.

To confirm unaltered levels of net FPG sensitive sites, we directly determined 8-OHdG concentrations in total placental tissue by ELISA. Concordantly, also 8-OHdG levels were not different in FT placental tissue from lean and obese women (Figure 9).

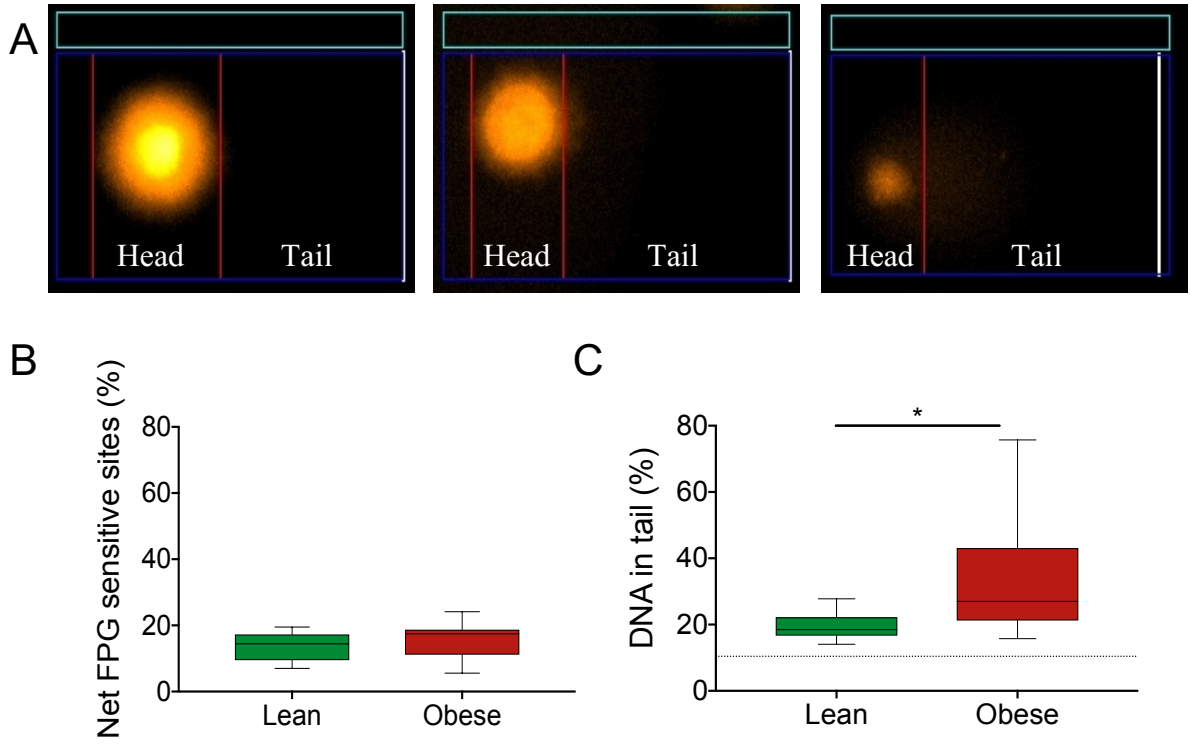

Figure 8: DNA damage in total FT tissue and *in vitro* H_2O_2 challenge. Alkaline COMET Assay with formamidopyrimidine DNA glycosylase (FPG) modification was used to determine oxygen-induced DNA stand breaks in total placental tissue from lean (BMI < 25, n = 10) and obese (BMI > 30, n = 14) women. (**A**) Representative images of different stages of DNA fragmentation. (**B**) Oxidative DNA damage was assessed by FPG COMET assay in total placental tissue from lean (BMI < 25, n =10) and obese (BMI > 30, n = 14) women. (**C**) Placental tissue was treated with H_2O_2 prior to alkaline COMET assay. Dotted line indicates basal DNA in tail in lean without H_2O_2 treatment (10.42%). Statistical analysis was performed using a multivariate linear regression analysis with BMI as categorical dependent variable and data was adjusted for gestational age and tissue processing time. Data shown as mean ± SD. n (lean / obese) = 10 / 14. Gestational week 5 – 12. *p < 0.05

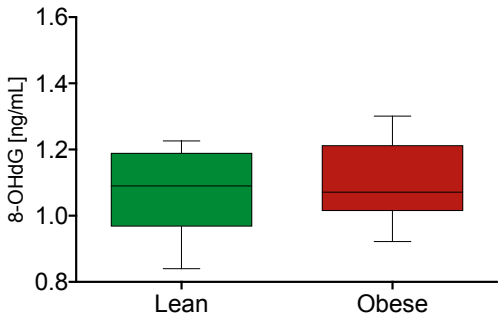

Figure 9: Levels 8-hydroxydeoxyguanosine (8-OHdG) in first trimester villous tissue. DNA was isolated from snap frozen first trimester placental tissues (gestational week 7) from lean (n=7) and obese (n=7) women. DNA was digested to nucleosides by incubating denatured DNA with 10 units of nuclease P1. Quantitative measurement of 8-OHdG by ELISA did not show changes in tissues from obese versus lean women. Unpaired student's t-test, all data mean ± SD. n (lean / obese) = 7 / 7. Gestational week 7

To further confirm the FPG COMET and 8-OHdG ELISA results in total placental tissue, we also assessed oxidative stress-induced DNA lesions in FT trophoblasts by 8-OHdG antibody staining in FFPE placental tissue from lean and obese women. Host specific IgG controls in appropriate dilutions served as negative control. After image segmentation and semi-automated cell layer identification, 8-OHdG positive cells were quantified *in situ* in the trophoblast layer and stromal cells (Figure 10A). The results show that FT trophoblast oxidative DNA damage, assessed by 8-OHdG IF staining, was not altered in FT trophoblast by maternal obesity (Figure 10B), which is in line with the FPG-COMET assay results in total tissue (Figure 8B).

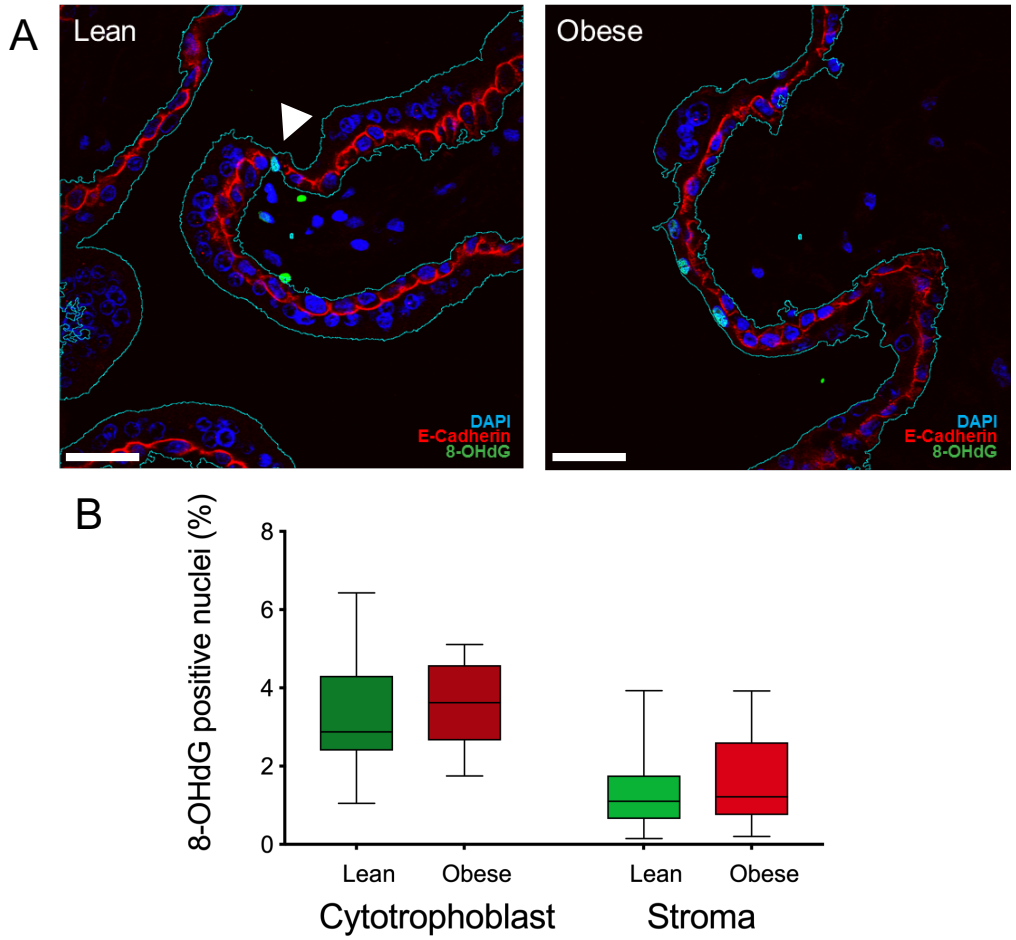

Figure 10: Detection of 8-hydroxy-desoyguanosine (8-OHdG) in paraffin embedded FT placenta sections. Fluorescence microscopic analysis of first trimester placental sections (FFPE, 3 µm) from lean and obese women. A mean of 924 trophoblast nuclei was analyzed in 10 randomly selected areas for each placental tissue and DNA damage was quantified using ImageJ. The trophoblast marker E-Cadherin was used as a mask during image segmentation and 8-OHdG (white arrow) quantification to demarcate trophoblasts from stromal cells. Statistical analysis was performed using a multivariate linear regression analysis with BMI as categorical dependent variable and data was adjusted for gestational age and tissue processing time. Results are presented as mean ± SD. n (lean / obese) = 12 / 12. n = 27. Gestational week 5 – 12

4.1.2. Lipid peroxidation and protein nitration

Next to the assessment of oxygen-induced DNA damage, we further assessed stress-associated modification of lipids and proteins by quantifying lipid peroxidation and protein nitration (Uchida, 2003).

Thus, we quantified 4-hydroxynonenal (4-HNE) and 3-nitrotyrosine (3-nitrotyr) modified proteins as markers for stress in the FT placenta by Western Blotting (Figure 11A, B). We used a MVLR model with data adjustments for gestational age and tissue processing time. No difference in 4-HNE and 3-nitrotyr adducts was observed in protein lysates of FT placental tissue from lean and obese women (Figure 11C, D).

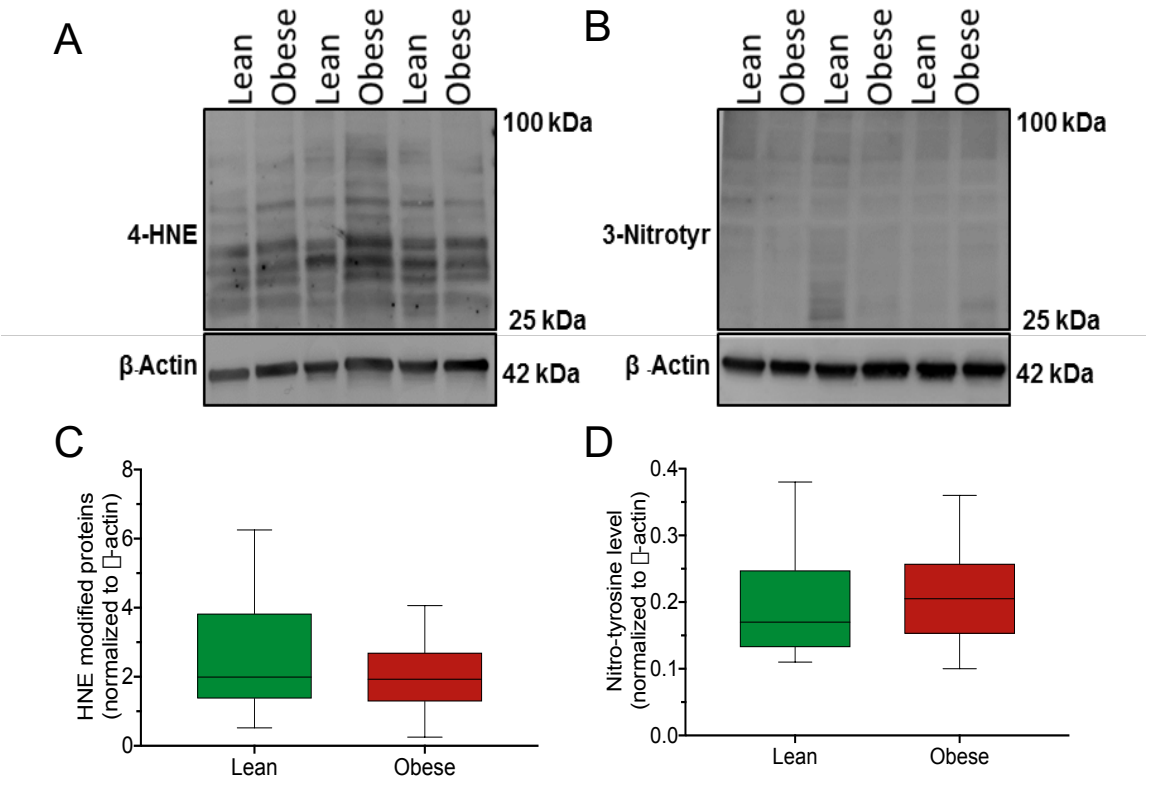

Figure 11: Lipid peroxidation adducts (4-HNE) and protein tyrosine nitration (3-nitrotyr) in first trimester placental tissue. 4-HNE and 3-nitrotyr protein levels were determined in first trimester placental tissue from lean (4-HNE: n = 19, 3-Nitrotyr: n =28) and obese (4-HNE: n = 33, 3-nitrotyr: n = 24) women by Western Blotting (**A**, **B**). Immunoblots for 4-HNE (**C**) and 3-nitrotyr (**D**) were quantified by densitometric analysis. β-actin was used for normalization as loading control. Statistical analysis was performed using a multivariate linear regression analysis with BMI as categorical dependent variable and data was adjusted for gestational age and tissue processing time. Results are presented as mean ± SD. n (lean / obese) = 19 - 28 / 33 - 24. Gestational week 5 – 12

To rule out a potential effect of gestational age (GA) that may have masked an effect of obesity, data analyses of lean and obese samples also included GA. GA did not affect levels of 4-HNE modified proteins (Figure 12A). However, we found a negative correlation between GA and 3-nitrotyr levels in obese FT placental tissue (Figure 12B).

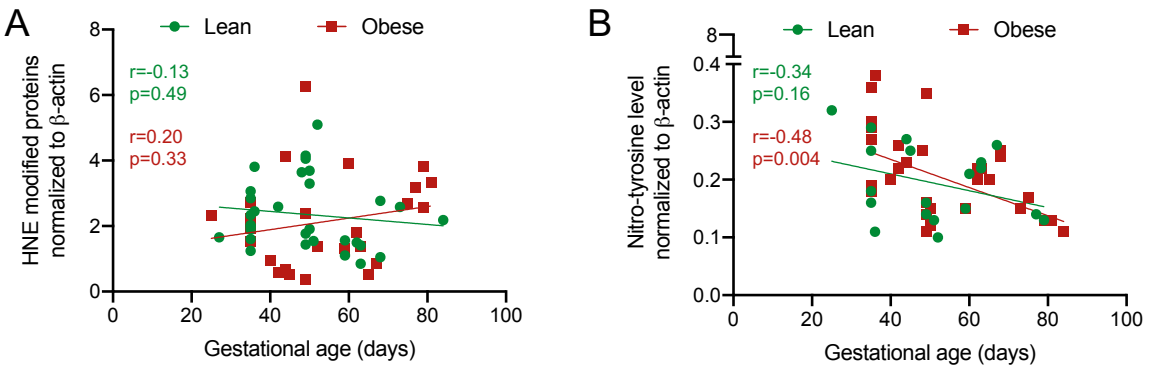

Figure 12: Correlation between gestational age and 4-HNE modified proteins or 3-nitrotyr levels in first trimester placental tissue stratified by BMI. Lean and obese tissue samples were stratified according to gestational age. 4-HNE modified proteins (**A**) and 3-nitrotyr (**B**) levels were determined by Western Blotting. Results were normalized to β -actin. Pearson correlation. n (lean / obese) = 19-28 / 33 -24. Gestational week 5 – 12

4.1.3. Placental antioxidants and stress markers

Due to a progressive increase in placental oxygen concentration after onset of maternal blood flow, a well-developed antioxidant defense system is particularly crucial for normal early placental development (Burton, Jauniaux and Charnock-Jones, 2010). Heme oxygenase 1 (HO-1) plays a protective role by heme degradation, as well as by regulating a wide variety of antioxidant, anti-inflammatory, and antiapoptotic pathways (Ndisang, 2010; Agarwal and Bolisetty, 2013). Therefore, we further studied antioxidant enzymes in FT placental tissue to test for potential effects of maternal obesity on the antioxidant signaling network in early pregnancy. If this were the case it could lead to reduced oxidative stress as reflected by lower *HO-1* expression in FT placentas from obese vs lean women.

Nanostring analysis of 18 enzymatic antioxidant defense enzymes showed that FT placental expression of superoxide dismutase 3 (SOD3, -30.2%, p = 0.02), microsomal glutathione S-transferase 3 (MGST3, -11.2%, p = 0.01), glutathione S-transferase P (GSTP1, -9.7%, p = 0.02), glutaredoxin (GLRX, -17.9%, p = 0.04) and thioredoxin reductase 1

(TXNRD1, -11.0%, p = 0.04) was decreased in obesity cases. All other antioxidant defense genes were unaltered (Table 4).

Table 4: Gene expression of antioxidant defense enzymes in first trimester tissue from lean and obese women.

		Unstandardized Coefficients		Standardized Coefficients		
Gene	Exposure	B	Std. Error	Beta	t	Sig.
MGST3	BMI (categorical)	-172.571	69.183	-0.241	-2.494	**0.014**
SOD3	BMI (categorical)	-25.233	10.415	-0.199	-2.423	**0.017**
GSTP1	BMI (categorical)	-48.850	20.811	-0.223	-2.347	**0.021**
GLRX	BMI (categorical)	-334.134	156.636	-0.215	-2.133	**0.035**
TXNRD1	BMI (categorical)	-37.285	18.253	-0.203	-2.043	**0.044**
PRDX3	BMI (categorical)	-104.245	61.033	-0.173	-1.708	0.091
SOD1	BMI (categorical)	-5.765	3.500	-0.157	-1.647	0.103
SOD2	BMI (categorical)	131.642	83.597	0.153	1.575	0.119
SRXN1	BMI (categorical)	-9.674	6.594	-0.145	-1.467	0.146
GPX3	BMI (categorical)	309.538	217.737	0.145	1.422	0.158
TXNRD2	BMI (categorical)	-6.852	5.151	-0.128	-1.330	0.187
GPX1	BMI (categorical)	-18.232	15.332	-0.113	-1.189	0.237
GPX2	BMI (categorical)	-4.367	3.687	-0.121	-1.185	0.239
MSH2	BMI (categorical)	-9.656	8.192	-0.121	-1.179	0.241
GSS	BMI (categorical)	-4.992	5.302	-0.092	-0.942	0.349
GSR	BMI (categorical)	13.764	21.807	0.056	0.631	0.529
TXN	BMI (categorical)	-16.333	33.926	-0.048	-0.481	0.631
NOX1	BMI (categorical)	-0.230	1.856	-0.013	-0.124	0.902

Dependent variable: Gene; Multivariate linear regression model; data adjusted for gestational age and tissue processing time. Significant genes are shown in bold. n = 101. Gestational week 5 – 12

One reason for some lower antioxidative defense systems could be the lack of need, i.e., reduced oxygen tension in the intervillous space in obesity. To test whether low oxygen is an underlying stimulus for reduced antioxidant defense enzymes in early pregnancies of obese womens, we cultured FT chorionic villous explants under physiologically low (2.5% O_2) and high (6.5% O_2) oxygen levels. Short term exposure of FT chorionic villous explants did not affect expression of *SOD3*. However, *MGST3* (14.1%, p = 0.02), *GLRX* (14.1%, p = 0.02) and *GSTP1* (17.8%, p = 0.02) gene expression was induced by raising oxygen tension to 6.5% O_2. Hence, placental antioxidative defense systems measured here rise with rising oxygen tension. This supports the notion that the lower antioxidative defense systems associated with maternal obesity are the results of lack of rising oxygen tension in the intervillous space.

Among all obesity affected antioxidant defense enzymes only *TXNRD1* (30.1%, p = 0.05) was downregulated by short term exposure to high oxygen levels *in vitro* (Figure 13). The specific consequence for placenta protection against oxidative stress is unclear.

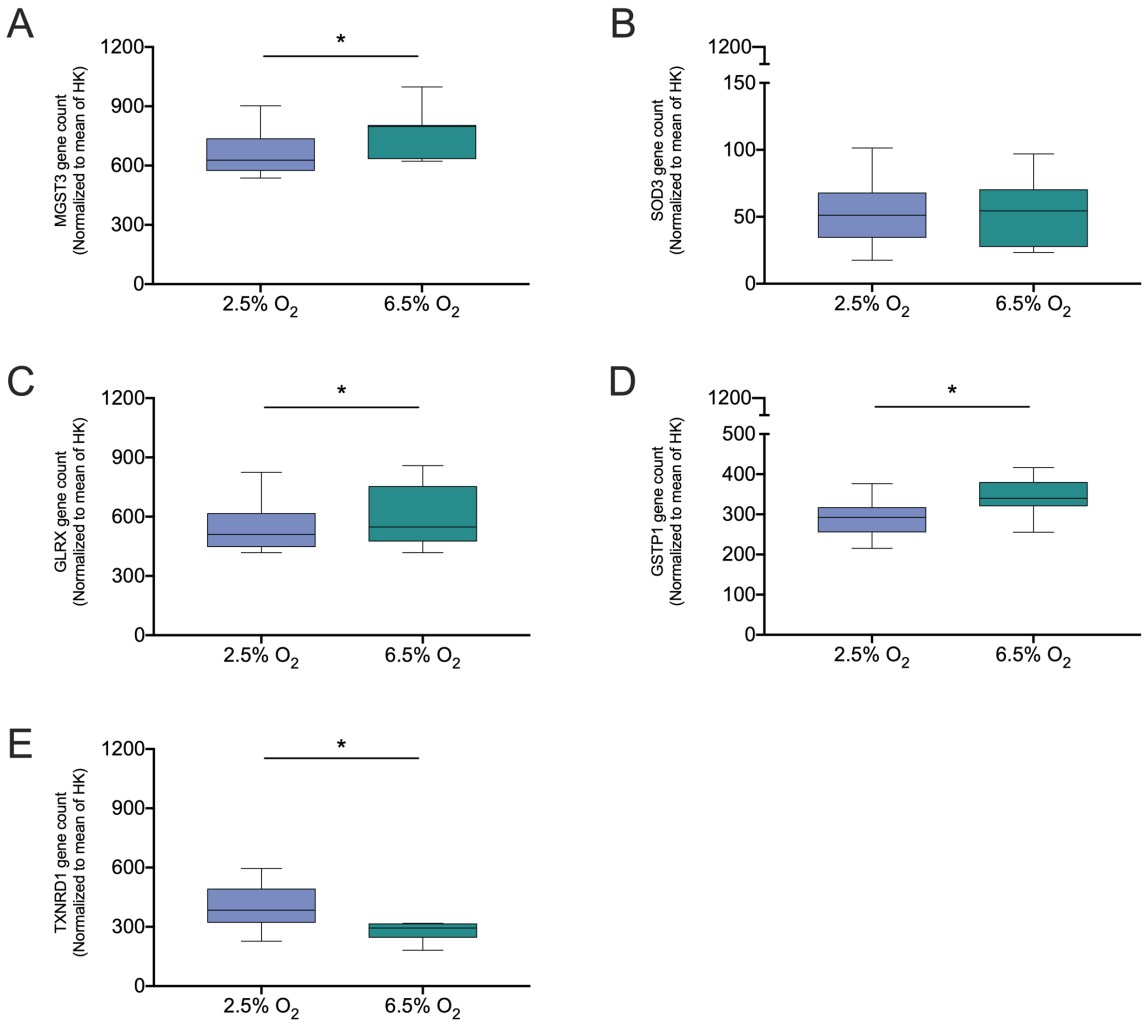

Figure 13: Effect of oxygen tension on antioxidants altered by obesity after short term exposure of first trimester placental chorionic villous explants to physiologically low (2.5% O_2) and high (6.5% O_2) oxygen levels. First trimester chorionic villous explants from different placental tissues (n = 8, gestational week 5 - 10) were cultured for 48 hours in triplicates at 2.5% O_2 or 65% O_2, respectively. Gene expression of *MGST1* (**A**), *SOD3* (**B**), *GLRX* (**C**), *GSTP1* (**D**) and *TXNRD1* (**E**) was analyzed by Nanostring gene expression analysis. Data was normalized to the mean of two different housekeeping (HK) genes WD repeat domain 45B (*WDR45L*) and TATA box binding protein (*TBP*). Statistical analysis included paired t-test or Wilcoxon matched-pairs signed rank test. * $p < 0.05$

So far, we found that maternal obesity downregulated placental expression of several genes involved in antioxidant defense in early pregnancy. Since these results were unexpected and only based on mRNA measurements, we further aimed to substantiate these findings. To this end we quantified the cytoprotective heat shock protein 70 (HSP70) and HO-1 protein by Western blotting (Figure 14A). Data was analyzed using a MVLR with BMI as categorical

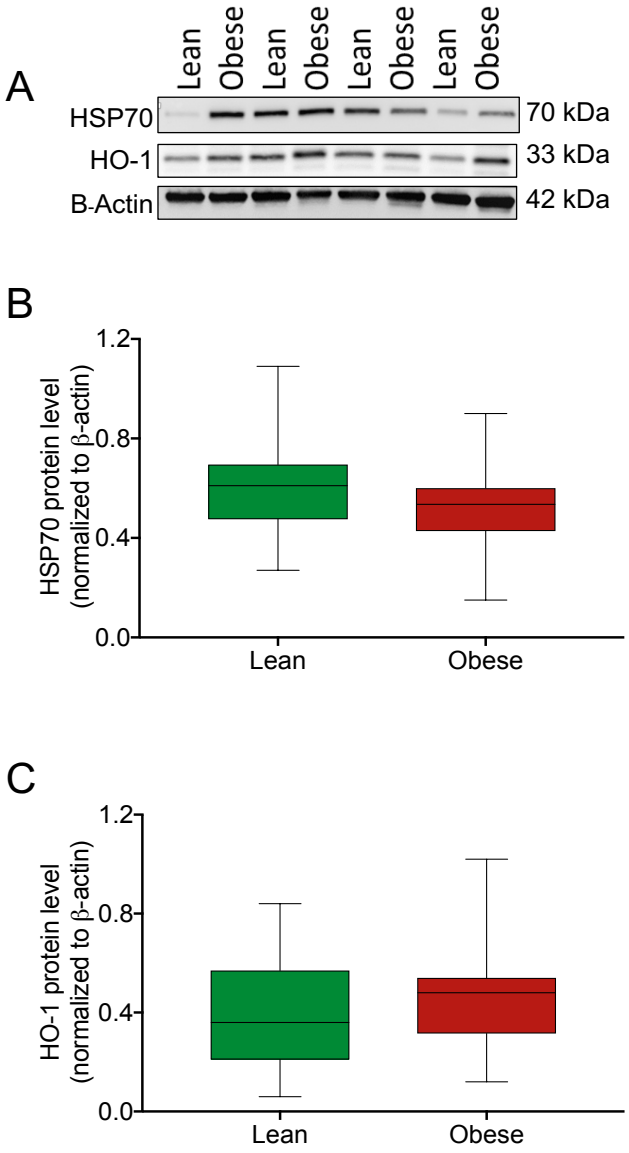

Figure 14. Heat shock protein 70 (HSP70) and hemeoxygenase 1 (HO-1) protein levels in lean and obese first trimester placental tissue. HSP70 and HO-1 protein levels were determined in first trimester placental tissue from lean and obese women by Western blotting (**A**). Immunoblots for HSP70 and HO-1 were quantified by densitometric analysis (**B**, **C**). β-actin was used for normalization as loading control. Statistical analysis was performed using a multivariate linear regression analysis with BMI as categorical dependent variable and data was adjusted for gestational age and tissue processing time. Results are presented as mean ± SD. n (lean / obese) = 21 / 36. Gestational week 5 – 12. *$p < 0.05$

variable and adjusted for gestational age and tissue processing time. The levels of both stress-induced proteins were not altered by maternal obesity in FT placental tissue (Figure 14B, C).

Furthermore, in univariate analysis, HSP70 and HO-1 protein levels did not correlate with gestational age in lean and obese FT placental tissue samples (Figure 15).

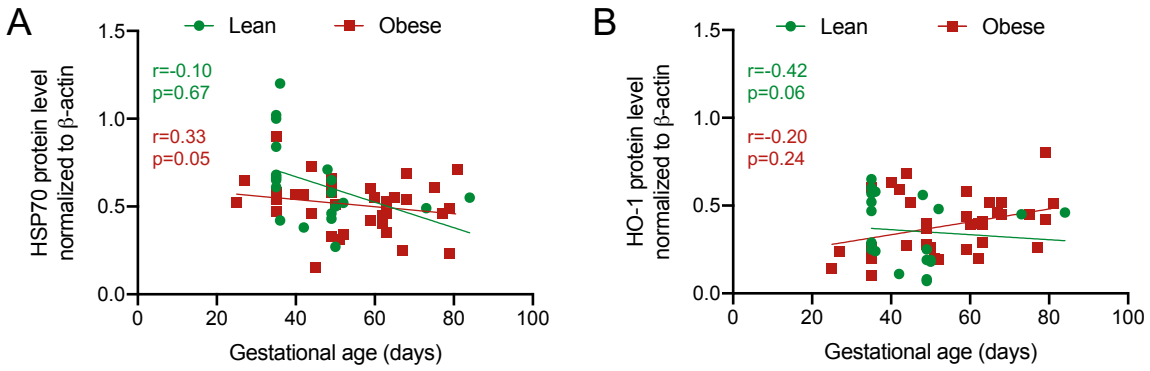

Figure 15: Correlation between gestational age, obesity and HSP70 or HO-1 protein levels in first trimester placental tissue. Lean and obese tissue samples were stratified according to gestational age. HSP70 (**A**) and HO-1 (**B**) protein levels were determined by Western Blotting. Results were normalized to β-actin. Pearson correlation. n (lean / obese) = 21/ 36. Gestational week 5 – 12

4.2. First trimester placental inflammatory response in obese pregnant women

In general, obesity is regarded as low-grade pro-inflammatory condition, associated with changes in the circulating cytokine profile (Fernandez, Gonzalez and Subirats, 1988). In late pregnancy, obesity-associated changes *in utero* directly affect placental inflammation as reflected by elevated cytokine production (Challier *et al.*, 2008). To interrogate if obesity associated placental inflammation is present already in the first trimester of pregnancy, we assessed changes in placental cytokine gene expression of lean and obese women using a qPCR panel. As expected, FT placentas from obese women showed elevated *IL6* (67.5%, p = 0.02) mRNA levels compared to lean samples. However, pro-inflammatory placental *IL1A* (-70.3%, p = 0.01) was lower in maternal obesity. Gene expression of placental *IL1B*, *IL18* and *TNF-α* was not affected by maternal obesity in gestational week 7 (Figure 16).

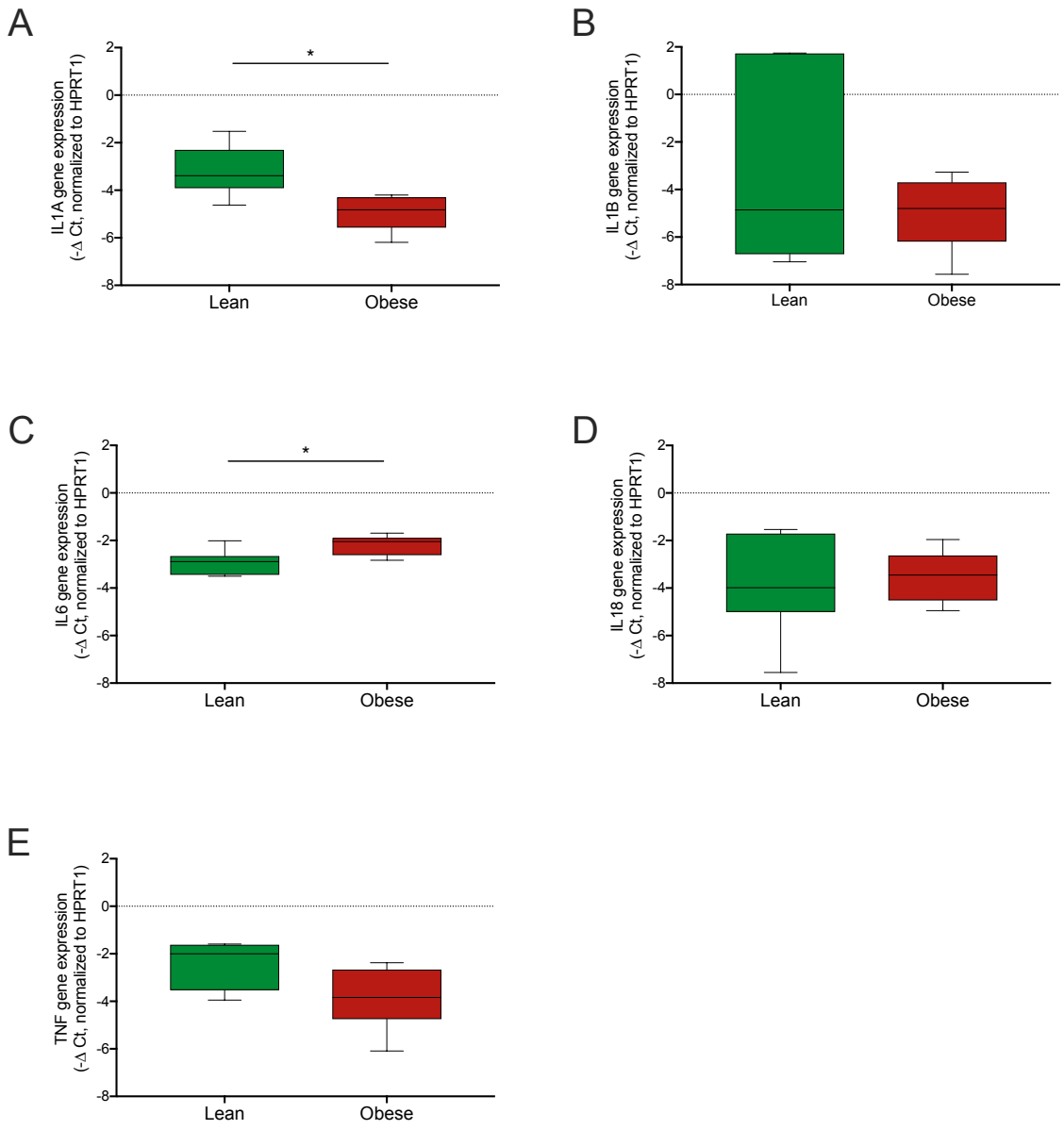

Figure 16: First trimester placental inflammatory response. First trimester (FT,gestational week 7) placental cytokine levels of lean and obese women were quantified by a qPCR panel. FT placental *IL1A* (**A**), *IL1B* (**B**), *IL6* (**C**), *IL18* (**D**) and *TNF-α* (**E**) gene expression was determined in placental tissue of lean and obese pregnant women. Gene expression data was normalized to the housekeeper hypoxanthine phosphoribosyltransferase 1 (*HPRT-1)*. Statistical analysis was performed using unpaired student's t-test or Wilcoxon rank-sum test. Results are presented as mean ± SD. Dashed line represents 0. n (lean / obese) = 7 / 7. *p < 0.05

4.3. First trimester placental stress signaling in obesity

To determine if maternal obesity activates classical stress response signaling pathways, we selected a set of prominent and well described signaling molecules and compared gene expression between lean and obese FT placentas. Therefore, we used the Nanostring gene expression approach to assess the pre-selected genes and used a MVLR, adjusted for gestational age and tissue processing time, to identify significant associations between maternal obesity and stress marker gene expression.

Among 11 targets that we surveyed, we found higher levels of Mitogen-Activated Protein Kinase Kinase Kinase 5 (*ASK1*) and Mitogen-Activated Protein Kinase 11 (*MAPK11*) and lower levels of Mitogen-Activated Protein Kinase Kinase Kinase 6 (*ASK2*), Mitogen-Activated Protein Kinase 13 (*MAPK13*), Mitogen-Activated Protein Kinase 12 (*MAPK12*) and Heme Oxygenase 1 (*HO-1*) in the samples from obese as compared to lean women. Interestingly, Hypoxia-inducible factor 1-alpha (*HIF1A)* was not affected by maternal obesity (Table 5).

Table 5: Gene expression of selected cellular stress markers.

		Unstandardized Coefficients		Standardized Coefficients		
Gene	Exposure	B	Std. Error	Beta	t	Sig.
ASK2	BMI (categorical)	-13.640	3.038	-0.402	-4.491	**0.000**
HO-1	BMI (categorical)	-90.374	35.139	-0.245	-2.572	**0.012**
MAPK13	BMI (categorical)	-20.798	8.486	-0.242	-2.451	**0.016**
MAPK12	BMI (categorical)	-5.623	2.299	-0.236	-2.445	**0.016**
JNK 1	BMI (categorical)	-6.176	2.774	-0.203	-2.226	**0.028**
ASK1	BMI (categorical)	24.924	12.105	0.192	2.059	**0.042**
MAPK11	BMI (categorical)	2.877	1.437	0.195	2.003	**0.048**
JNK2	BMI (categorical)	-8.604	8.264	-0.106	-1.041	0.300
Nrf2	BMI (categorical)	11.741	12.818	0.084	0.916	0.362
HIF1A	BMI (categorical)	17.727	24.575	0.071	0.721	0.472
MAPK14	BMI (categorical)	-1.640	21.696	-0.007	-0.076	0.940

Dependent variable: Gene; Multivariate linear regression model; data adjusted for gestational age and tissue processing time. Significant genes are shown in bold. n = 101. Gestational week 5 – 12

Since the genes with significantly altered expression levels in maternal obesity belong to the TNF-α signalling pathway, we treated FT chorionic villous explants with TNF-α (50 ng/mL) and assessed stress marker gene expression by Nanostring analysis using same target

genes. Villous tissue was cultured under physiological oxygen concentration (2.5% O_2) for 48 hours. Despite involvement in TNF-α signalling, only *MAPK11* and *MAPK12* were downregulated by TNF-α in first trimester chorionic villous explants by 46.7% and 42.2%, respectively. All other genes altered in FT total tissue with obesity were not affected by short term treatment with TNF-α *in vitro* (Figure 17).

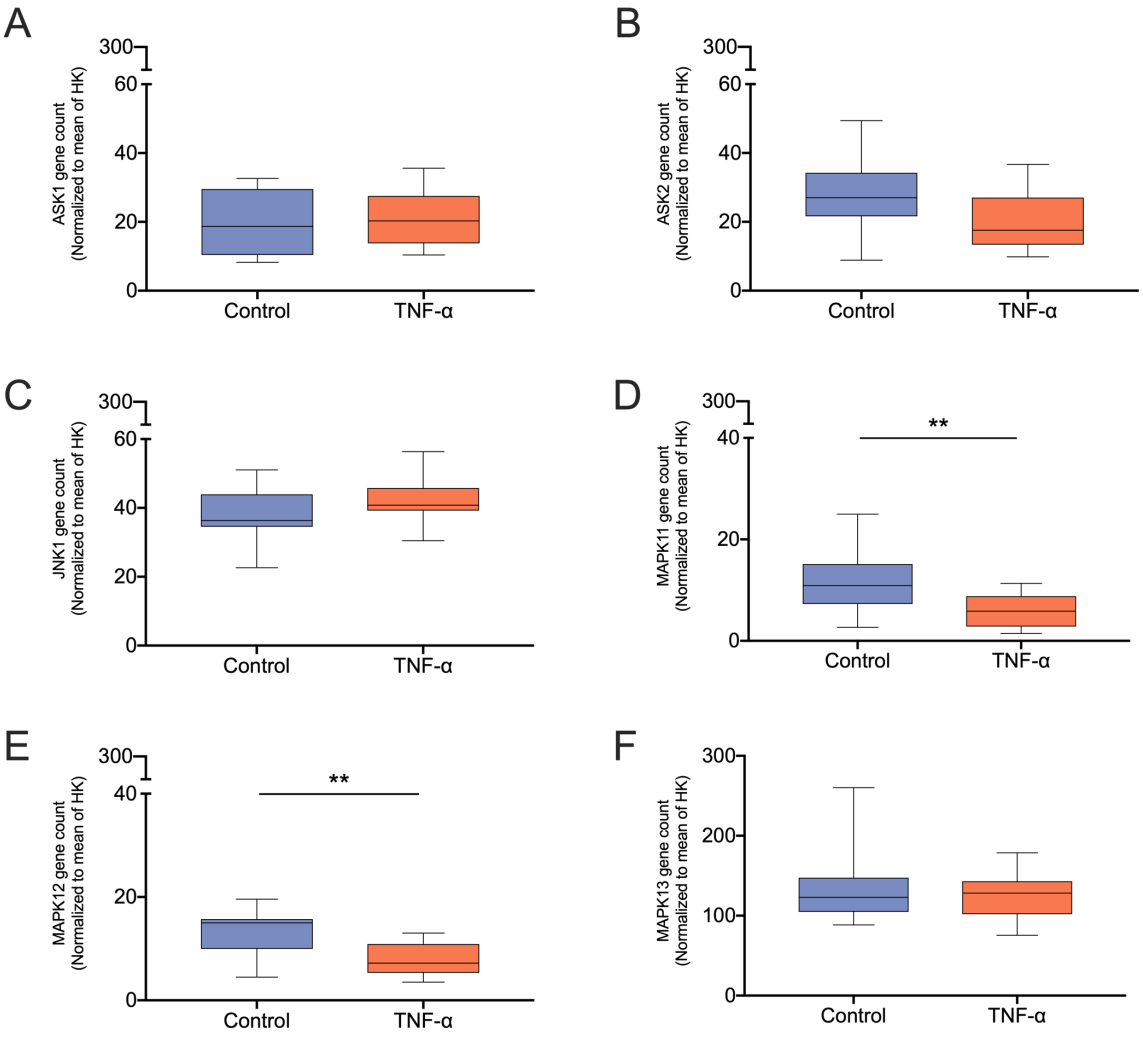

Figure 17: Assessment of obesity affected stress signaling genes after short term treatment with tumor necrosis factor α (TNF-α) in first trimester placental explants. First trimester chorionic villous explants from different placental tissues (n=8, gestational week 5-10) were cultured at 2.5% O_2 with TNF-α (50 ng/mL) for 48 hours in triplicates. Gene expression was analyzed by Nanostring gene expression analysis. Data was normalized to the mean of two different housekeeping (HK) genes WD repeat domain 45B (WDR45L) and TATA box binding protein (TBP). Only MAPK11 and MAPK12 were downregulated by TNF-α treatment. Statistical analysis included Paired t-test or Wilcoxon matched-pairs signed rank test. * $p < 0.05$, ** $p < 0.01$

4.4. First trimester placental DNA integrity in obese pregnant women

One major consequence of not only oxidative, but also nitrative or inflammatory stress is DNA damage, which includes DNA fragmentation, base modifications and strand breaks (Stein *et al.*, 2008; Kim *et al.*, 2009). Furthermore, cellular stress accelerates telomere shortening, which, in turn, correlates with DNA damage and contributes to DNA damage response (Barnes, Fouquerel and Opresko, 2019).

4.4.1. Placental DNA damage

To test whether an obesity-associated intrauterine environment affects genomic DNA damage in the FT placenta, we performed an alkaline COMET assay with a cell suspension from total tissue. Representative images of different stages of DNA fragmentation are shown in Figure 18A. Levels of DNA single- and double- strand breaks in FT placental tissue of obese women was increased by 2.6-fold compared to lean controls ($p < 0.001$, Figure 18B).

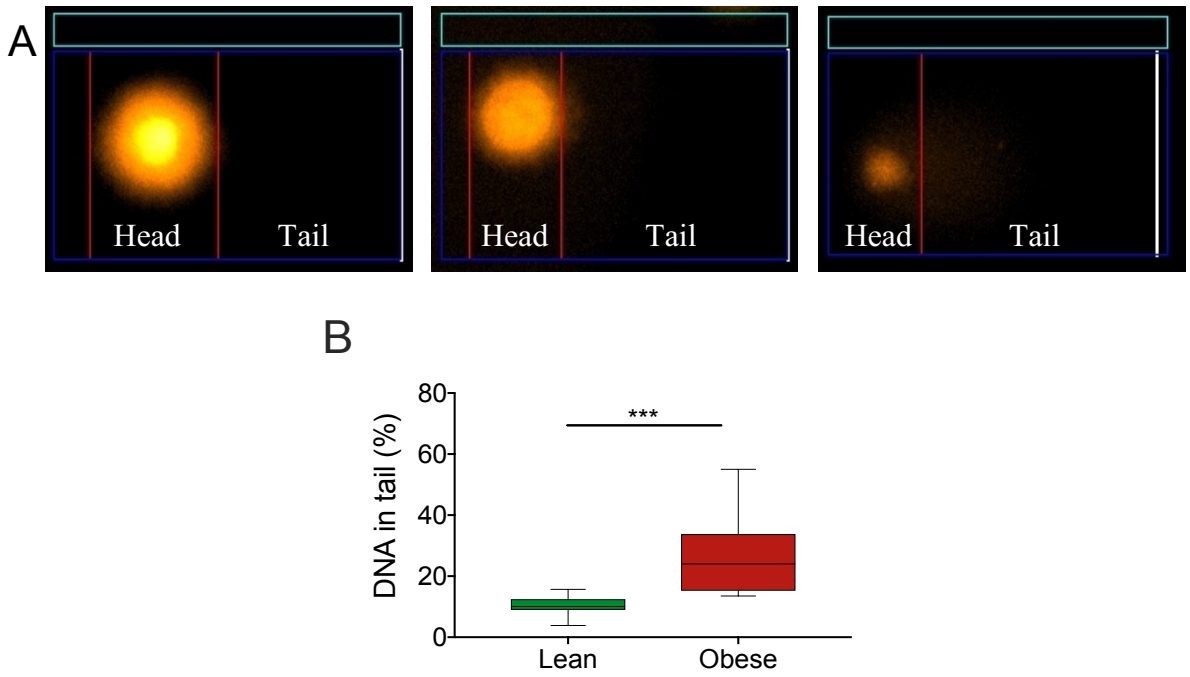

Figure 18: *In situ* DNA damage in total FT tissue. Alkaline COMET Assay was used to assess DNA stand breaks in total placental tissue from lean (BMI < 25, n = 10) and obese (BMI > 30, n = 14) women. (**A**) Representative images of different stages of DNA fragmentation. (**B**) First trimester placentas from obese mothers show a 2.6-fold increase in DNA strand breaks compared to lean. Statistical analysis was performed using a multivariate linear regression analysis with BMI as categorical dependent variable and data was adjusted for gestational age and tissue processing time. Data shown as mean ±SD. n (lean / obese) = 10 / 14. Gestational week 5 – 12. ***p < 0.001

As an early reaction to double-strand breaks, the histone variant H2AX becomes phosphorylated at serine 139 (γH2AX) by ATM, ATR or DNA-PK. Therefore, genomic DNA damage specifically in trophoblasts was semi-quantified by staining using antibodies against γH2AX (DNA strand breaks) and E-Cadherin (trophoblast marker). FT placental tissue exposed to X-Ray was used as positive control and host specific IgG controls in appropriate dilutions served as negative control. After image segmentation and semi-automated cell layer identification, γH2AX foci were quantified *in situ* specifically in the trophoblasts (Figure 19A).

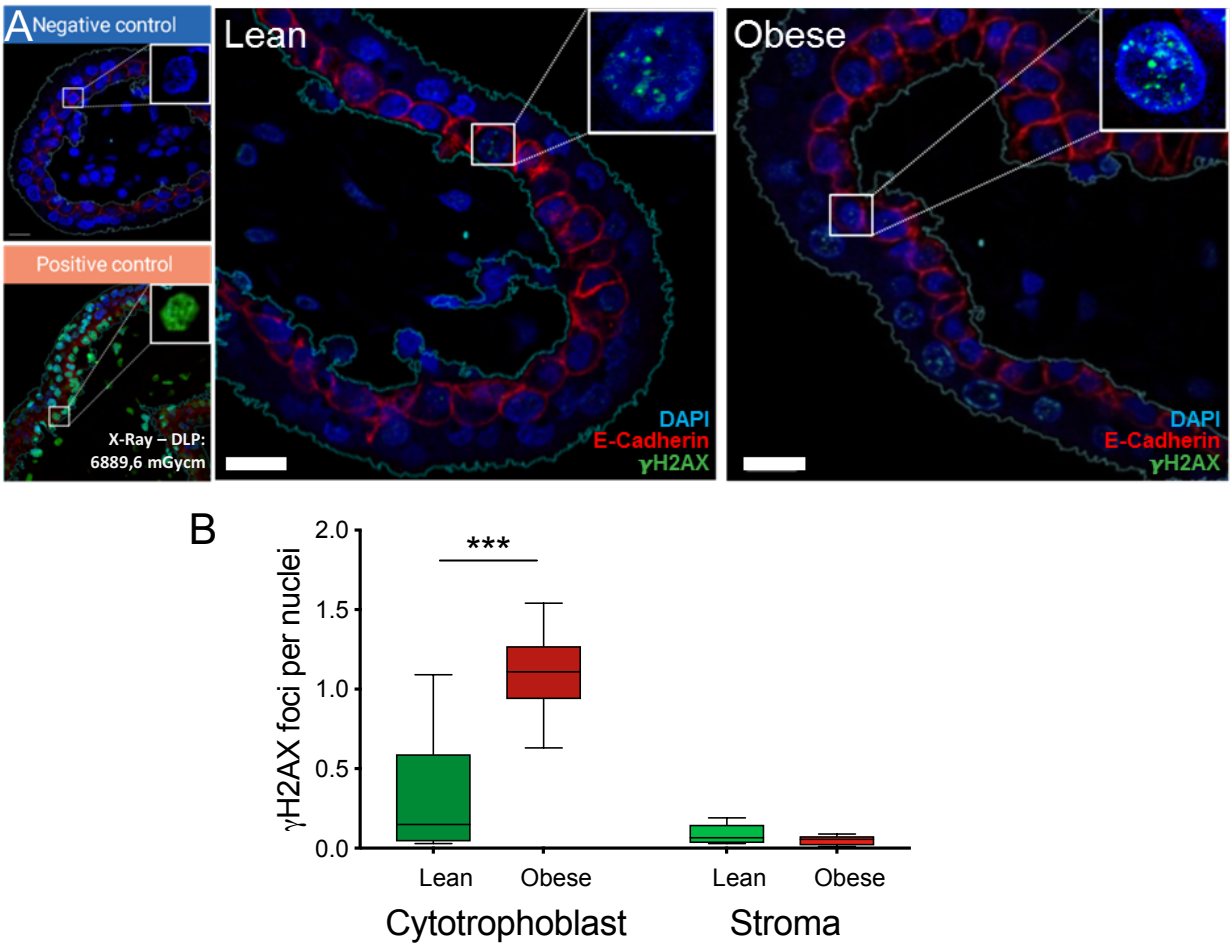

Figure 19: *In situ* DNA damage analysis in FT villous trophoblasts and stromal cells. (**A**) Fluorescence microscopic analysis of first trimester placental sections (FFPE, 3 µm) from lean and obese women. A mean of 1375 trophoblast nuclei was analyzed in 10 randomly selected areas for each placental tissue and DNA damage was quantified using ImageJ. The trophoblast marker E-Cadherin was used as a mask during image segmentation and γH2AX quantification to demarcate trophoblasts from stromal cells. (**B**) Trophoblasts from obese women showed an increase in DNA damage sites (6.9-fold, p=0.001) while stromal cells remain unaffected. Statistical analysis was performed using a multivariate linear regression analysis with BMI as categorical dependent variable and data was adjusted for gestational age and tissue processing time. Results are presented as mean ± SD. n (lean / obese) = 5 / 7. Gestational week 5 – 12. ***p < 0.001

Trophoblasts from obese women showed an increase in DNA damage sites (6.9-fold, p=0.001), while non-trophoblast cells representing stromal cells remained unaffected (Figure 19B). This suggest that obesity accompanied changes *in utero* affect only the trophoblast as the cell compartment in direct contact with maternal blood.

4.4.2. Telomere length in total FT tissue and villous trophoblasts

In addition to genomic DNA damage, the intrauterine environment may also affect telomere length (Gardner *et al.*, 2005). In general, critically short telomeres lead to genomic instability that triggers the DNA damage response. Telomere shortening was assessed by a qPCR-based protocol and quantitative fluorescence *in situ* hybridization in total tissue lysates, of laser capture-microdissected FT trophoblasts and tissue sections, respectively. The results were also analyzed in relation to maternal metabolic factors, such as serum leptin, glucose, C-peptide and maternal insulin sensitivity. These could be quantified, because maternal blood was available for these samples.

Total placenta telomere length was assessed using an adapted qPCR protocol by calculating the ratio (T/S) of telomere repeat length (T) to β-globin (BG), a single copy gene (S). Statistical analysis was performed using a MVLR with adjustment for gestational age and tissue processing time. First, we used DNA isolated from total FT placental villous tissue. Here, neither maternal BMI nor maternal metabolic parameters such as C-peptide and insulin sensitivity were associated with placental telomere length (Table 6).

Table 6: Relative telomere length in first trimester placental tissue.

	Unstandardized Coefficients		Standardized Coefficients	T	Sig.
	B	Std. Error	Beta		
Maternal BMI (continuous, Kg/m^2)	-1.173E-03	0.002	-0.104	-0.505	0.618
Maternal BMI (categorical, Kg/m^2)	-0.021	0.029	-0.141	-0.714	0.482
Maternal serum leptin (ng/mL)	-0.003	0.003	-0.263	-1.095	0.291
Maternal serum glucose (mg/dL)*	-0.002	0.002	-0.303	-1.176	0.258
C-peptide (pmol/L)	4.820E-05	0.000	0.160	0.652	0.524
Insulin sensitivity (HOMA)*	-0.013	0.058	-0.056	-0.220	0.829

Dependent variable: Relative telomere length; Multivariate linear regression model; data adjusted for gestational age and tissue processing time. 2 BMI categories: lean (BMI < 25) / obese (BMI > 30). n = 29. Gestational week 5 – 12. *Glucose values are corrected for blood processing time

As villous trophoblasts are in direct contact with maternal blood, changes in the intrauterine environment might predominately affect the trophoblast compartment.

Non-trophoblast cells may have 'diluted' a trophoblast-specific effect in above analyses of total placental tissue. Therefore, we performed laser-capture microdissection on FFPE tissue sections to specifically separate the trophoblast layer from the surrounding tissue. After trophoblast DNA isolation and quality control, the same set up and qPCR protocol was used as in the total tissue telomere analysis. Strikingly, in multivariate analysis trophoblast specific telomere length analysis showed shorter telomeres with increased serum C-peptide levels (r = -0.51, p = 0.02) and decreased insulin sensitivity (r = 0.66, p = 0.01), while telomere length was not associated with maternal BMI or any other metabolite measured (Table 7).

Table 7: Relative telomere length of laser-capture microdissected first trimester trophoblasts.

	Unstandardized Coefficients		Standardized Coefficients	T	Sig.
	B	Std. Error	Beta		
Maternal BMI (continuous, Kg/m^2)	9.105E-05	0.001	0.018	0.077	0.939
Maternal BMI (categorical, Kg/m^2)	0.009	0.013	0.150	0.709	0.486
Maternal serum leptin (ng/mL)	0.000	0.001	0.084	0.343	0.736
Maternal serum glucose (mg/dL)*	0.000	0.001	-0.083	-0.296	0.771
C-peptide (pmol/L)	-8.011E-05	0.000	-0.511	-2.548	**0.020**
Insulin sensitivity (HOMA)*	0.047	0.016	0.598	2.888	**0.013**

Dependent variable: Relative telomere length; Multivariate linear regression model; data adjusted for gestational age and tissue processing time. 2 BMI categories: lean / obese. n = 27. Gestational week 5 – 12. Significant results shown in bold. *Glucose values are corrected for blood processing time

Similar results were obtained using univariate correlation analysis between relative telomere length and C-peptide or insulin sensitivity, respectively (Figure 20).

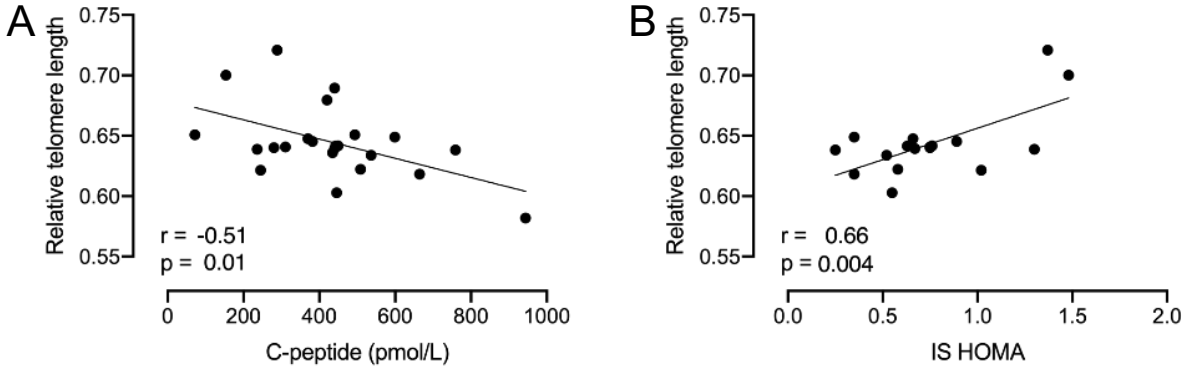

Figure 20: Relative telomere length of laser-capture microdissected first trimester trophoblasts and maternal C-peptide and IS HOMA. Laser-capture microdissection was performed to specifically obtain trophoblast DNA from lean (n = 13) and obese (n = 17) women. Subsequent telomere qPCR analysis was performed according to an adjusted protocol and raw data was normalized to the single copy gene (β-globin). Telomere length was correlated with maternal C-peptide (**A**) levels and IS HOMA (**B**). n = 27. Gestational week 5 – 12

Trophoblast telomere qPCR results were confirmed using quantitative fluorescence *in situ* hybridization (Q-FISH) on FT tissue sections (Figure 21A). Here, a Cy5-telomere probe ((CCCTAA)-peptide nucleic acid (PNA) probe) was used and data analyzed using multivariate analysis adjusted for gestational age and processing time. Quantified fluorescence intensity was normalized to DAPI intensity in each image. Maternal obesity was associated with shorter telomeres (-58.6%, $p < 0.001$, Figure 21B). In line with the qPCR findings, (Figure 20), trophoblast telomeres are shorter with high maternal C-peptide levels ($r = -0.58$, $p < 0.001$, Figure 21C) and low insulin sensitivity ($r = 0.75$, $p < 0.001$, Figure 21D).

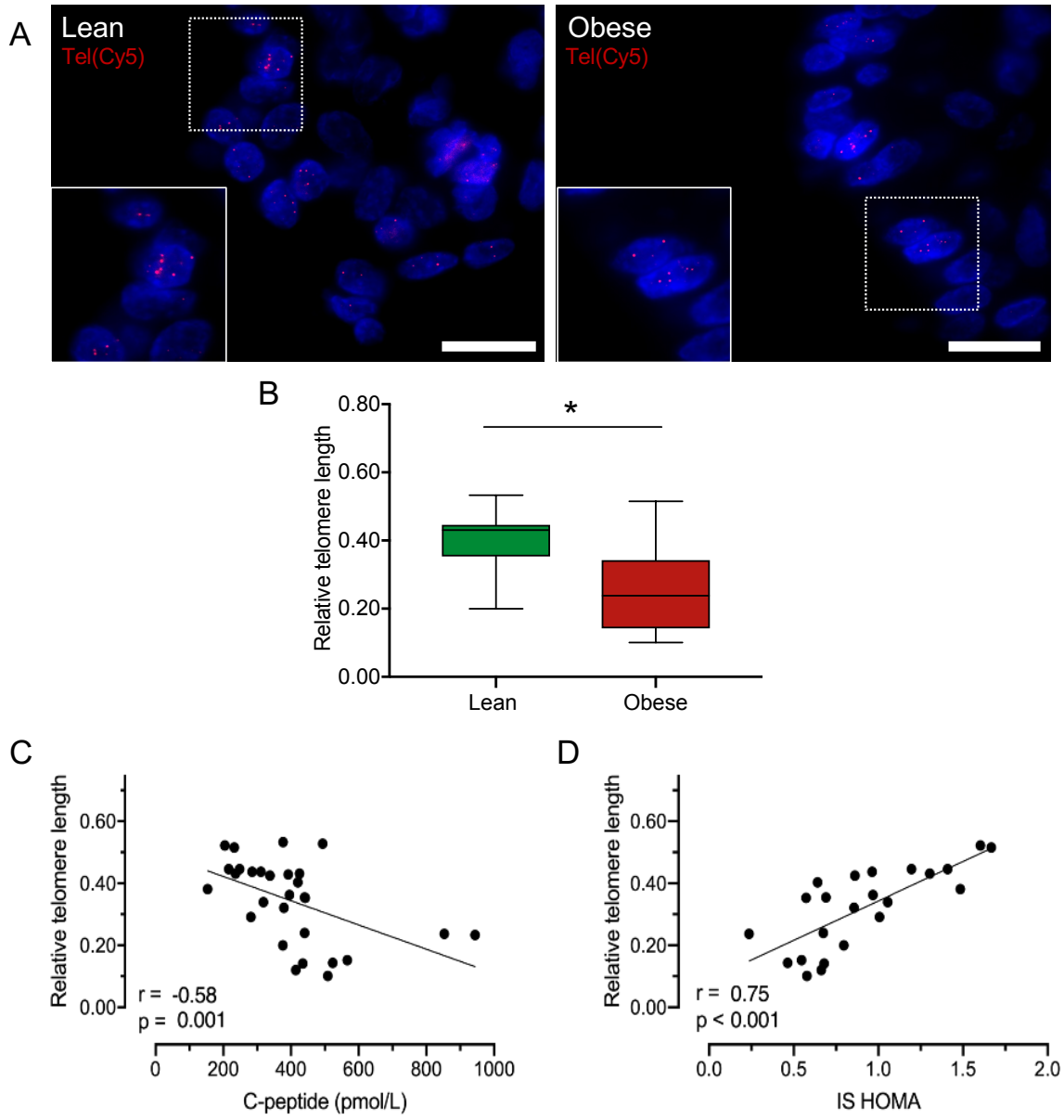

Figure 21: Trophoblast telomere *in situ* hybridization. (**A**) Representative images of telomere Q-FISH signals in FT placenta villous tissue from lean and obese women. Hybridization was performed on sectioned (3 um) and

deparaffinized FFPE placental tissue after antigen retrieval. Red/green colors indicate telomeres (Cy5-telomere probe ((CCCTAA)$_3$ PNA probe) and nuclei were counterstained with DAPI. Ten randomly selected areas within every placental tissue section were captured by a single blinded investigator within 24 hours after hybridization. Telomere signals are evident in the nuclei while signal intensity was lower in obese FT placental tissue specimens (**A**). Quantified telomere signals are normalized to DAPI intensity in each image and analyzed according to maternal BMI (**B**), serum C-peptide levels (**C**) and maternal insulin sensitivity calculated as IS HOMA index (r = (**D**). Categorical results are presented as mean ± SD. Statistical analysis was performed using a multivariate linear regression analysis with BMI as categorical dependent variable or continuous C-peptide/IS HOMA and data was adjusted for gestational age and tissue processing time. *p < 0.05. n = 32. Gestational week 5 – 12

4.5. First trimester placental response to DNA damage in obesity

To preserve DNA integrity, a complex cellular protein network, described as DNA damage response (DDR), is activated to repair single- and double strand breaks (Barzilai and Yamamoto, 2004). After damage sensing, the actual repair mechanism depends on the type of damage. The most prominent response pathways for single stranded DNA damage are base excision repair (BER), nucleotide excision repair (NER) and DNA mismatch repair (MMR). Double strand break repair signaling includes non-homologous end joining (NHEJ) and homologous recombination (HR). One of the first steps in response to DNA damage is cell cycle arrest to allow DNA repair (Barzilai and Yamamoto, 2004). This study determines DNA damage repair and placental cell cycle changes as potential downstream consequences of obesity-associated DNA damage.

4.5.1. Placental DNA damage repair

Placental expression of DNA damage related genes was analyzed in human FT placental tissue from lean (BM < 25, n = 7) and obese (BMI ≥ 30, n = 7) women using a qPCR array including 187 DNA damage related genes.

Already in gestational week 7, maternal obesity upregulated 8 out of 187 analyzed genes (4.3%) while downregulated genes did not reach significance. The DNA strand break sensors H2A Histone Family Member X (*H2AFX*) and p53 binding protein (*TP53BP1*) by 2.3-fold (p = 0.05) and 41% (p = 0.05), respectively. Furthermore, obese placental tissue from obese women showed an increase in *ATRIP* (80%, p = 0.01), *APEX1* (85%, p = 0.05), *PCNA* (97%, p = 0.09) and *TP53* (42%, p = 0.09) gene expression compared to placentas from lean women. Expression levels of *RAD52* (82%, p = 0.01) and XPA (65%, p = 0.03) were significantly increased in the obese group, both important factors in DNA double-strand break repair and

NER, respectively. Gene expression of bloom syndrome RecQ like helicase (*BLM*), participating in DNA repair and replication, is higher by 2.6-fold (p = 0.04) in obesity (Table 8).

Table 8: DNA damage repair related gene expression in gestational week 7.

Gene	Gene name	FC	Sig.
ATRIP	ATR Interacting Protein	1.80	**0.01**
HDAC1	Histone deacetylase 1	1.96	**0.01**
RAD52	RAD52 Homolog, DNA Repair Protein	1.82	**0.01**
XPA	DNA Damage Recognition and Repair Factor	1.65	**0.03**
BLM	Bloom Syndrome RecQ Like Helicase	2.55	**0.04**
TP53BP1	p53 binding protein	1.41	**0.05**
H2AFX	H2A Histone Family Member X	2.30	**0.05**
APEX1	Apurinic/Apyrimidinic Endodeoxyribonuclease 1	1.85	**0.05**
BRCA1	BRCA1, DNA Repair Associated	2.15	0.06
PCNA	Proliferating Cell Nuclear Antigen	1.98	0.06
PARP1	Poly(ADP-Ribose) Polymerase 1	1.97	0.09
TP53	Tumor Protein P53	1.42	0.09
CHAF1A	Chromatin Assembly Factor 1 Subunit A	2.12	0.09

PCR Panel, FC: Fold change. Significant results in bold. Gestational week 7

In summary, various genes involved in central DNA repair processes, such as DNA damage sensing, DNA double-strand break repair, NER and BER are dysregulated by maternal obesity already in gestational week 7.

These analyses resulting in pilot data raised the question if the effects of maternal obesity can be confirmed in a larger cohort by an independent method. Moreover, since the pilot data were obtained at one defined gestational week in the first trimester, we aimed to assess if these effects of maternal obesity on early placental DNA damage response can also be found at other weeks in the first trimester. Therefore, we performed Nanostring gene expression analysis for 29 prominent DNA damage repair signaling genes in a larger cohort (n = 101) covering a gestational age range from week 5 - 12 and used a MVLR model with BMI as a categorical variable adjusted for gestational age and tissue processing time to analyze gene expression data.

Surprisingly, 22 out of 29 analyzed genes were not affected by maternal obesity. Figure 22 shows a heatmap of all DNA damage repair signaling genes assessed in this study. Only histone deacetylase 8 (*HDAC8*) gene expression was upregulated by 14.53% (p = 0.001) in FT placental tissue of obese women. However, *HDAC1* (-19.7%, p < 0.001), *FEN1* (-19.4%, p = 0.01), *Ku70* (-9.7%, p = 0.007), *PARP1* (-20.6%, p = 0.002) and *BLM* (-37.0%, p < 0.001) were downregulated by maternal obesity (Figure 22, App. Figure 1). We further performed a sub-analysis, assessing Nanostring DNA damage repair genes only in gestational week 7. Similar to the analysis including samples from gestational weeks 5 - 12, *BML, POLG* and *PARP1*were

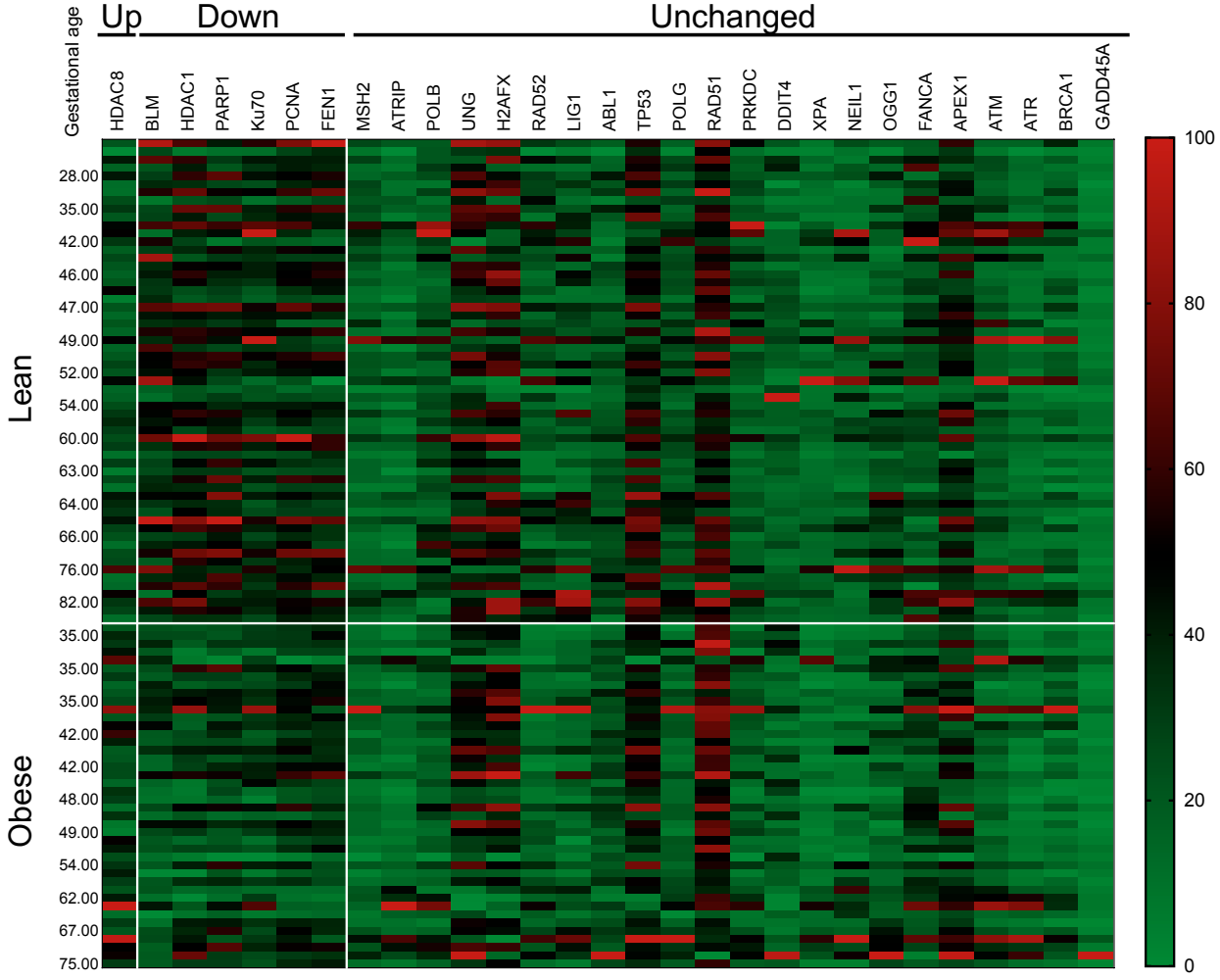

Figure 22: DNA damage repair signalling in early placental villous tissue. Gene expression was determined in first trimester placental tissue from lean (n = 59) and obese (n = 41) women by Nanostring analysis. Gene counts were normalized to the mean of two different housekeeping (HK) genes WD repeat domain 45B (*WDR45L*) and TATA box binding protein (*TBP*). Statistical analysis was performed using a multivariate linear regression analysis with BMI as categorical dependent variable adjusted for gestational age and tissue processing time, n=101. Gestational week 5 -12

downregulated in FT placentas from obese women (App. Table 2). Samples used for the Nanostring analysis differ from those used in the DNA damage specific PCR panel which may explain the differences in obesity effects.

To assess specific DNA damage repair signaling pathways, we grouped the Nanostring gene expression data accordingly (Table 6). Maternal obesity affected gene expression of key transducers not only in single stand break repair (BER), but also in double stand break repair, e.g., non-homologous end joining (NHEJ) and homologous recombination (HR, Table 9).

To further investigate whether a physiological change in oxygen levels or inflammation-associated TNF-α triggers changes of obesity-associated DNA damage repair genes, we used FT chorionic villous explants *in vitro* and cultured them for 24 hours at 2.5% or 6.5% oxygen in culture medium, or treated the tissue at 2.5% oxygen with TNF-α (50 ng/mL). This experiment was followed by Nanostring gene analysis. Physiologically high oxygen levels (6.5%) induced gene expression of *HDAC1* (25.0%, p = 0.03), and *PCNA* (30.0%, p = 0.03), while all other obesity induced DNA damage repair related genes (*HDAC8, BLM, PARP1, Ku70* and *FEN1*) remained unaffected (Figure 23). FT chorionic villous explants treated *in vitro* with TNF-α show a significant downregulation of *HDAC8* (-24.0%, p = 0.04), *BLM* (-46.9%, p = 0.02), *PARP1* (-49.3%, p = 0.008), *PCNA* (-38.0%, p = 0.008) and *FEN1* (-25.5%, p = 0.04) genes, but did not affect *HDAC1* and *Ku70* gene expression (Figure 24).

The ATM/ATR signaling pathway is a central regulatory network in response to different types of DNA lesions with consequences for expression of genes involved in damage repair, cell cycle arrest and apoptosis. Therefore, we specifically assessed AMT, ATR and AMT/ATR substrate phosphorylation (serine or threonine in the S*/T*Q motif) (Cimprich and Cortez, 2008) in FT placental tissue of lean and obese women by Western blotting. Representative blots are shown in Figure 25A. Densitometry results were statistically analyzed using a MVLR model adjusted for gestational age and tissue processing time with BMI as a continuous (Figure 25B, D, F) or categorical variable (Figure 25C, E, G), respectively. High maternal BMI in the first trimester of pregnancy was significantly associated with increased levels of placental ATR (B = 0.03, p < 0.001) and ATM (B = 0.003, p < 0.001) (Figure 25B and D).

Table 9: Genes related to DNA damage repair (DDR) pathways.

Gene	Gene name	DDR pathway	Unstandardized Coefficients		Standardized Coefficients		
			B	Std. Error	Beta	t	Sig.
Double strand break repair							
ATM	ATM serine/threonine kinase	NHEJ	-0.25	2.10	-0.01	-0.12	0.91
H2AFX	H2A histone family member X		-1.80	1.42	-0.13	-1.27	0.21
PRKDC	protein kinase, DNA-activated, catalytic subunit		-3.60	5.93	-0.06	-0.61	0.55
Ku70	**ATP-dependent DNA helicase 2 subunit**		-9.75	3.50	-0.28	-2.78	**0.01**
BRCA1	BRCA1 DNA repair associated	HR	-0.03	0.42	-0.01	-0.06	0.95
RAD52	RAD52 homolog, DNA repair protein		-0.66	0.54	-0.13	-1.22	0.22
ABL1	ABL proto-oncogene 1		1.19	1.13	0.11	1.05	0.29
BLM	**BLM RecQ like helicase**		-0.97	0.21	-0.43	-4.54	**<0.001**
FANCA	FA complementation group 1		0.14	0.74	0.02	0.19	0.85
GADD45A	Growth arrest and DNA damage inducible alpha		-0.14	2.35	-0.01	-0.06	0.95
RAD51	RAD51 recombinase		0.24	0.38	0.07	0.64	0.52
TP53	tumor protein p53		-0.44	0.46	-0.10	-0.96	0.34
CHEK2	Checkpoint kinase 2		9.50	10.29	0.09	0.92	0.36
Single strand break repair							
ATR	ATM- and PI-3K–like essential kinase		0.21	1.92	0.01	0.11	0.91
NEIL1	Nei like DNA glycosylase 1	BER	-0.06	0.21	-0.03	-0.31	0.75
OGG1	8-oxoG opposite C		0.08	0.34	0.02	0.25	0.81
APEX1	AP endonuclease		-0.13	0.90	-0.01	-0.14	0.89
FEN1	**Flap structure-specific endonuclease 1**		-2.36	0.92	-0.26	-2.57	**0.01**
UNG	Uracil DNA glycosylase		-1.03	0.81	-0.13	-1.28	0.20
PCNA	**Proliferating cell nuclear antigen**		-3.53	1.28	-0.27	-2.76	**0.01**
POLG	DNA polymerase gamma, Catalytic subunit		-1.18	1.23	-0.10	-0.95	0.34
POLB	DNA polymerase beta		-0.92	0.61	-0.15	-1.50	0.14
XPA	DNA damage recognition and repair factor	NER	-0.36	0.84	-0.04	-0.42	0.67
MSH2	MutS Homolog 2	MMR	-1.40	0.83	-0.17	-1.68	0.10
CHEK1	Checkpoint kinase 1		-6.96	4.19	-0.17	-1.66	0.10
Damage repair associated genes							
HDAC1	Histone deacetylase 1		-6.38	1.69	-0.37	-3.77	**<0.001**
HDAC8	Histone deacetylase 8		2.07	0.86	0.24	2.40	**0.02**
PARP1	Poly(ADP-ribose) polymerase 1		-12.67	4.49	-0.27	-2.82	**0.01**
LIG1	DNA ligase 1		-0.72	0.64	-0.12	-1.13	0.26

NHEJ: Non-homologous end joining, HR: Homologous recombination, BER: Base excision repair, NER: Nucleotide excision repair, MMR: DNA mismatch repair. Multivariate linear regression analysis adjusted for gestational age and processing time,n=101. Gestational week 5 – 12

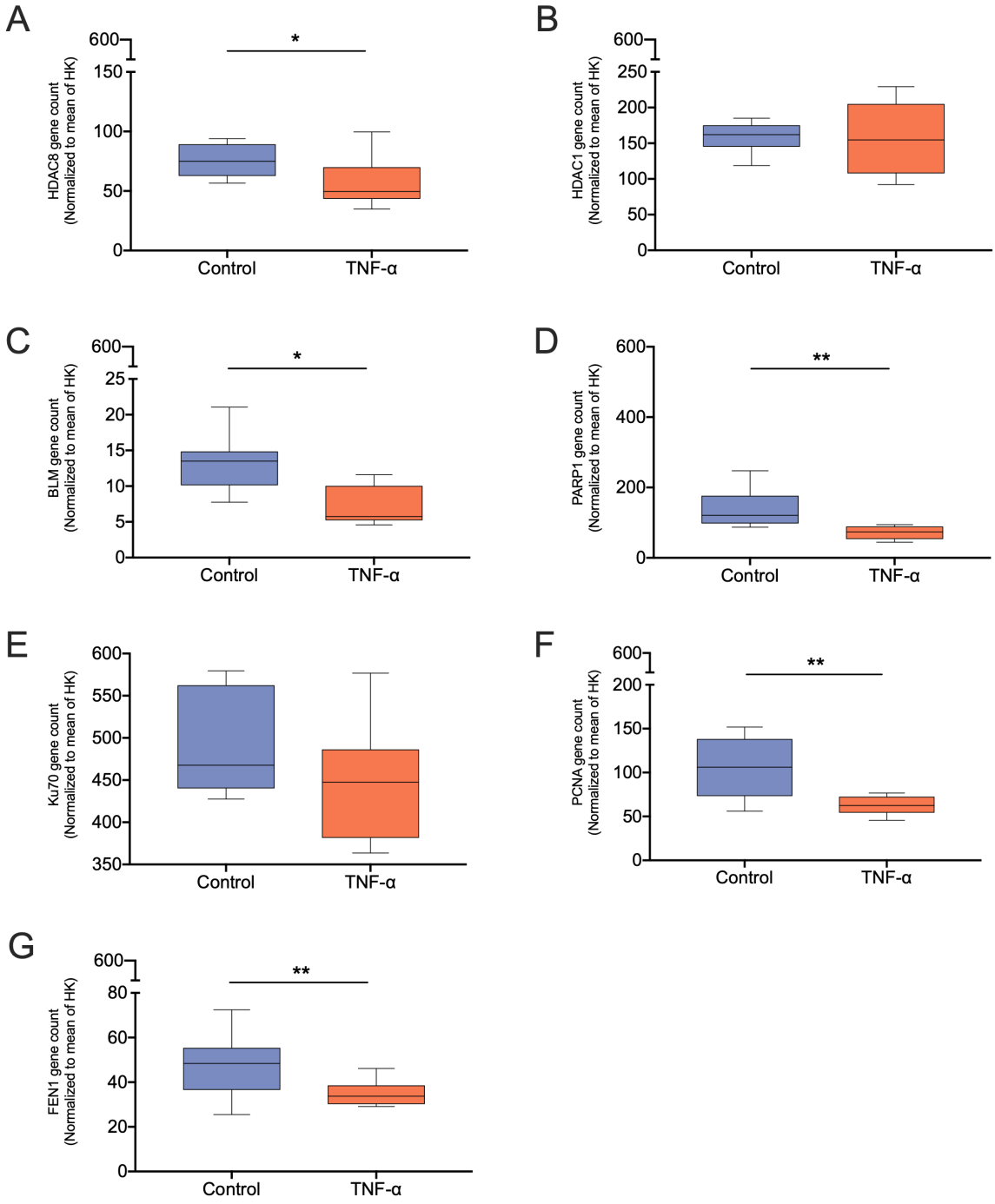

Figure 23: Assessment of DNA damage repair genes after short term treatment with tumor necrosis factor α (TNF-α) in first trimester placental explants. First trimester chorionic villous explants (n = 8, gestational week 5 - 10) were cultured at 2.5% O_2 with or without TNF-α (50 ng/mL) for 48 hours in triplicates. Gene expression of *HDAC8* (**A**), *HDAC1* (**B**), *BLM* (**C**), *PARP1* (**D**), *Ku70* (**E**), *PCNA* (**F**) and *FEN1* (**G**) was determined by Nanostring analysis. Data was normalized to the mean of two different housekeeping (HK) genes WD repeat domain 45B (*WDR45L*) and TATA box binding protein (*TBP*). Statistical analysis included paired t-test or Wilcoxon matched-pairs signed rank test. * $p < 0.05$, ** $p < 0.01$

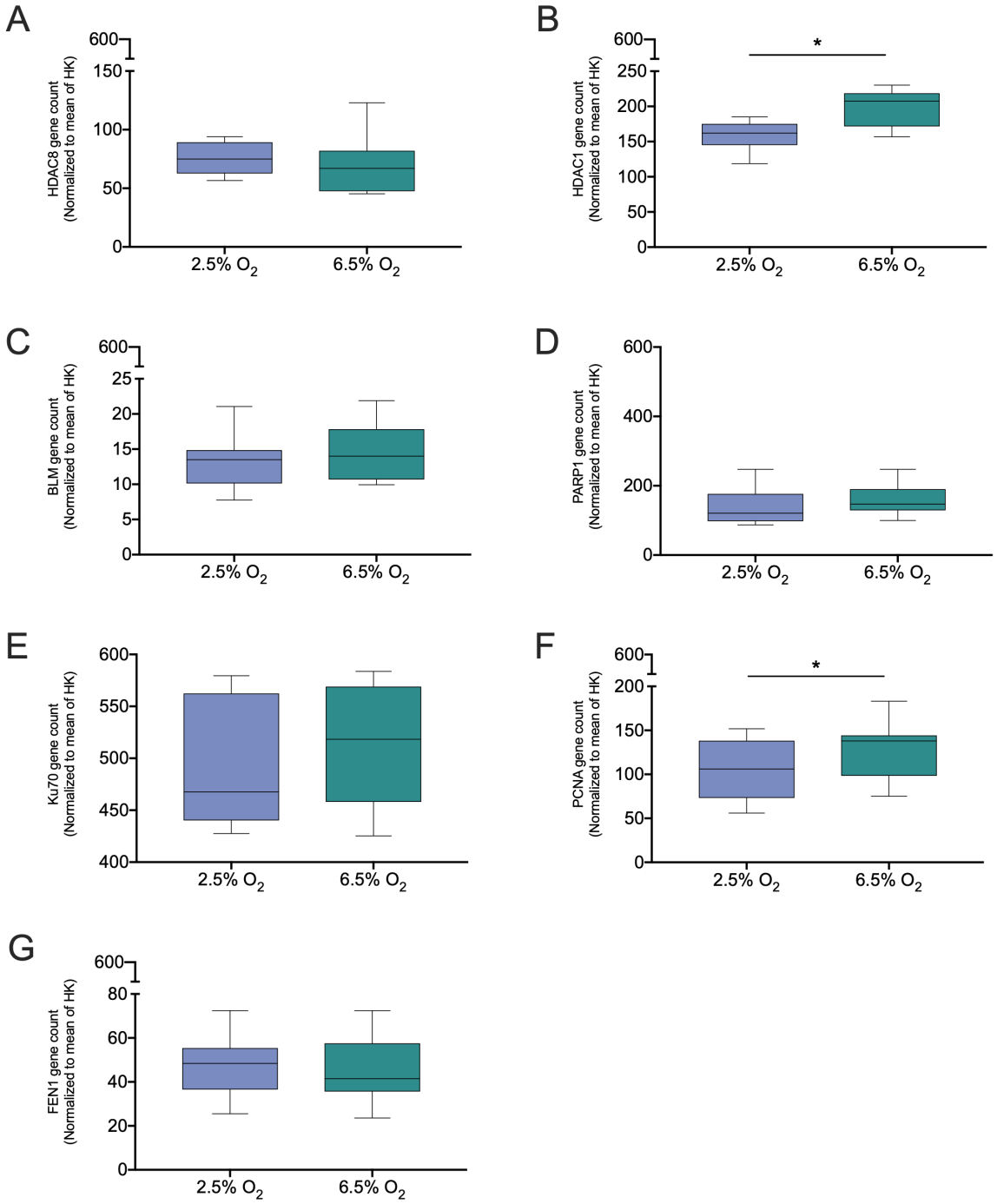

Figure 24: Assessment of DNA damage repair genes after short term exposure of first trimester placental chorionic villous explants to physiologically low (2.5% O_2) and high (6.5% O_2) oxygen levels. First trimester chorionic villous explants from different placental tissues (n = 8, gestational week 5 - 10) were cultured for 48 hours in triplicates at 2.5% O_2 or 65% O_2, respectively. Gene expression of *HDAC8* (**A**), *HDAC1* (**B**), *BLM* (**C**), *PARP1* (**D**), *Ku70* (**E**), *PCNA* (**F**) and *FEN1* (**G**) was determined by Nanostring analysis. Data was normalized to the mean of two different housekeeping (HK) genes WD repeat domain 45B (WDR45L) and TATA box binding protein (TBP). Statistical analysis included paired t-test or Wilcoxon matched-pairs signed rank test. * $p < 0.05$

Furthermore, phosphorylation levels of serine or threonine in the S*/T*Q motif were increased in FT placentas from obese women (B = 0.01, p = 0.05) (Figure 25F). Analyzing the data with BMI stratified into lean and obese groups, ATR and ATM protein levels were higher in the obese cohort by 5.9-fold ($p < 0.001$, Figure 24C) and 2.8-fold ($p < 0.01$, Figure 25E), respectively. However, obesity-induced changes in phosphorylation of ATM/ATR substrates did not reach significance (Figure 25G). All together this data indicates activation of the ATM/ATR signaling pathway in placentas associated with maternal obesity already in the first trimester of human pregnancy.

To further assess the effect of gestational age, we stratified the data accordingly. In line with MVLR analysis (App. Table 2), ATM, ATR and AMT/ATR substrate phosphorylation did not correlate with gestational age (Figure 26).

We further quantified protein levels of proteins associated with ATM/ATR damage repair signaling, e.g., growth arrest and DNA damage inducible alpha (GADD45a), proliferating cell nuclear antigen (PCNA), nei-like DNA glycosylase 3 (NEIL3) and apurinic/apyrimidinic endodeoxyribonuclease 1 (APE1) in FT placental tissue lysates by Western Blotting. Again, data analysis was performed using a MVLR model with BMI as categorical dependent variable and data was adjusted for gestational age and tissue processing time. Maternal obesity in early pregnancy tended to increase GADD45a (9.0%, p = 0.07), NEIL3 (7.8%, p = 0.08) and PCNA (62.9%, p = 0.06) and increased APE1 (21.6%, p = 0.03) protein levels (Figure 27).

ATM/ATR-dependent phosphorylation events lead to stabilization and activation of p53 via phosphorylation at serine 15, the classical ATM phosphorylation site. As substrates of the ATM/ATR signaling pathway were affected by maternal obesity by trend, we further determined protein levels of phosphorylated p53 at serine 15 (Lavin, 2008) and of ATM/ATR downstream effector nibrin (NBS1). Both proteins are key regulators of cell cycle checkpoint activation and DNA damage repair. Figure 28A and B shows representative blots. Total p53 protein level was increased by trend (p = 0.07, data not shown) in FT placental tissue from obese women. However, phosphorylation of placental p53 at serine 15 was not affected by maternal obesity in early pregnancy (Figure 28C). Furthermore, NBS1 protein level were not altered in obese FT placentas compared to the lean cohort (Figure 28D).

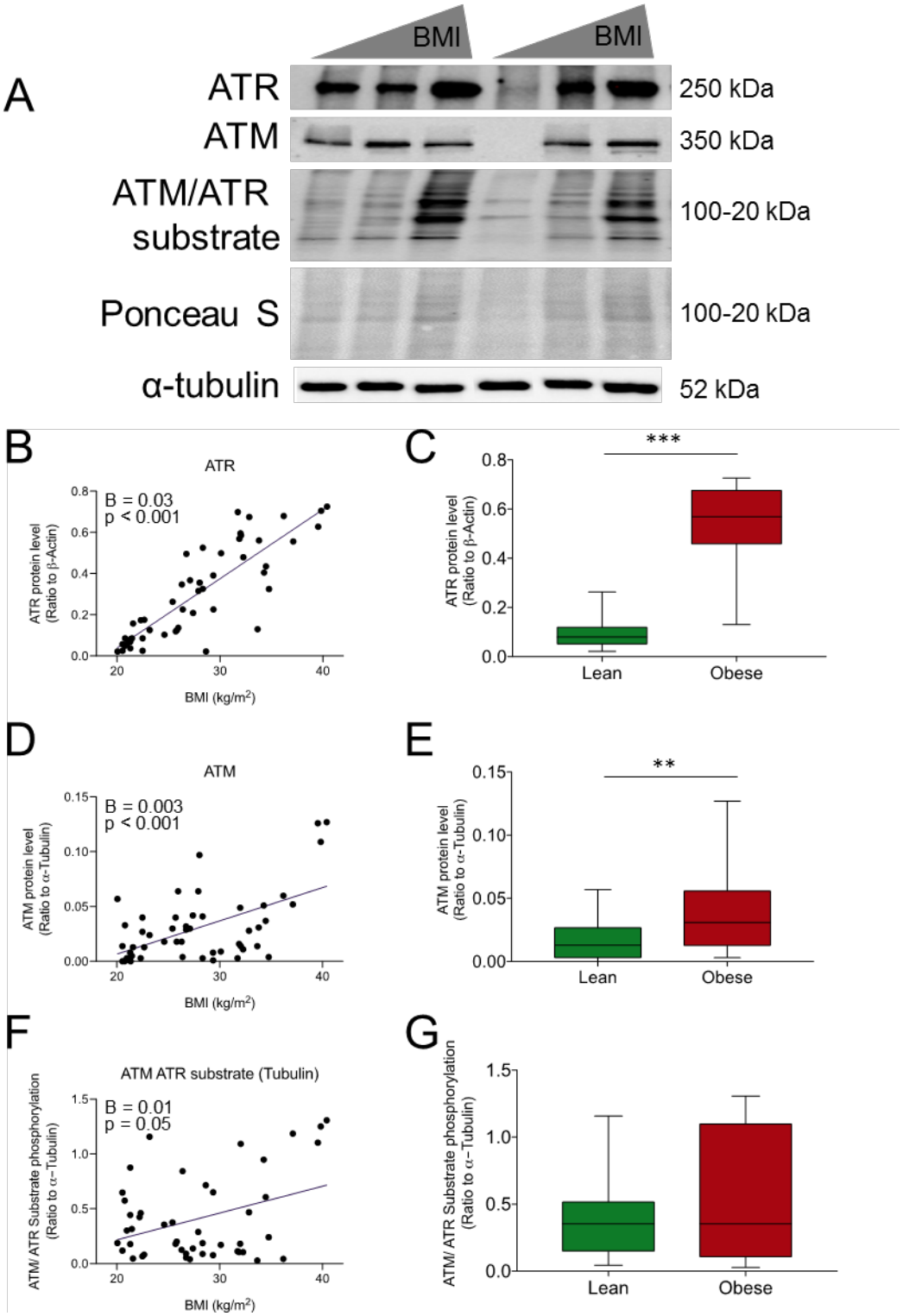

Figure 25: ATM/ATR signaling in first trimester placenta of lean and obese women. Total protein of first trimester placental cell lysates was extracted and subjected to Western blot analysis (**A**). The density of each band was quantified using Evolution-Capt software. The relative density ratio of each protein was calculated to *α*-tubulin. Statistical analysis was performed using a multivariate linear regression analysis with BMI as linear (**B, D, F**) or categorical (**C, E, G**) dependent variable and data was adjusted for gestational age and tissue processing time. Categorical BMI data is shown as means ± SD, n = 54. ** $p < 0.01$ *** $p < 0.001$

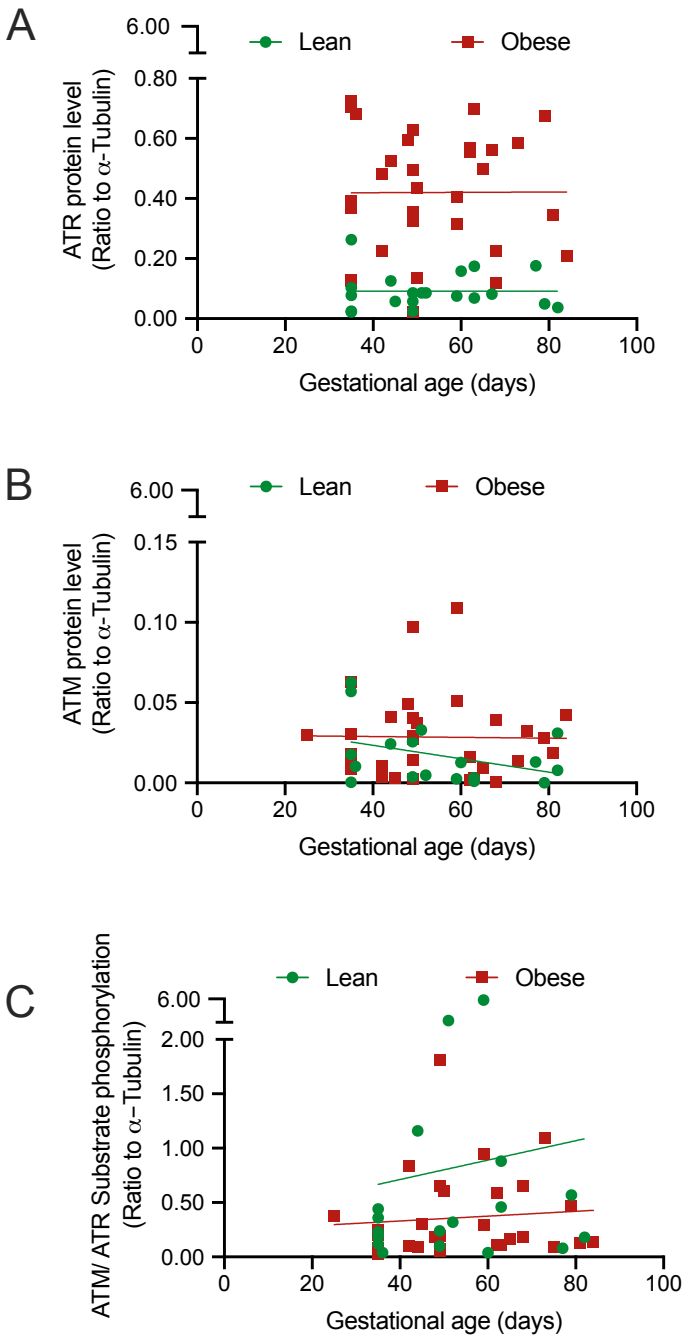

Figure 26: ATM, ATR and ATM/ATR substrate phosphorylation with gestational age stratified by BMI category. Total protein of first trimester placental cell lysates was extracted and subjected to Western blot analysis. The density of each band was quantified using Evolution-Capt software. The relative density ratio of each protein was calculated to α-tubulin. ATM (**A**), ATR (**B**) and AMT/ATR substrate phosphorylation (**C**) were correlated to gestational age. Statistical analysis was performed using Pearson correlation. n = 54.

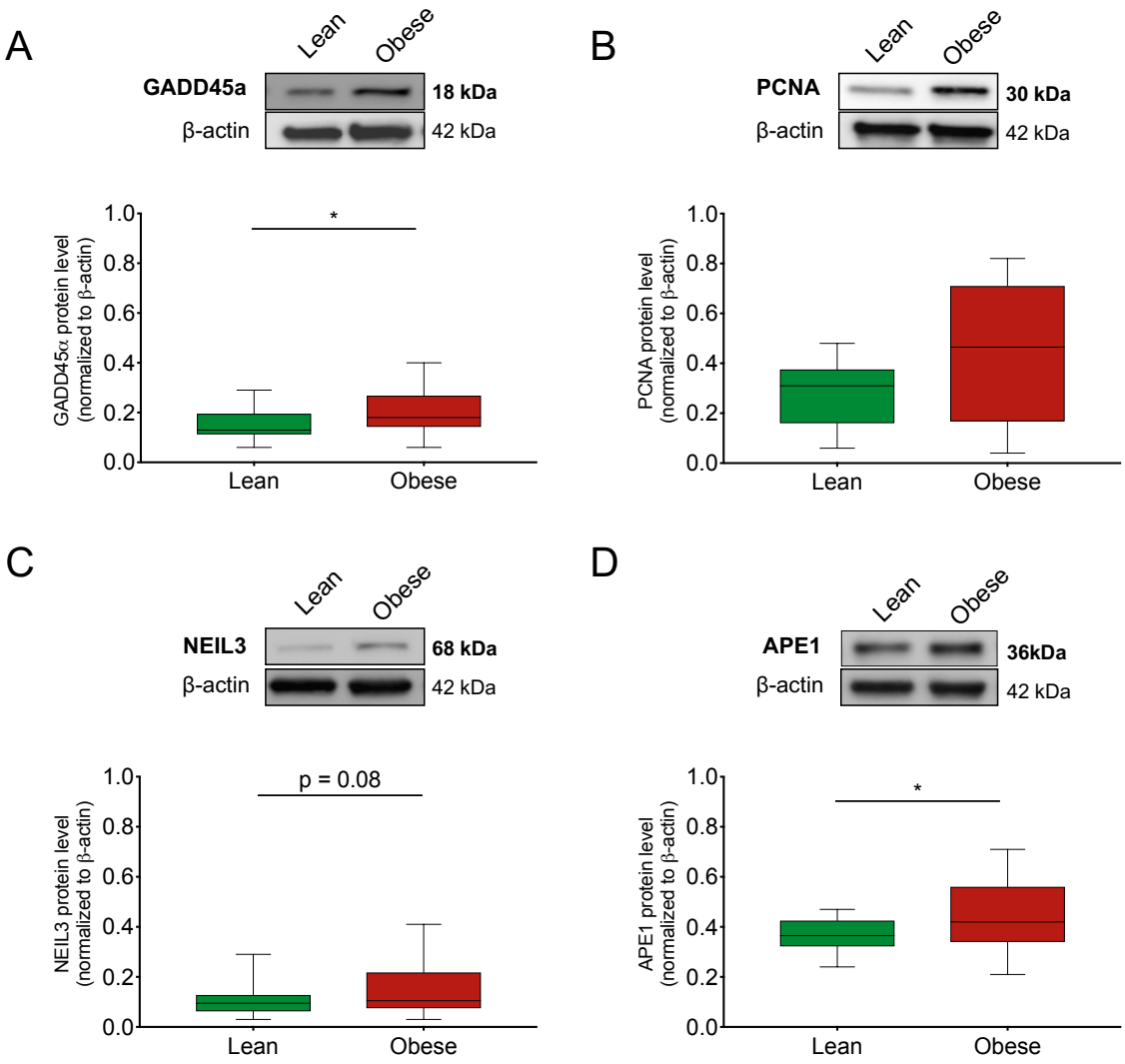

Figure 27: Protein level of double strand break repair proteins in the first trimester placenta of lean and obese women. Total protein of first trimester placental cell lysates was extracted and subjected to Western blot analysis. The density of each band was quantified using Evolution-Capt software. The relative density ratio of each protein was calculated to β-actin. Statistical analysis was performed using a multivariate linear regression analysis with BMI as categorical dependent variable and data was adjusted for gestational age and tissue processing time Gestational week 5 – 12. Data are means ± SD. n (lean / obese) = 18 / 16. *p < 0.05. GADD45a: Growth Arrest and DNA Damage Inducible Alpha, PCNA: Proliferating Cell Nuclear Antigen, NEIL3: Nei Like DNA Glycosylase 3, APE1: Apurinic/Apyrimidinic Endodeoxyribonuclease 1

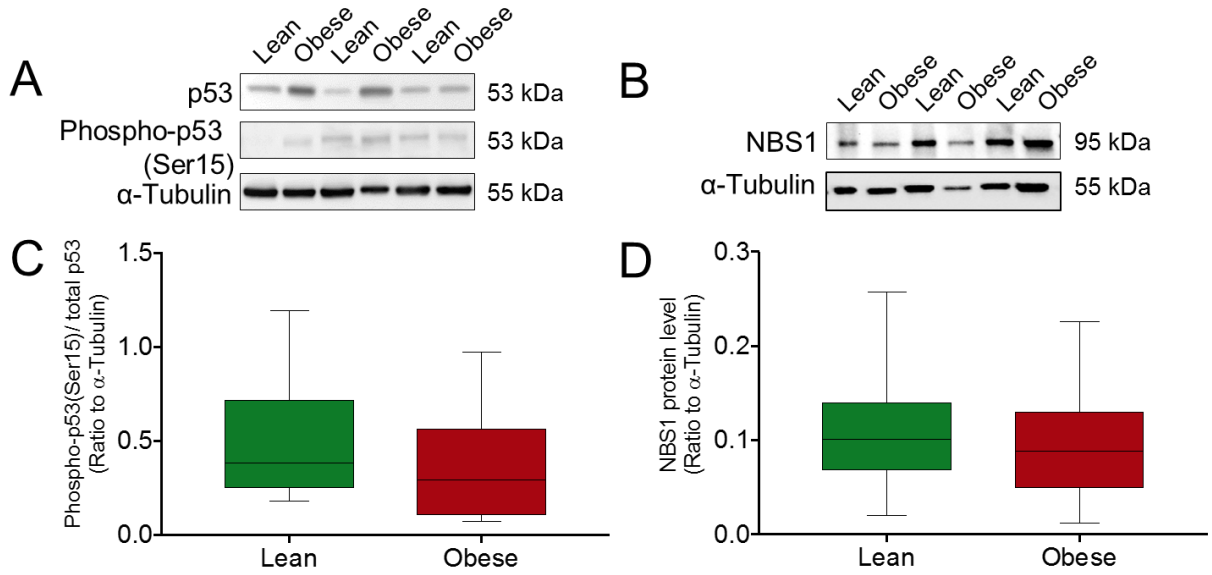

Figure 28: ATM/ATR downstream effectors p53 and NBS1 in first trimester placenta of lean and obese women. Total protein of first trimester placental cell lysates was extracted and subjected to Western blot analysis. The density of each band was quantified using Evolution-Capt software and relative density ratio of each protein was calculated to α-tubulin. (**A, B**) Immmunoblotting with subsequent densitometry of phosphor-p53/total p53 (**C**) and NBS1 (**D**) show that both protein levels of ATM/ATR downstream effectors were not altered by maternal obesity in the first trimester human placenta. Statistical analysis was performed using a multivariate linear regression analysis with BMI as categorical dependent variable and data was adjusted for gestational age and tissue processing time. Data is shown as means ± SD, n (lean / obese) = 17 / 17. NBS1: Ninbrin

4.5.2. Cell cycle regulation

Cell cycle arrest is mandatory for DNA damage repair as it gives cells time to repair critical DNA damage. Once DNA damage has been repaired, the cell cycle progression can resume or, if the damage is too extensive, the cell will undergo apoptosis (Awasthi *et al.*, 2016). As this study described obesity-induced DNA damage and activated ATM/ATR DNA damage signaling in FT placentas from obese women, we further assessed placental cell cycle regulation in the context of maternal obesity.

First, a qPCR panel (187 genes) and a cell cycle specific protein array (95 proteins) were used to measure gene expression and protein levels of several cell cycle regulators in placental tissue from gestational week 7. Results were statistically analyzed using a MVLR model with BMI as a categorical variable adjusted for gestational age and tissue processing time. Only proteins and genes with a fold change (FC) > 1.3 and $p < 0.05$ were considered significant.

Maternal obesity affected gene expression of 9 out of 187 (4.8%) cell cycle regulators, with excision repair 5 (*ERCC5*) and *BRCA1* showing the highest fold increase in samples from obese vs lean women (1.5-fold, $p = 0.02$ and 2.0-fold, $p = 0.03$, respectively, Figure 29A). Furthermore, maternal obesity increased the levels of 22 out of 95 (26.3%) analyzed proteins, e.g., Rad52 (fold change: 1.5, $p < 0.0001$) and BRCA1 (fold change: 1.4, $p = 0.003$, Figure 29B). Interestingly, also phospho(Ser1423)-BRCA1 protein level was increased in maternal obesity (30.0%, $p = 0.009$, Figure 29B). Among all cell cycle regulators analyzed in this study, only BRCA1 gene expression and protein level were concordantly altered by maternal obesity (Figure 29C). We further confirmed gene panel and protein array data by Nanostring analysis (52.3% , $p = 0.03$, Figure 30A) and BRCA1 and pBRCA1 protein levels by Western blotting (49.1%, $p = 0.04$ and 57.4%, $p = 0.001$, respectively, Figure 30B-D) (Hoch, Bachbauer, *et al.*, 2020). Gestational age and fetal sex had no effect on BRCA1 gene expression and protein level (data not shown) (Hoch, Bachbauer, *et al.*, 2020).

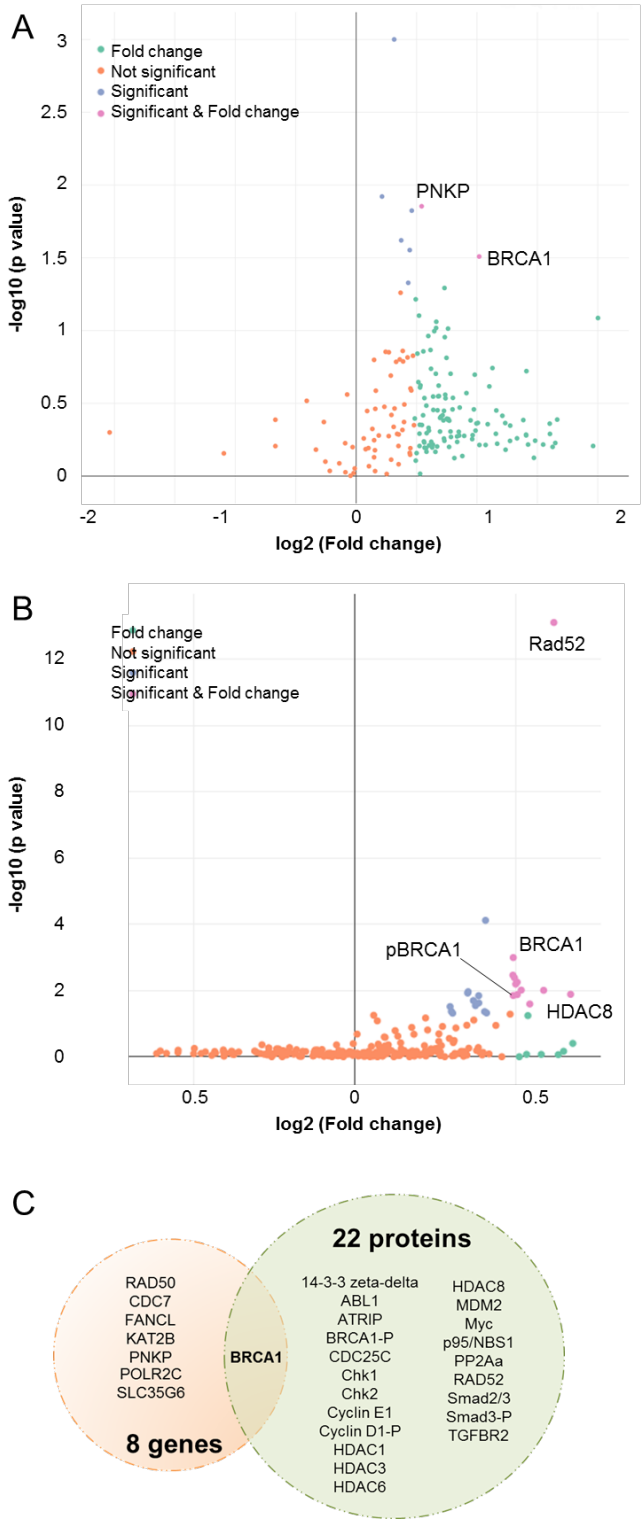

Figure 29: Cell cycle regulators in first trimester placenta villous tissue. (**A**) Volcano plot shows fold change for genes differentially expressed between lean and obese samples. (**B**) Volcano plot shows fold change for proteins differentially expressed between lean and obese placenta tissue (gestational week 7). (**C**) Venn diagram depicting genes and proteins induced by a high maternal BMI in the first trimester of pregnancy with BRCA1 as common factor. Genes and proteins were considered as significant with $p < 0.05$ and fold change threshold was

set to 1.3. On all volcano plots, x axis = log2 fold change (lean vs. obese), n (lean / obese) = 7 / 7. y axis = multivariate linear regression p-value. Legend: ERRC5, excision repair 5; BRCA1, breast cancer 1; pBRCA1, phospho-BRCA1. This figure was adapted from Hoch, Bachbauer *et al.* (2020) with publisher's permission as for all subsequent figures in this thesis, wherever applicable.

As BRCA1 gene expression and protein level are affected by maternal obesity already in early pregnancy, immunohistochemistry was used to assess BRCA1 location in early, mid, and late FT first trimester placental tissue. Both CTB and evCTB displayed strong BRCA1 immunostaining which localized to both, nuclei and the cytosol (Figure 31A, C, E). BRCA1 staining in the ST was located to the nuclei.

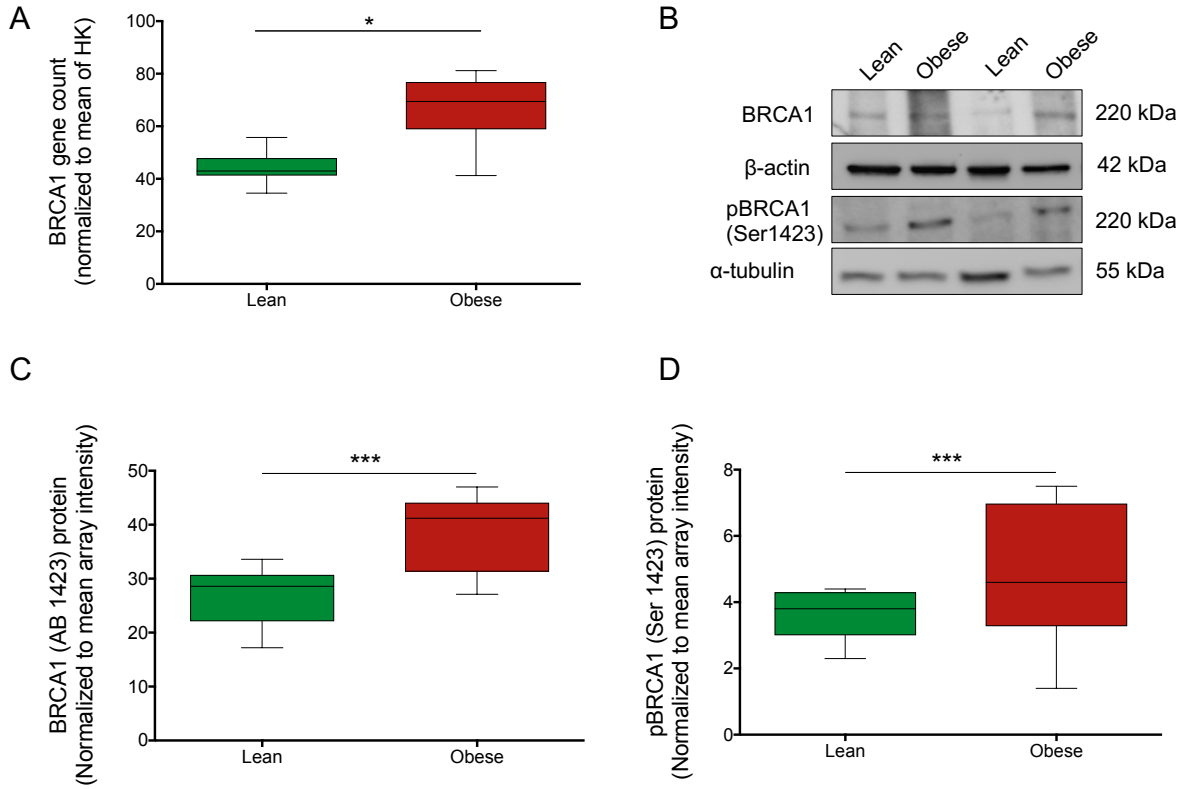

Figure 30: BRCA1 gene expression and protein level validation. (**A**) Nanostring gene expression analysis confirms BRCA1upregulation in FT placental tissue from obese women (52.3%, lean: 44±6.5, obese 67±14.0). Nanostring gene counts were normalized to the mean of two different housekeeping (HK) genes (WDR45L and TBP) (**B**) Immmunoblotting with subsequent densitometry of (**C**) BRCA1 and (**D**) phosho(Ser 1423)-BRCA1 show higher protein levels in FT placentas from obese women. Results are presented as ratio of BRCA1 or phosho-BRCA1 protein and beta-actin band densities. * $p < 0.05$, *** $p < 0.001$ This figure was adapted from Hoch, Bachbauer *et al.* (2020).

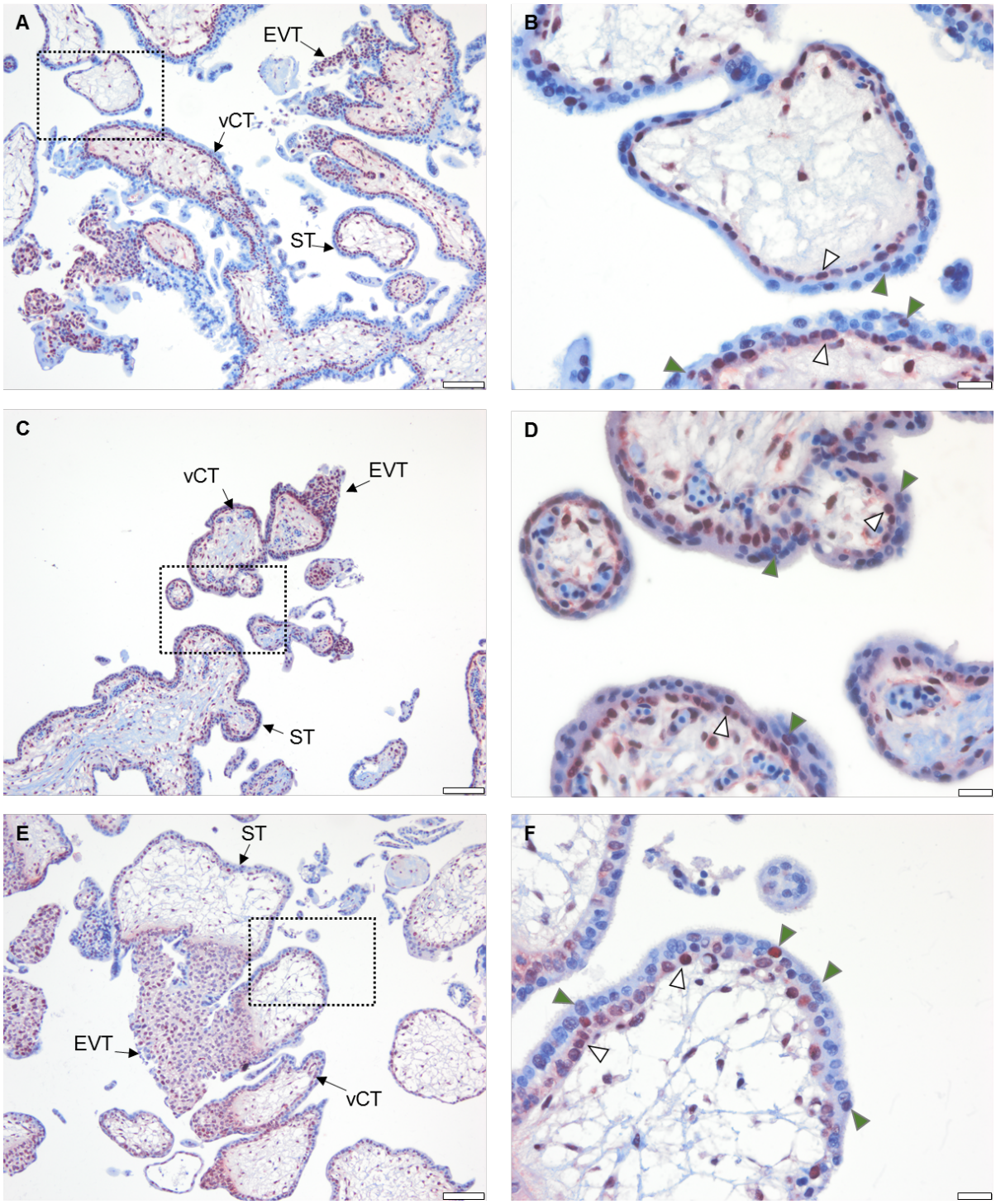

Figure 31: BRCA1 immunohistochemistry of FT placental tissue from gestational week 5 (A and B), week 8 (C and D) and week 12 (E and F). BRCA1 localizes to the nuclei and cytoplasm of villous cytotrophoblasts (CTB) and extravillous cytotrophoblasts (evCTB) (**A**, **C** and **E**). In Syncytiotrophoblasts (STB) BRCA1 was also located in the nuclei (**B**, **D**, and **F**, green arrowheads. Open arrowheads point towards CTB). Scale bar indicates 100 µm in **A**, **C** and **E** or 20 µm in **B**, **D** and **F**. Fields shown in **B**, **D** and **F** are indicated as dotted frames in **A**, **C** and **E.** This figure was adapted from Hoch, Bachbauer *et al.* (2020).

Furthermore, stromal cells were also positive for BRCA1 (Figure 31B, D, F, green arrowheads).We found no differences in location between early, mid, and late first trimester placental sections (Hoch, Bachbauer, *et al.*, 2020).

As obesity is a low-grade pro-inflammatory condition associated with inflammatory stress (Shoelson, Herrero and Naaz, 2007) and specifically with increased levels of TNF-α (La Vignera *et al.*, 2011), we investigated a potential role of TNF-α in cell cycle dysregulation in FT chorionic villous explants. To this end, we used Nanostring gene expression analysis to assess expression of the prominent cell cycle regulatory cyclins, cyclin depended kinases, checkpoint kinases and genes of the RAD family after TNF-α exposure.

Short term treatment (24h) of FT chorionic villous explants with TNF-α (50 ng/mL) decreased gene expression of *cyclin A1* (-62.36%, p = 0.008), *cyclin B1* (-56.7%, p = 0.008), *cyclin E1* (-59.8, p = 0.02), checkpoint kinase 1 (*CHEK1*, -48.9%, p =0.02), checkpoint kinase 2 (*CHEK2*, -27.8%, p =0.008) and RAD 51 recombinase (*RAD51*, -45.2%, p = 0.008). In concordance with *cyclin E1* downregulation, cyclin dependent kinase inhibitor 1 (*CDKN1A*) that inhibits cell cycle progression in G1 via binding to cyclin CDK2 was upregulated by 36.3% (p = 0.008) in FT chorionic villous explants after TNF-α treatment (Figure 32).

To further investigate whether oxygen is the underlying stimulus for dysregulation of cell cycle mediators in early pregnancies of obese mothers, we cultured FT chorionic villous explants under physiologically low (2.5% O_2) and high (6.5% O_2) oxygen levels. Among all analyzed genes, only *cyclin A1* (-66.2%, p =0.03) and *cyclin D1* (-14.3%, p = 0.05) was downregulated, while *cyclin B1* gene expression was induced (48.0%, p = 0.02) by high oxygen, respectively (Figure 33).

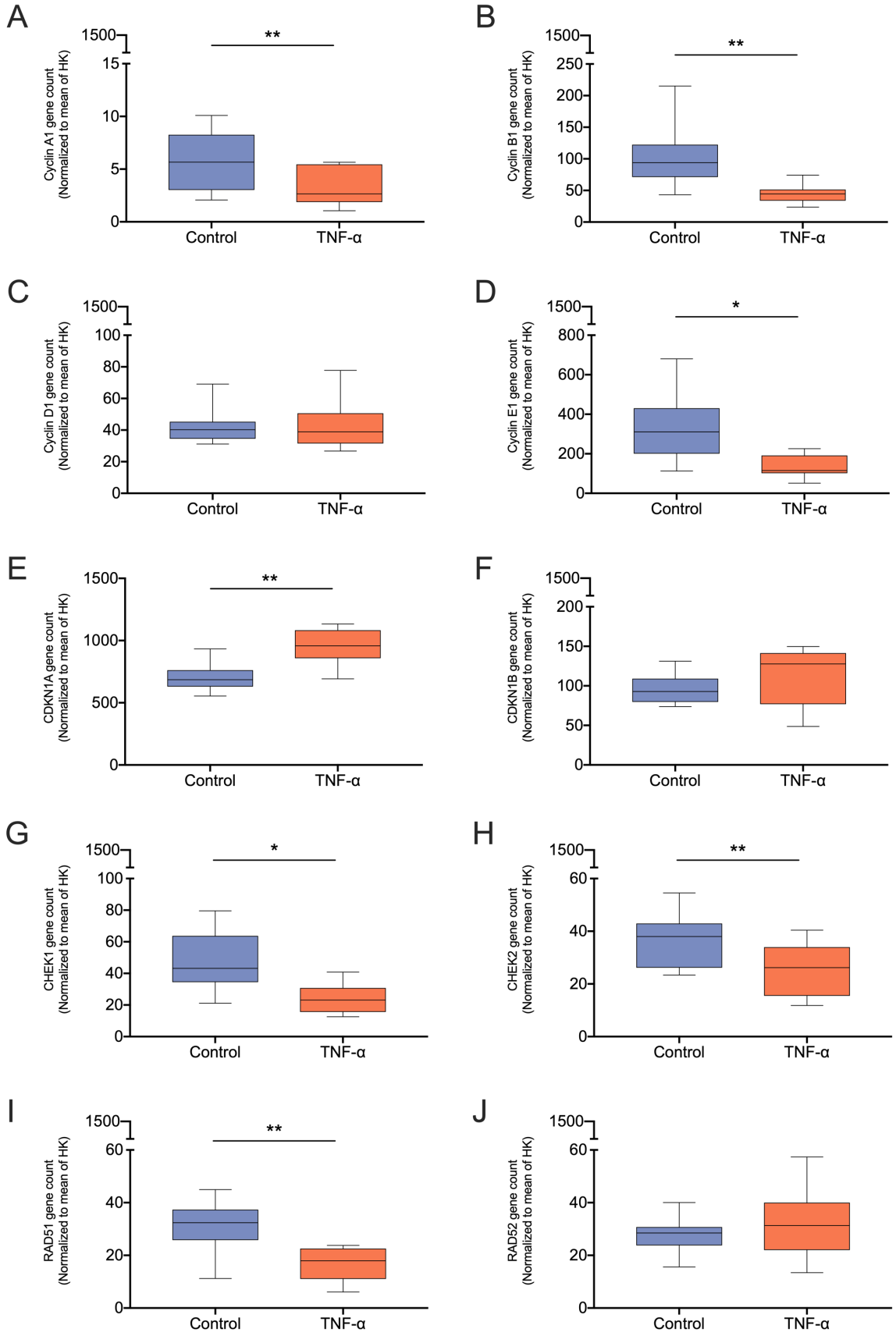

Figure 32: Assessment of cell cycle regulatory genes after short term treatment with tumor necrosis factor α (TNF-α) in first trimester placental explants. First trimester chorionic villous explants from different placental

explants from different placental tissues (n = 8, gestational week 5 - 10) were cultured at 2.5% O_2 with TNF-α (50 ng/mL) for 48 hours in triplicates. Genes by Nanostring gene expression analysis. Gene expression of *cyclin A1* (**A**), *cyclin B1* (**B**), *cyclin D1* (**C**), *cyclin E1* (**D**), *CDKN1A* (**E**), *CDKN1B* (**F**), *CHEK1* (**G**), *CHEK2* (**H**), *RAD51* (**I**) and *RAD52* (**J**) was normalized to the mean of two different housekeeping (HK) genes WD repeat domain 45B (*WDR45L*) and TATA box binding protein (*TBP*). Statistical analysis included paired t-test or Wilcoxon matched-pairs signed rank test. * $p < 0.05$, ** $p < 0.01$

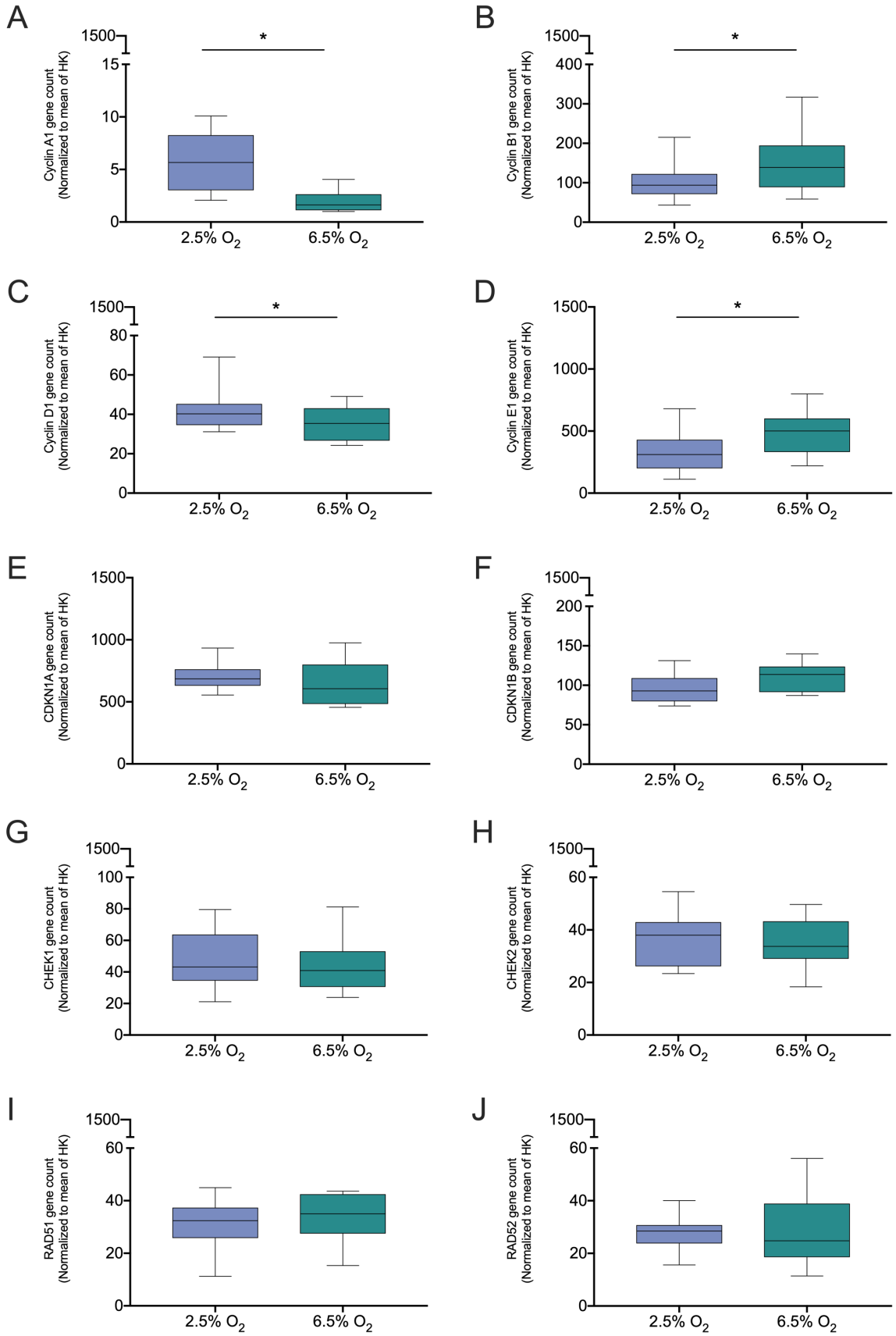

Figure 33: Assessment of cell cycle regulatory genes after short term exposure of first trimester placental chorionic villous explants to physiologically low (2.5% O_2) and high (6.5% O_2) oxygen levels. First trimester

chorionic villous explants from different placental tissues (n = 8, gestational week 5 - 10) were cultured for 48 hours in triplicates at 2.5% O_2 or 65% O_2, respectively. Genes by Nanostring gene expression analysis. Gene expression of *cyclin A1* (**A**), *cyclin B1* (**B**), *cyclin D1* (**C**), *cyclin E1* (**D**), *CDKN1A* (**E**), *CDKN1B* (**F**), *CHEK1* (**G***), CHEK2* (**H**), *RAD51* (**I**) and *RAD52* (**J**) was normalized to the mean of two different housekeeping (HK) genes WD repeat domain 45B (*WDR45L*) and TATA box binding protein (*TBP*). Statistical analysis included Paired t-test or Wilcoxon matched-pairs signed rank test. * $p < 0.05$

4.6. Consequences for first trimester CTB turnover in obesity

Disruption of normal cell cycle progression, unrepaired DNA damage or critically short telomeres directly affect cell viability by reducing proliferation rate and/or initiation of apoptotic events. We demonstrated that obesity in pregnant women affects those cellular processes already in the FT placenta. This raised the question about potential consequences for placental, i.e., trophoblast turnover. To test this, we assessed trophoblast viability by measuring proliferation and apoptosis *in situ,* and senescence. We used quantitative *in situ* analysis to specifically determine trophoblast proliferation and apoptosis as reflected by Ki67 (Figure 34A) and TUNEL assay (Figure35A)/M30 (Figure 36A) IF staining, respectively. We further assessed p16 protein levels to determine cellular senescence as a potential obesity-induced

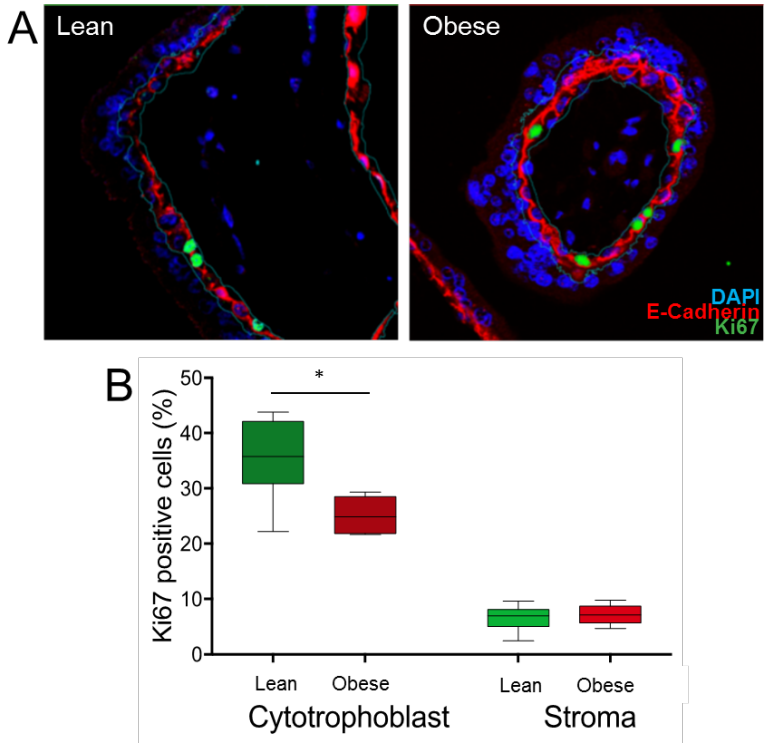

Figure 34: Quantification of cytotrophoblast and stromal cell proliferation *in situ*. Trophoblast and stromal cell proliferation was assessed using semi-quantitative *in situ* analysis of Ki67 and TUNEL assay, respectively. Formalin fixed, paraffin embedded first trimester tissue (week 5-8) was cut (3 µm), de-paraffinized, rehydrated and stained for E-Cadherin and Ki67 or TUNEL reagent. Ten randomly selected villi were captured per section using the Zeiss LSM 510 META Axiovert 200M Zeiss confocal system. Blue lines indicate cytotrophoblast cell border. Statistical analysis was performed using a multivariate linear regression analysis with BMI as categorical dependent variable adjusted for gestational age and tissue processing time. Results are presented as mean ± SD. n (lean / obese) = 13 / 17. *$p < 0.05$

consequence. Data was analyzed using a MVLR model with BMI as a categorical variable adjusted for gestational age and tissue processing time.

Cytotrophoblast proliferation was reduced (-52.2%, p = 0.02) in FT placental tissue from obese women. However, proliferation of stromal cells was unaffected by maternal obesity (Figure 34B).

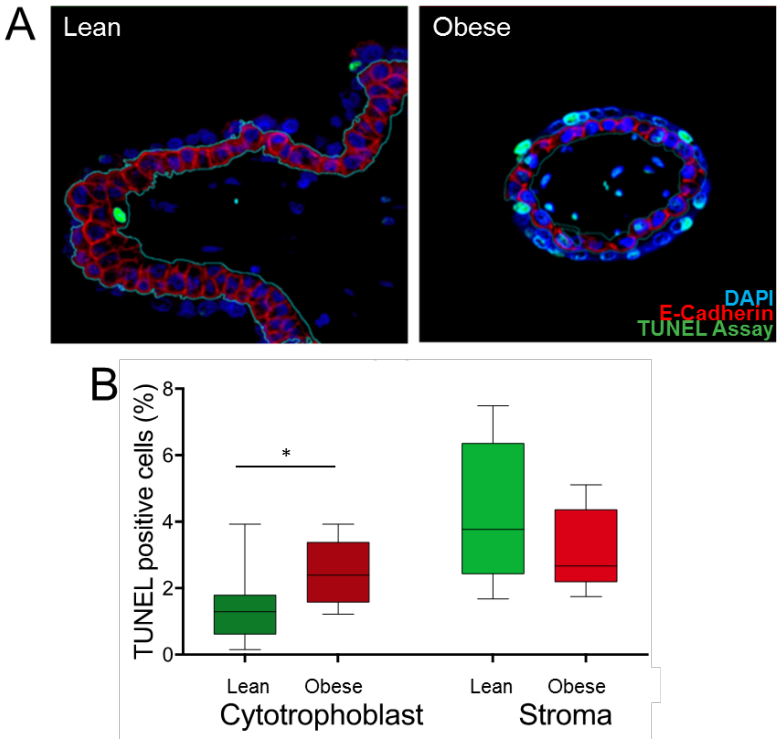

Figure 35: Assessment of trophoblast apoptosis *in situ* using TUNEL assay. Trophoblast proliferation was assessed using semi-quantitative in-situ analysis of Ki67 and TUNEL assay, respectively. Formalin fixed, paraffin embedded first trimester tissue (week 5 - 8) was cut (3 µm), de-paraffinized, rehydrated and stained for E-Cadherin and TUNEL reagent. Ten randomly selected villi were captured per section using the Zeiss LSM 510 META Axiovert 200M Zeiss confocal system. Blue lines indicate cytotrophoblast cell border. Statistical analysis was performed using a multivariate linear regression analysis with BMI as categorical dependent variable adjusted for gestational age and tissue processing time. Results are presented as mean ± SD. n (lean / obese) = 13 / 17. *p < 0.05

Furthermore, we used two different methods to assess trophoblast apoptosis. The TUNEL reaction labels DNA strand breaks generated during apoptosis and is, therefore, a widely used marker for DNA degradation, an early-stage event of apoptosis (Yasuda *et al.*, 1995). Caspase-cleaved cytokeratin 18 (CK18) is an epithelial cell-specific marker for

apoptosis as it is cleaved by caspases at multiple sequence sites during early apoptosis (Caulín, Salvesen and Oshima, 1997).

In this study, maternal obesity induced cytotrophoblast apoptosis (5.6-fold, $p < 0.01$), reflected by TUNEL positive cells within the E-Cadherin layer. However, the number of TUNEL positive cells within the stroma of FT placental villi was not affected by maternal obesity in early pregnancy (Figure 35B).

TUNEL assay results were confirmed by CK18 immunofluorescent staining. Nuclei were counted as CK18 positive with at least one fluorescent signal. Trophoblasts of FT

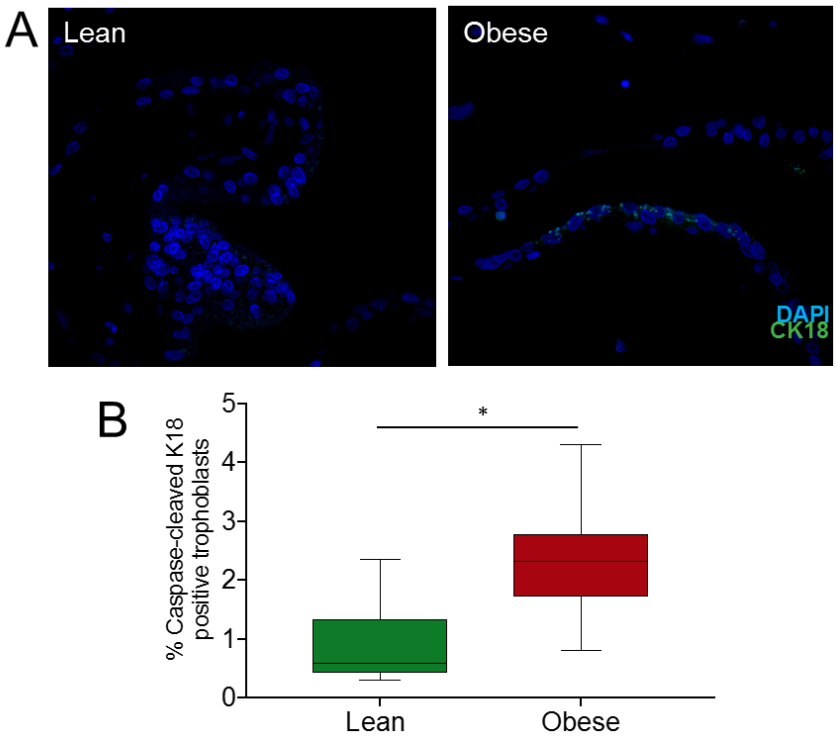

Figure 36: Assessment of trophoblast apoptosis *in situ* using Caspase-cleaved cytokeratin 18. Trophoblast apoptosis was assessed using semi-quantitative in-situ analysis of Caspase-cleaved cytokeratin 18 (CK18). Formalin fixed, paraffin embedded first trimester tissue (week 5 - 8) was cut (3 µm), de-paraffinized, rehydrated and stained for. Ten randomly selected villi were captured per section using the Zeiss LSM 510 META Axiovert 200M Zeiss confocal system. (**A**) Representative images of stained lean and obese first trimester placenta tissue sections. (**B**) Statistical analysis was performed using a multivariate linear regression analysis with BMI as categorical dependent variable adjusted for gestational age and tissue processing time. Categorical BMI data is shown as mean ± SD, n (lean / obese) = 13 / 17. Gestational week 5 – 12. *$p < 0.05$

placentas exposed *in utero* to an obesity environment show increased apoptosis (2.5-fold, p = 0.01) reflected by CK18 IF staining *in situ* (Figure 36B).

To test if maternal obesity-induced DNA damage activates cellular senescence in the FT placenta, we assessed p16 protein level in tissues from lean and obese women by Western blotting (Figure 37A). Densitometry results show that maternal obesity did not affect protein levels of p16 in the FT placenta (Figure 37B).

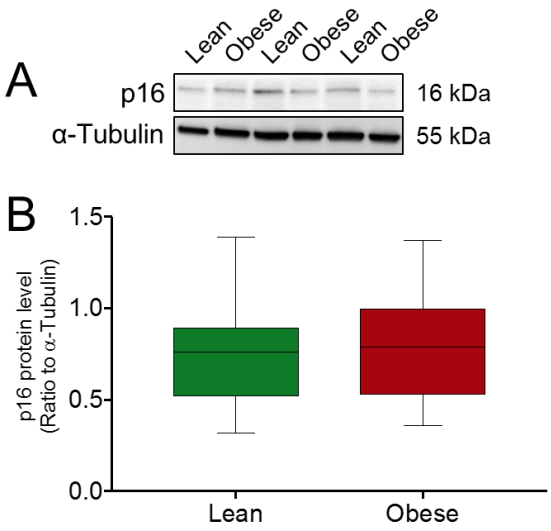

Figure 37: Senescence marker p16 in first trimester placenta of lean and obese women. Total protein of first trimester placental cell lysates was extracted and subjected to Western blot analysis. The density of each band (**A**) was quantified using Evolution-Capt software and relative density ratio of each protein was calculated to α-tubulin (**B**). Statistical analysis was performed using a multivariate linear regression analysis with BMI as categorical dependent variable and data was adjusted for gestational age and tissue processing time. Categorical BMI data is shown as mean ± SD, n (lean / obese) = 17 / 17. Gestational week 5- 12

5. Discussion

Obesity is a global pandemic, and its prevalence keeps increasing worldwide (World Health Organization (WHO), 2018). In general, obesity is accompanied by metabolic alterations resulting from imbalanced energy intake and expenditure leading to increased adipose tissue volume (Shoelson, Herrero and Naaz, 2007). Obesity related metabolic derangements associate with hypertension or type 2 diabetes mellitus (T2DM), conditions that affect the patient's quality of life (Conway and Rene, 2004). Lymphocytes of obese non-pregnant women showed various DNA lesions, and obesity also correlated with increased oxidative DNA damage in lymphocytes (Al-Aubaidy and Jelinek, 2011; Włodarczyk *et al.*, 2018). Altered systemic function in obesity, reduced insulin sensitivity and higher inflammation lead to manifold consequences for specific tissues and organs (Keaney *et al.*, 2003; Olivares-Corichi *et al.*, 2011).

The prevalence of overweight and obesity in women in reproductive age is rising every year (James, 2004), with the resulting adverse consequences for the growing fetus. Thus, understanding the underlying mechanisms and effects of obesity on placental function has recently gained increasing attention. So far, the majority of pregnancy-related studies on obesity effects have been carried out at the end of pregnancy and, thus, have focused on term placenta. At that stage in pregnancy, the placenta mainly adapts to changes associated with maternal obesity, e.g., reflected by hypervascularization, to protect the fetus. Furthermore, maternal obesity alters placental gene expression of stress and inflammatory markers, while also antioxidant gene expression is lower (Challier *et al.*, 2008; Roberts *et al.*, 2009, 2011; Malti-Boudilmi *et al.*, 2010; Saben *et al.*, 2014). Further studies demonstrated an obesity-associated reduction in mTOR signaling as well as increased NFkB, but decreased AMPK expression (Martino *et al.*, 2016). Some of these changes may be regarded as adaptive responses to protect the fetus in a metabolically adverse environment (Santos-Rosendo *et al.*, 2020). Taken together, at the end of pregnancy maternal obesity is associated with changes in placental function at the end of pregnancy.

In early human pregnancy, adequate trophoblast proliferation, differentiation, fusion, and survival are required for successful placental development and function (Velicky *et al.*, 2018). These crucial biological processes might be disturbed by cellular stress that characterizes

the maternal obese intrauterine environment (Desoye, 2018). Therefore, early placental development and function might directly be affected by obesity, since the early placenta is exposed to metabolic changes in the mother during the most critical periods of its development, but this has been scarcely investigated. While potential obesity effects on FT trophoblast invasion have been studied (Castellana *et al.*, 2018; St-Germain *et al.*, 2020), consequences of obesity on villous placental cell types and function still remain to be elucidated.

Therefore, this study aimed to shed first light on the effects of maternal obesity on first trimester villous DNA integrity, placental stress and antioxidative response, damage repair and associated cell cycle alterations, to finally focus on its consequences on villous trophoblast viability. We used FT placental tissue of non-smoking women after pregnancy termination for psychosocial reasons after an overnight fast and preserved the tissue or performed chorionic villous explant studies *in vitro*. We took into account that the oxygen level in the intervillous space and villous tissue gradually rises during the first trimester of pregnancy (Burton, 2009). Therefore, when we analyzed total FT placental tissue, the MVLR model used for statistical analyses was always adjusted for gestational age. Because of a lag time between the surgical procedure to terminate the pregnancy and fixation or freezing of placental tissue, we also always included this 'tissue processing time' as a further confounder in MVLR analyses. Furthermore, we cultured chorionic villous explants under two different low oxygen tensions during the time of the experiments, and processed the tissue also under low oxygen until fixation or snap-freezing. In this set of experiments, the influence of changes in oxygen levels, which may be accompanied by oxidative stress, on gene expression was studied. In addition, tissue exposure to TNF-α was used as experimental paradigm to evaluate whether inflammation modulates *in vitro* obesity-induced genes of interest.

5.1. FT placental oxidative stress in obese pregnant women

5.1.1. Oxidative stress-induced DNA damage

Obesity *per se* is linked to hyperglycemia-induced, systemic, oxidative stress (Keaney *et al.*, 2003). In such an oxidative stress environment, highly reactive ROS can further react with biological molecules, e.g., DNA. 8-oxo-7,8-dihydroguanine (8-OGdH) is derived from the reaction of guanine with the hydroxyl radical and is a classical marker of oxidative DNA damage (Gonzalez-Hunt, Wadhwa and Sanders, 2018). The DNA repair enzyme

formamidopyrimidine DNA glycosylase (FPG) converts damaged bases, including 8-OGdH, to DNA single strand breaks (Anderson *et al.*, 1998).

Previous studies have shown that the percentage of 8-OHdG positive nuclei was increased in placentas associated with preeclampsia or intrauterine growth restriction (IUGR) compared to controls (Cindrova-Davies *et al.*, 2018). We, therefore, hypothesized that obesity-associated oxidative stress can also induce DNA damage in the FT placenta. Using FPG COMET assay (single cell gel electrophoresis) and immunofluorescence staining of 8-OHdG followed by trophoblast specific analysis, we demonstrated that neither total placental tissue nor trophoblast (STB and CTB) show altered levels of oxygen-induced DNA damage in obese pregnant women in early pregnancy. This unexpected absence of enhanced oxidative stress signs vis-à-vis the hypothesized increased oxidative stress in obesity, raised the question, whether first trimester trophoblast is susceptible to oxygen-mediated DNA damage. Therefore, we challenged FT placenta tissue from lean and obese pregnant women with H_2O_2 prior to DNA damage quantification by alkaline COMET assay. In these experiments, FT placentas from obese women showed higher levels of DNA damage after *in vitro* induced stress compared to lean controls. Our results are not unprecedented, because term placental explants challenged with H_2O_2 (1 M) for 24 or 48 hours also showed an increased percentage of 8-OHdG immunopositive nuclei (Cindrova-Davies *et al.*, 2018).

This demonstrates i) that oxidative stress can induce DNA damage in FT placentas *in vitro*, and ii) a higher susceptibility of FT placentas from obese pregnant women to oxidative stress-induced DNA damage. Collectively, these results can be interpreted to indicate absence of oxidative stress in first trimester trophoblasts of obese pregnant women at an extent that induces oxidative DNA modification.

5.1.2. Lipid peroxidation and protein nitration

To further test the hypothesis of absent placental oxidative stress in FT placentas associated with maternal obesity, we determined lipid peroxidation and protein nitration in FT placental tissue from lean and obese women.

Oxidative stress cannot only attack DNA, but also lipids and proteins resulting in lipid peroxidation and protein nitration. In order to assess whether an obesity-associated intrauterine environment affects lipids and proteins, we determined 4-HNE and nitrotyrosine-protein

modifications. In presence of oxidative stress or high glucose levels, lipid peroxidation and protein nitration are further stress-induced cellular consequences (Esterbauer, Schaur and Zollner, 1991; Alvarez and Radi, 2003). While 4-HNE is derived from the oxidation of polyunsaturated fatty acids of the n-6 series, nitrotyrosine is formed by the reaction between protein-tyrosin and peroxynitrite radical, which is the generated through superoxide reacting with nitric oxide (Alvarez and Radi, 2003; Uchida, 2003). 4-HNE and nitrotyrosine modifications unspecifically occur on a range of proteins. Therefore, in immunoblots antibody binding results in several bands covering a broad molecular weight. Overall, 4-HNE and nitrotyrosine levels were not affected by maternal obesity in FT placental tissue of obese women. HSP70 is involved in the degradation of 4-HNE modified proteins (Hirata *et al.*, 2009), but the lower HSP70 levels found here make it unlikely to have affected nitrotyrosine levels. In a previous study, high maternal BMI was also not associated with increased levels of placental oxidative stress, but nitrotyrosine residues were increased in placenta samples from obese women (Roberts *et al.*, 2009). As our results differ from this study it is important to highlight that we used FT placenta tissue to assess the effect of maternal obesity on protein nitration, while the study by Roberts *et al*. focused on term placenta. Taken together, neither classical stress markers nor products of oxidative stress on DNA (8-OHdG), lipids (lipid peroxidation) and proteins (nitration) indicate placental stress associated with maternal obesity.

5.1.3. Antioxidants, HSP70 and HO-1

If confirmed by measurements of protein levels and kinase activity, downregulation of most stress-related genes may argue against placental stress in obese pregnant mothers in the first trimester. This can be the result of either absence of oxidative stress or of increased antioxidant defence capable of coping with enhanced oxidative stress. The first option is difficult to test directly. Hence, we focussed on antioxidant defence systems.

To evaluate the FT placental antioxidant defense system, we selected 18 antioxidants based on literature and performed Nanostring gene expression analysis. A MVLR model was used for data analysis with adjustments for gestational age and tissue processing time to account for oxygen changes. Among the 18 antioxidants, five were downregulated by maternal obesity, namely *SOD3, MGST3, GSTP1, GLRX, TXNRD1*. Figure 38 shows a scheme of the

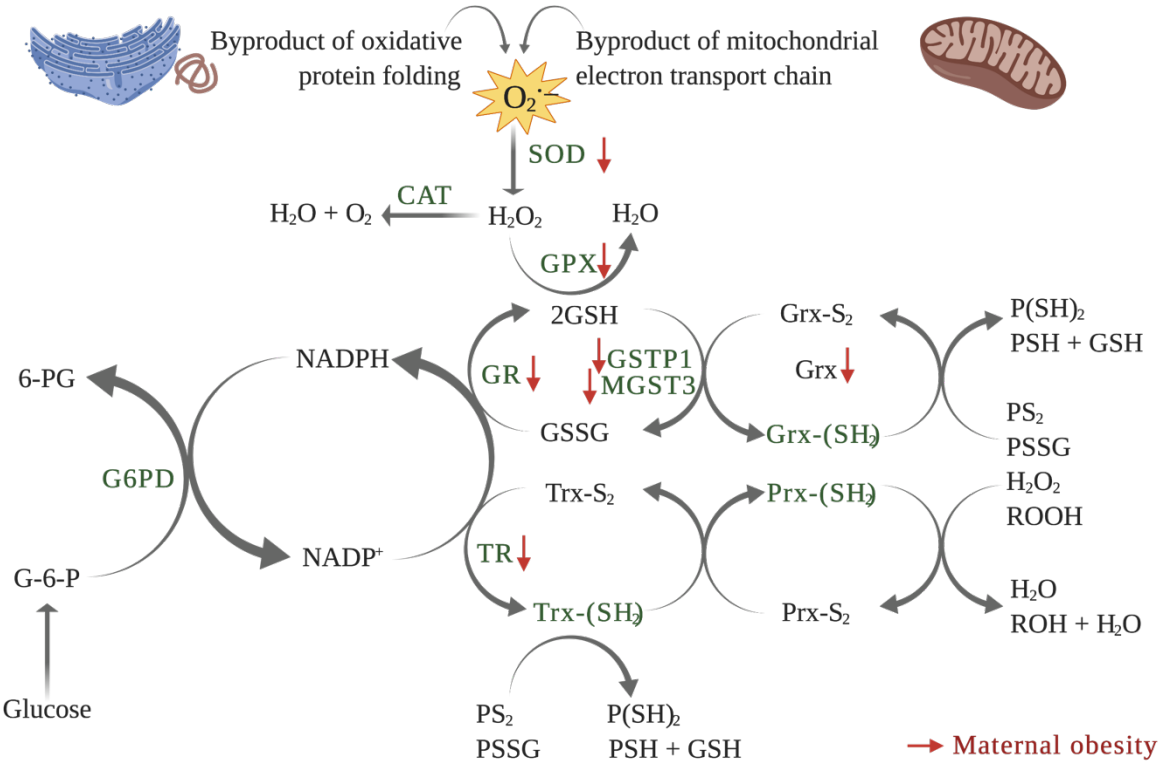

Figure 38: Schematic representation of the placental antioxidant defense system in the context of maternal obesity. Gene expression levels were determined in first trimester placental tissue from lean (n = 59) and obese (n = 41) women by Nanostring. Gene counts of Nanostring analysis were normalized to the mean of two different housekeeping (HK) genes WD repeat domain 45B (WDR45L) and TATA box binding protein (TBP). Pathway was created with Biorender.com. SOD2: Superoxide Dismutase 2, GPX: Glutathione Peroxidase, GSTP: Glutathione S-Transferase Pi, MGST3: Microsomal Glutathione S-Transferase 3, Grx: Glutaredoxin, TR: Thioredoxin Reductase

interrelationship of the antioxidants. The lower antioxidant levels were found mostly proximal to superoxide radical.

Interestingly, several of these genes are regulated by nuclear factor (erythroid-derived 2)-like 2 (Nrf2). Nrf2 is a key transcription factor in response to metabolic and oxidative stress that regulates genes containing antioxidant response elements (ARE) in their promoters (Wu and Papagiannakopoulos, 2020). Figure 39 shows metabolic and oxidative stress as Nrf2 inputs leading to regulation of iron metabolism via *HO-1* and glutathione or thioredoxin metabolism to counteract ROS and toxins. Although *Nrf2*-regulated genes were downregulated in FT placental tissue from obese pregnant women compared to lean controls, maternal obesity was not associated with altered expression of *Nrf2* in early pregnancy.

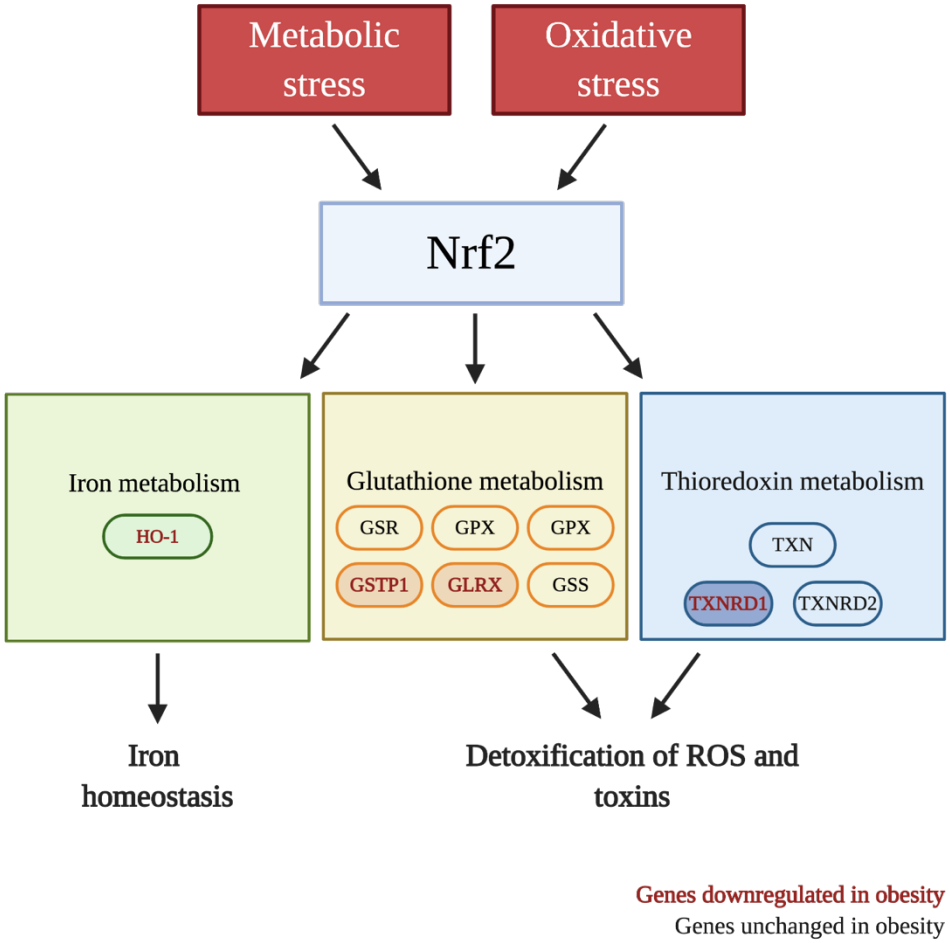

Figure 39: Major activating inputs and functional outputs of the NRF2 pathway including analyzed genes in this study. Obesity regulated are presented in bold and red. Black genes are not altered in first trimester placental tissue from obese pregnant women compared to lean controls. Modified from Wu and Papagiannakopoulos, 2020. Figure created with BioRender.com

So far, there are no other studies available on the effect of maternal obesity on FT placental antioxidative response. In general, chemical agents, e.g., drugs and environmental metabolites, may lead to downregulation or inactivation of antioxidants. Downregulated or inhibited cellular antioxidants may also cause oxidative stress, which contributes to tissue injury and disease pathophysiology (Zhu *et al.*, 2013). Although this study did not assess placental ROS directly, downregulation of placental antioxidants in the context of maternal obesity was not associated with an increase in various markers for oxidative stress. This is in concordance with our previous results showing no oxidative DNA modifications in the first trimester. Furthermore, we showed by *in vitro* H_2O_2 treatment and subsequent COMET assay, that FT placentas from obese pregnant women are more susceptible to oxidative DNA damage. Again,

this data indicates no oxidative stress environment, which could explain why antioxidants are not induced in placentas from obese pregnant women in early pregnancy.

In vitro culture of FT chorionic explants demonstrated that a physiological low oxygen environment (2.5% O_2) downregulated three of five obesity-downregulated antioxidants, while only TXNRD1 gene expression was higher and SOD3 was unaltered. This suggests that altered oxygen may be, at least for some FT placental antioxidants, a stimulus in the context of obesity. The results provide further evidence for absence of oxidative stress in FT placentas of obese mothers. One can speculate that spiral artery opening is insufficient or delayed, a notion supported by uterine leukocyte dysfunction in maternal obesity (St-Germain *et al.*, 2020). This would entail lower oxygen tension in intervillous space and placenta for the given gestational age. Hence, the stimulus for upregulation of defence systems would be absent.

To further test the hypothesis of absent placental oxidative stress in FT placentas associated with maternal obesity, we quantified classical stress marker HSP70 and HO-1 in FT placental tissue from lean and obese women. HSP70 is a molecular chaperone involved in repair of misfolded or aggregated proteins triggering cellular stress response mechanisms, e.g., unfolded protein response. Moreover, HSP70 suppresses stress-induced apoptosis (Daugaard, Rohde and Jäättelä, 2007; Reeg *et al.*, 2016). HO-1, i.e., the inducible isoform of heme oxygenase, catalyses the rate-limiting step in heme degradation. Reaction products are known to possess antioxidant, anti-inflammatory and cytoprotective functions (Wegiel *et al.*, 2014). Therefore, HSP70 and HO-1 exert cytoprotective functions and are upregulated by oxidative stress and inflammation (Zhao *et al.*, 2015; Radons, 2016). In the first trimester of pregnancy, protein levels of HSP70 and HO-1 are elevated in placentas of T1DM women linking placental cellular stress in T1DM with disturbances in placental development (Gauster *et al.*, 2017). In the present study, both stress-induced proteins HSP70 and HO-1 were not altered by maternal obesity in FT placental tissue arguing against an obesity-associated oxidative stress response in the FT placenta.

5.2. FT placental inflammatory stress in obese pregnant women

Obesity is described as a low-grade inflammatory condition that is associated with an increased production of pro-inflammatory factors (Xu *et al.*, 2003). Also pregnancy is considered as a natural inflammatory state as reflected by activation of maternal leucocytes and increased systemic concentrations of cytokines (Sacks *et al.*, 2004). The placenta is a source of a variety

of adipocytokines and cytokines, whose expression may be dysregulated by maternal obesity. Already in the first trimester of pregnancy placental villi express interleukin (*IL*) *6*, *IL10*, *IL1B* and *TNF-α* and others (Siwetz *et al.*, 2016). In late pregnancy, maternal obesity directly affects placental inflammation as is reflected by elevated cytokine production (Challier *et al.*, 2008; Roberts *et al.*, 2011). However, it is unknown if these changes already occur in the first trimester of pregnancy.

To close this knowledge gap, we assessed a selection of prominent cytokines in FT placentas from lean and obese women using a qPCR panel. At gestational week 7, gene expression of placental *IL1B*, *IL18* and *TNF-α* was not altered by maternal obesity. However, *IL6* mRNA levels were elevated compared to samples from lean pregnant women, while pro-inflammatory placental *IL1A* was lower in obese pregnant women. Early studies demonstrated an interaction of trophoblast-derived IL6 with IL6 receptor on the trophoblasts resulting in hCG release (Nishino *et al.*, 1990). IL1A significantly increases secretion of fetal fibronectin and the gene activity of matrix metalloproteinase gene 9 (Meisser *et al.*, 1999). This dysregulation of placental cytokines already in gestational week 7 might, therefore, not only indicate enhanced placental inflammation status, but may also affect trophoblast function.

5.3. First trimester placental stress signaling in obesity

In general, adaptive responses of cells and tissues include various signaling pathways eventually affecting cell fate (Kyriakis and Avruch, 2001; Takeda *et al.*, 2008). As an example, the classical stress response ASK/JNK pathway, comprising members of the MAP kinase family, is activated by a variety of environmental stress inputs and inflammatory cytokines. Hence, the obesity-associated placental environment might thus trigger placental stress signaling pathways. Therefore, we determined whether obesity in early pregnancy activates classical stress response signaling pathways in the FT placenta. To this end, we selected a set of prominent and well described stress signaling mediators and compared their gene expression levels between lean and obese FT placentas using the Nanostring gene expression approach. A MVLR model was used for statistical analysis with adjustments for gestational age and tissue processing time.

We found higher *ASK1* and *MAPK11* levels and lower *JNK1, ASK2*, *MAPK12* and *MAPK13* levels in FT placentas of obese pregnant women. The serine/threonine kinases ASK1 and ASK2 are MAP3K family members that induce apoptosis through the activation of classical

stress kinases JNK and p38 (Takeda *et al.*, 2008). In general, ASK1 and JNK downregulation points towards a decrease in stress response resulting in an anti-apoptotic effect (Figure 40). The three dysregulated MAPKs (*MAP3K, MAPK12, MAPK13*) are three of four p38 MAPKs isoforms that play an important role in responses induced by extracellular stimuli, e.g. proinflammatory cytokines or physical stress, that lead to direct activation of transcription factors (Kyriakis and Avruch, 2001). During early pregnancy cytotrophoblast differentiation and invasion involve p38 MAPK (Peters *et al.*, 2000; Delidaki *et al.*, 2011; Liu *et al.*, 2017).

TNF-α has been traditionally associated with obesity and is known to be elevated in the circulation of obese pregnant and non-pregnant women (Tzanavari, Giannogonas and Karalis, 2010; Stone *et al.*, 2014). Therefore, we treated FT chorionic explants with TNF-α for 24 hours using a physiological concentration (Siwetz *et al.*, 2016). Only two p38 MAPKs were significantly downregulated after treatment compared to untreated controls. Treating placental explants with only one selected cytokine may oversimplify the biological complexity of obesity effects on the first trimester of pregnancy. Furthermore, we cannot rule out concentration- and time-dependent effects in culture.

Our data suggest a complex interplay between placental environment in obesity and stress response pathways. Maternal obesity-induced dysregulation of MAPK gene expression may be a response to an altered intrauterine environment affecting not only placental cell fate pathways, but also important developmental function in the first trimester, which might in turn affect fetal development.

Future studies need to measure TNF-α concentrations in the maternal circulation and in culture supernatants of FT placental explants. This will allow assessing if TNF-α is elevated in obesity and if it may induce changes FT trophoblasts in obesity in an endocrine or para/autocrine manner.

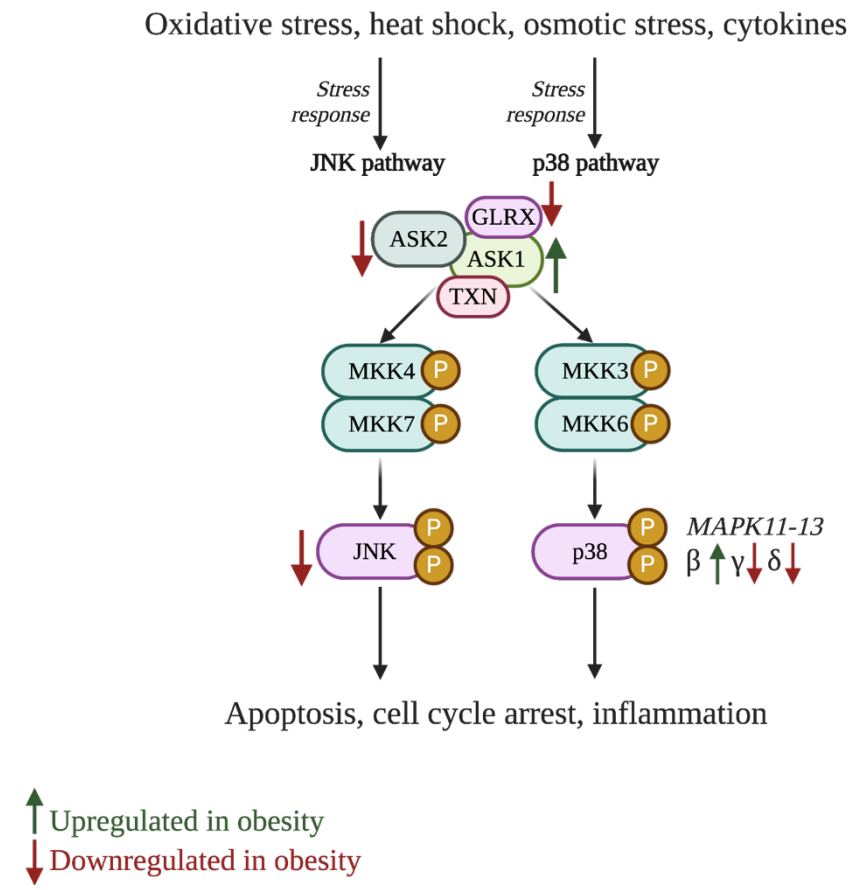

Figure 40: Major activating inputs and functional outputs of the JNK and p38 stress response pathways including analyzed genes in this study. Green arrows indicate upregulation in first trimester placental tissue from obese pregnant mothers while red arrows indicate downregulation compared to lean. Created with BioRender.com

5.4. DNA damage and telomere length in obesity

CTB growth and differentiation is the basis of tertiary villous tree expansion and leads to formation of different villus types (Castellucci *et al.*, 2000). The rate of CTB proliferation and turnover decreases during gestation. However, as the placenta grows exponentially during the first trimester of pregnancy, high CTB proliferation rates are necessary to accommodate growth. Alterations of either CTB proliferation or rate of syncytial fusion may have profound effects on the integrity of the syncytiotrophoblast. STB integrity is essential as this cell layer actively regulates placental transport from the mother to the fetus and releases hormones and extracellular vesicles to facilitate maternal adaptation to pregnancy. Altered villus growth, especially of gas-exchanging villi, may also impair diffusional exchange (Caniggia *et al.*, 2000).

In addition to oxidative DNA modification, also single- or double-strand breaks affect DNA integrity (Fontes *et al.*, 2015). In this study, we demonstrated higher levels of DNA damage in total first trimester placental tissue of obese pregnant woman compared to lean controls. We further aimed to identify the placental cell type that is affected by obesity-induced DNA damage and performed fluorescent triple staining with γH2AX. This trophoblast-specific *in situ* analysis included E-cadherin as trophoblast marker. E-cadherin was selected due to its higher fluorescence intensity on CTB, which enabled CTB specific analysis. The semi-automated image analysis script allowed a precise and unbiased count of CTB and positive signals. We did not assess STB DNA damage as we were interested in the CTB as trophoblast stem cells. We specifically showed that DNA damage in CTB is increased in the obese cohort, while stromal cells remained unaffected. High levels of DNA damage in CTB may directly affect cell proliferation or fusion leading to impaired STB integrity, which, in turn, may affect fetal growth. So far, studies have only focused on DNA damage in early pregnancies associated with later pregnancy pathologies, e.g., preeclampsia and IUGR. Recently, Cindrova-Davies *et al.* demonstrated increased levels of villous p21 and γH2AX in STB in both pathologies and suggested activation of DNA damage repair pathways in these first trimester placentas (Cindrova-Davies *et al.*, 2018).

Measuring telomere length is another way to estimate stability of the genetic material. Telomeres are gradually shortened with each cell division and are also affected by environmental factors such as oxidative stress (Gardner *et al.*, 2005). A previous study using quantitative fluorescence *in situ* and immunohistochemistry reported telomere shortening in third trimester placentas from IUGR and preeclampsia pregnancies (Biron-Shental *et al.*, 2010). Also in the third trimester, high maternal pre-pregnancy BMI was associated with significantly shorter placental telomeres (Martens *et al.*, 2016). Considering the association between obesity-associated telomere shortening, cellular aging and DNA damage signaling even in the absence of oxidative stress (Tzanetakou *et al.*, 2012), there is a clear lack of studies relating maternal obesity to early placental telomere length. In this present study we used a RT-qPCR-based approach for total placental tissue telomere analysis and also performed the same analysis with DNA isolated after laser-capture microdissection of trophoblasts. Neither maternal BMI nor maternal metabolic parameters, such as C-peptide and insulin sensitivity, were associated with placental telomere length in total FT placental tissue. However, laser-capture microdissected trophoblasts showed shorter telomeres with increased serum C-peptide levels and decreased

maternal insulin sensitivity, while telomere length was not associated with maternal BMI. This discrepancy between total tissue and trophoblast-specific results supports the concept of a cell-specific effect of obesity on telomere length in early pregnancy. Although telomere length was decreased in CTB from obese placentas, it might remain unaffected in the other cell types, i.e. stromal cells, thus masking the effect of obesity in total tissue. Due to the direct contact with the maternal circulation, trophoblasts are exposed to obesity-associated changes in the intervillous space. Therefore, consequences on this cell type are expected.

We further used quantitative fluorescence *in situ* hybridization (Q-FISH) to assess telomere length on FT tissue sections. After image segmentation, only trophoblast nuclei were analyzed. Again, trophoblast telomeres were shorter with increasing C-peptide levels and low insulin sensitivity in the pregnant women confirming above results. However, in this analysis also maternal BMI, i.e. obesity, was associated with shorter telomeres *in situ*. This data may differ from the laser-capture microdissection qPCR results, because we used different samples for both methods as the amount of FT material was not sufficient enough to be used for both methods.

Outside pregnancy, shorter telomeres have been associated with increasing BMI, increased adiposity and excess visceral fat accumulation , thus, linking obesity with accelerated aging processes that also trigger DNA damage response (Demissie *et al.*, 2006). Telomere shortening might not only induce DNA damage signaling but may also affect CTB turnover finally impairing syncytialization. Telomere length is generally related to cellular ageing as the repetitive sequences get shorter at each DNA replication. As soon as a critical length is reached, telomeres trigger DNA repair and cell cycle checkpoint modification resulting in cell cycle arrest, senescence and/or apoptosis (Shin *et al.*, 2006).

5.5. Placental DNA damage repair and consequences for cell cycle progression

We found elevated levels of DNA damage in placenta tissue of obese women with predominant location to the CTB. Thus, obesity-associated placental DNA damage in CTB may ultimately lead to mutations and genomic instability affecting cell fate (Fontes *et al.*, 2015). This DNA damage in the form of single and double strand breaks needs repair to make CTB proliferation possible. To this end, cells will have to undergo cell cycle arrest to allow the repair machinery to act. Ultimately, only adequate removal of damaged DNA will ensure proper CTB function.

5.5.1. DNA damage repair

Cells with defects in DNA damage repair are more sensitive towards DNA damaging agents leading to cytotoxicity, mutagenesis, cell death, and disease. Repair of different types of DNA lesions involves a variety of proteins that undergo crosstalk and form a network to protect the cellular genome (Moreli *et al.*, 2014). According to a recent study in mouse placentas, impaired function of cohesins, protein complexes stabilizing 3D-structure of chromatins, results in persistent DNA damage triggering cytokine production and senescence (Singh, McKinney and Gerton, 2020).

Although eight DNA damage repair genes were higher in placentas of obese women at pregnancy week 7 (qPCR), Nanostring analysis of 101 FT placentas spanning a broad gestational age and BMI range showed lower levels of five DNA damage related genes, while only HDAC8 was higher. The heatmap further shows gene expression changes associated with gestational age, as observed using a MVLR model. Also, Nanostring sub-analysis of week 7 samples is not in line with qPCR data, showing also downregulation of 3 repair genes. These differences may be explained due to biological and technical variability, since different samples and different target genes were included in each assay. Nevertheless, affected pathways included base excision repair, non-homologous end joining and homologous recombination regardless of the method used.

This data indicates a complex and gestational age-dependent orchestration of various signaling pathways, e.g., BER, NER and double strand break repair, as consequences of obesity-associated DNA damage. Inter-individual variations in the activity of DNA repair transducers have been described (Allione *et al.*, 2013). Thus, extensive differences in efficiency of DNA repair can be expected (Nagel, Chaim and Samson, 2014). Importantly, all genes with lower expression levels in obesity also showed lower expression after *in vitro* treatment of chorionic villous explants with TNF-α (*HDAC8, HDAC1, BLM, PAFP1, Ku70, PCNA, FEN1*). Furthermore, *HDAC1* and *PCNA* expression decreased after culture at 2.5% O_2. Thus, reduced expression of genes involved in DNA damage repair in FT placental tissue may be the result of obesity-associated increase in circulating TNF-α levels (Challier *et al.*, 2008) or of lower oxygen levels in the intervillous space in this condition. Should gene expression translate into less protein and less DNA damage repair activity, then increased DNA damage in FT placentas

may be the result of either more damage induced by the environment, reduced repair activity or both.

Although gene expression data argues for functioning repair at week 7 and decreased DNA repair capacity when corrected for gestational age, protein analysis is crucial to understand signaling and activation of repair transducers. In mammalian cells, the ATM, ATR, and DNA-PKcs kinases are the most upstream DNA damage repair kinases. In response to damaged DNA, hundreds of proteins are phosphorylated at Ser/Thr-Glu motifs in an ATM- or ATR-dependent manner (Maréchal and Zou, 2013). Therefore, we performed Western blot analysis for ATM, ATR and for phosphorylation of AMT/ATR substrates. Furthermore, we assessed levels of downstream proteins p53, NBS1, GADD45α, PCNA, NEIL3 and APE1. Both, ATM and ATR protein levels were higher in FT placentas of obese women compared to lean controls independent of gestational age. Increase in placental AMT/ATR substrate phosphorylation in obesity was also borderline significant. While p53 phosphorylation, NBS1 and PCNA protein levels were not altered by maternal obesity, NEIL3 was increased by trend and obesity induced GADD45a and APE1 protein levels. All together this data indicates partial activation of the ATM/ATR signaling pathway in placentas of obese pregnant women already in the first trimester of pregnancy.

To the best of our knowledge this is the first study on placental DNA damage signaling in the context of obesity. However, DNA damage repair was evaluated in lymphocytes of non-pregnant subjects with T1DM and T2DM (Blasiak *et al.*, 2004; Pácal *et al.*, 2011). The results suggest that T2DM may not only be associated with elevated levels of DNA damage, but also with decreased efficacy of DNA damage repair (Blasiak *et al.*, 2004). Lymphocyte DNA damage was more pronounced and DNA repair capacity more decreased in individuals with T2DM when compared with T1DM (Pácal *et al.*, 2011). This impaired efficacy of DNA repair may lead to DNA damage accumulation in the FT placenta of obese women affecting specifically CTB function.

5.5.2. Cell cycle regulation

Cell cycle arrest is mandatory for DNA damage repair as it gives cells time to repair critical DNA damage before replication continues. After successful DNA damage repair, the cell cycle can resume or, if the damage is too extensive, the cell will undergo apoptosis (Awasthi et al., 2016). The effect of increased DNA damage and alterations in DNA damage repair may thus affect placental cell cycle. In this study, we used a qPCR panel and a cell cycle specific protein array to assess FT placental cell cycle of lean and obese pregnant women. Obesity affected gene expression of 9 out of 187 cell cycle regulators, with *ERCC5* and *BRCA1* showing the highest fold increase between samples from lean and obese women. Moreover, obesity increased the level of 22 out of 95 analyzed proteins, e.g., Rad52 and BRCA1. Figure 41 shows obesity-

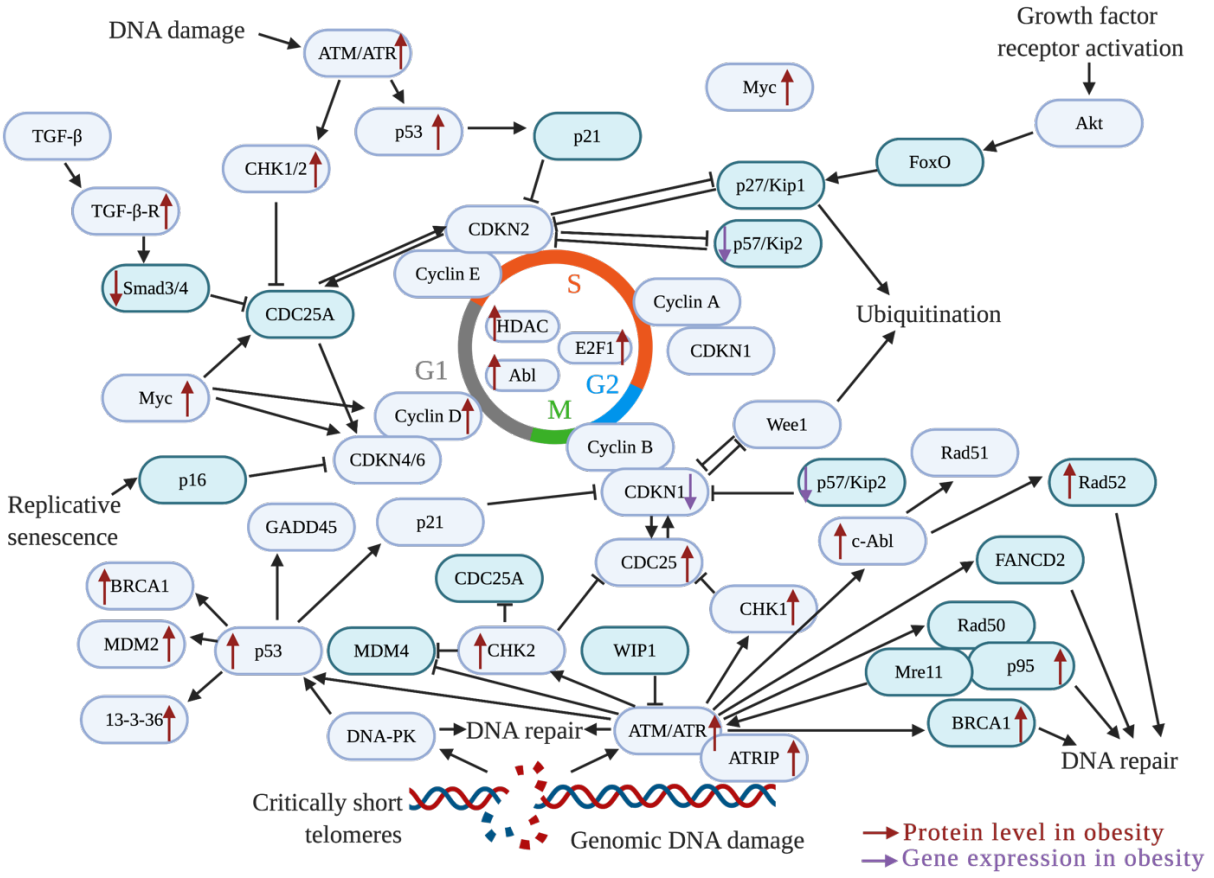

Figure 41: Maternal obesity-induced cell cycle dysregulation in first trimester (FT) placenta. Despite triggering repair responses and upregulation of DNA damage checkpoint kinases CHK1 and CHK2, maternal obesity does not alter cell cycle master regulators (Cyclins, cyclin-dependent kinases, cyclin-dependent kinase inhibitors). Expression of 238 cell cycle related proteins in human FT placental tissue lysates (week 5-7) were compared using a protein array. Pathway was created with Biorender.com

associated alterations in gene expression and protein levels in the context of cell cycle regulation.

In general, data suggests that obesity negatively affects placental cell cycle control already in the FT of pregnancy. This may in turn compromise CTB proliferation and differentiation into EVTs, altering invasion and spiral artery remodeling, and might set the basis for obesity-associated pregnancy disorders, e.g. preeclampsia (Lopez-Jaramillo *et al.*, 2018).

Based on its consistent upregulation at the gene and the protein level, we subsequently characterized the effect of maternal obesity on BRCA1 as a specific cell cycle modulator. BRCA1 upregulation was further confirmed by Nanostring and Western blotting and localized to nuclei of CTB, STB and extravillous cytotrophoblasts. Classically, BRCA1 has been studied in the context of ovarian and breast cancer (Varol *et al.*, 2018), where it mainly functions to establish adequate DNA damage response (Savage *et al.*, 2014; Krieger *et al.*, 2019). Furthermore, it also plays a pivotal role in cell cycle checkpoint regulation via p27 activation inducing G1-cell cycle arrest, p53-dependent blocking of S-phase entry, and activation of G2/M-arrest through 14-3-3 zeta/delta activation (Deng, 2006; Wu, Lu and Yu, 2010). In our study, not only BRCA1, but also several of its protein binding partners were upregulated by maternal obesity. These include 14-3-3 zeta/delta, chk1, and chk2. The latter is part of a pathway involving cdc25 and pSer1423-BRCA1 leading to cell cycle arrest (Kastan and Bartek, 2004; Ouchi, 2006). BRCA1 phosphorylation at Ser1423 fine-tunes its function. Obesity-associated upregulation of BRCA1 phosphorylation may involve several kinases, including CHK2, Akt, and ATM, the latter is directly involved in BRCA1 phosphorylation at Ser 1423 (Ouchi, 2006). Enhanced BRCA1 phosphorylation in maternal obesity may reflect additional BRCA1 interactions with various cell cycle regulators (Okada and Ouchi, 2003).

To identify short-term drivers of changes in FT placental cell cycle regulators, we tested TNF-α and low, i.e., 2.5%, oxygen in FT chorionic villus explants. Short term treatment with TNF-α decreased gene expression of *cyclin A1, cyclin B1, cyclin E1, CHEK1, CHEK2* and *RAD51*. In concordance with *cyclin E1* downregulation, the specific inhibitor *CDKN1A* was upregulated in FT chorionic villous explants after TNF-α treatment. We further assessed the effect of altered oxygen levels on core cell cycle regulators. Here, only *cyclin A1* and *cyclin D1* were upregulated while *cyclin B1* gene expression was decreased by low oxygen, respectively. *In vitro* treatment of explants from lean women only allows testing for short-term

effects (48 h). This short time period may not be sufficient to induce changes similar to those seen as the result to the obesity environment after long-term tissue exposure *in vivo*.

Interestingly, CHK1 and CHK2 protein levels were also higher in FT placentas from obese pregnant women. Together with ATR interacting protein (ATRIP), they establish the main link between DNA damage response and cell cycle arrest. ATRIP interacts with ATR which results in its accumulation at intranuclear foci after DNA damage (Saldivar, Cortez and Cimprich, 2017).

The proposed interplay between obesity-induced DNA damage and telomere shortening with subsequent damage recognition via γH2AX (Fernandez-Capetillo *et al.*, 2003; Plesca, Mazumder and Almasan, 2008) and ATM/ATR induced damage repair with subsequent cell cycle arrest is shown in Figure 42.

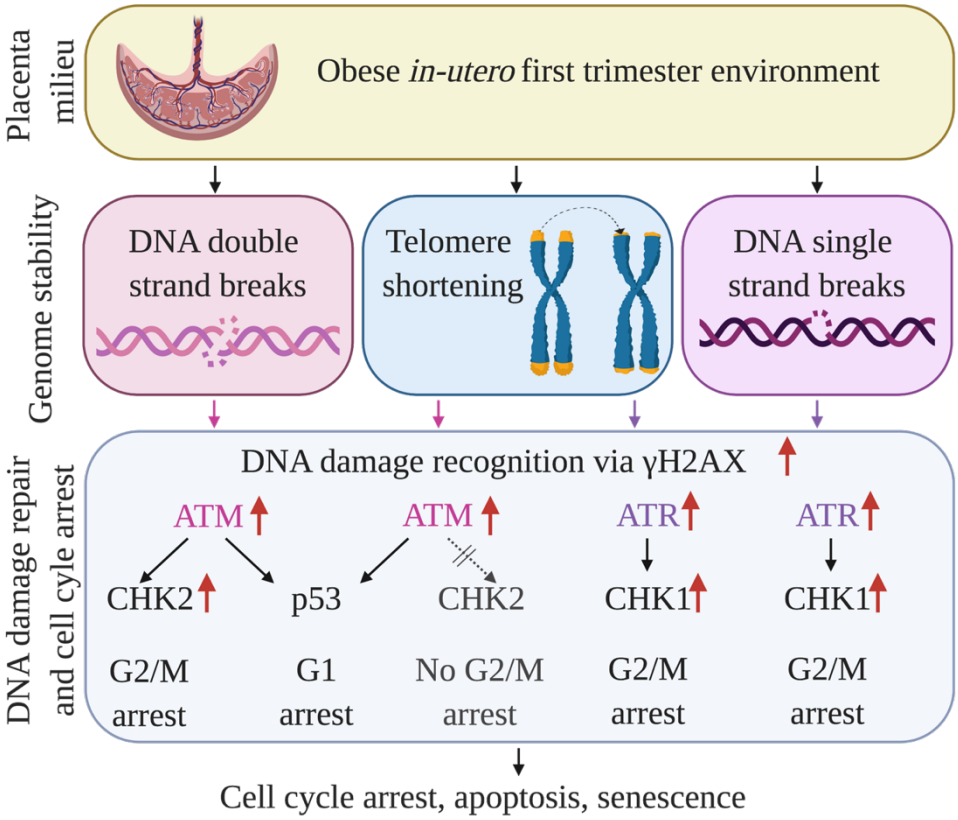

Figure 42: Placental milieu affects genome stability with consequences for DNA damage repair and cell cycle regulation. DNA damage and telomere shortening may activate placental DNA damage response and upregulate CHK1 and CHK2 – two critical messengers of the genome integrity checkpoints – with

potential consequences for cell cycle regulation in first trimester placenta of obese women. Scheme was created with Biorender.com

5.6. FT CTB turnover in an obesity-associated in utero environment

The villus trophoblast compartment undergoes continuous turnover as a physiologic process to maintain cellular homeostasis. It includes CTB stem cell proliferation, fusion of daughter CTB into the overlying syncytium, progression towards apoptotic cell death and, finally, removal of apoptotic nuclei by their shedding into the maternal circulation in syncytial knots. It has been proposed that pathological pregnancy conditions may result from altered trophoblast turnover. This would not only affect placental function, but also the mother and, indirectly, the fetus (Huppertz, Kaufmann and Kingdom, 2002). In general, DNA instability directly affects cellular turnover by DNA damage repair activating cell cycle arrest (Lavin, 2008).

In this study, we aimed to assess obesity-associated alterations in trophoblast turnover reflected by changes in CTB proliferation and apoptosis. To this end, we used semi-quantitative *in situ* analysis to specifically determine proliferation and apoptosis reflected by quantifying Ki67 (proliferation) and TUNEL assay/CK18 (apoptosis) IF staining, respectively. Data was analyzed using a MVLR model with BMI as a categorical variable adjusted for gestational age and tissue processing time. The TUNEL reaction labels DNA strand breaks generated during apoptosis. Therefore, it is a marker for DNA degradation, an early-stage event of apoptosis. TUNEL assay is generally used to assess cell apoptosis as labelling DNA fragments is a well-accepted and widely used histological method for detecting apoptotic cells. However, apoptotic and necrotic cells cannot always be distinguished by TUNEL staining and sometimes this assay falsely identifies cells in the process of DNA damage repair (Watanabe *et al.*, 2002). Therefore, TUNEL assay results need to be often supported by a second method for apoptosis assessment. Here, CK18 staining was the method of choice as cleavage of CK18 is an early apoptotic event specifically in epithelial cells, e.g. FT trophoblasts (Caulín, Salvesen and Oshima, 1997). CK18 is cleaved by caspases at multiple sequence sites during early apoptosis CK18 fragments can be specifically detected by M30 antibody.

CTB proliferation was reduced in first trimester placental tissue from obese women, while proliferation of stromal cells was unaffected. A study in obese mice found significantly reduced cell proliferation and a reduced number of cytotrophoblasts that may further be associated with reduced STB formation (Kim *et al.*, 2014). Also, our data may suggest that

reduced cytotrophoblast proliferation leads to less syncytialization, contributing to reduced STB expansion and, ultimately, compromised early placental growth. This may lead to placental dysfunction in the first trimester of pregnancies of obese women.

Reduced proliferation was paralleled by enhanced cytotrophoblast apoptosis, reflected by TUNEL positive cells within the trophoblast compartment. However, number of TUNEL positive cells within the stroma was not affected by maternal obesity. TUNEL assay results were confirmed by CK18 staining. Correspondingly, trophoblasts of FT placentas exposed to an obesity-associated *in utero* environment show increased CK18 intensity. This increase in CTB apoptosis might also affect CTB differentiation and syncytial fusion with consequences for STB morphology (Huppertz, Kaufmann and Kingdom, 2002), ultimately affecting placental function.

Cellular senescence may be one potential consequence of obesity-induced DNA damage. Thus, we quantified a key protein in the senescence pathway, p16 protein (Cox and Redman, 2017), in placental tissues from lean and obese women. Results demonstrate that maternal obesity did not affect protein levels of p16 in the FT placenta. Placental senescence is often studied in the context of ageing characterized by high levels of telomere aggregates, triggered DNA damage response, altered cell cycle regulation and mitochondrial dysfunction (Manna, McCarthy and McCarthy, 2019). Thus, our study may indicate that maternal obesity in early pregnancy rather induces apoptosis and decreases CTB turnover without an irreversible arrest of cell proliferation, while the cell maintains its metabolic function.

5.7. Strengths and limitations

In general, first trimester material matched with maternal serum samples are very rare worldwide. It is an asset of this study that exclusively tissue from human first trimester placentas was used without isolating its cellular constituents. In total tissue the spatial arrangement of cells is maintained, and the cells are embedded in extracellular matrix. Tissue sampling and processing were standardized and well-documented. We included samples from very early in gestation (starting from gestational week 4^{+0}) and spanned the full range until the end of the first trimester (gestational week 11^{+6}). However, we excluded women with co-morbidities and under current medication. Because of the well-known effect of smoking to induce oxidative stress, it was mandatory to carefully exclude smokers. Hence, these were

identified by both self-report in a questionnaire and by measuring cotinine levels in the maternal circulation.

In the first trimester of human pregnancy oxygen tension in the intervillous space and within the placenta physiologically rise, a process that is essential for proper development and adequate trophoblast function (Jauniaux *et al.*, 2000; Burton, Jauniaux and Charnock-Jones, 2010; Cindrova-Davies *et al.*, 2014). Therefore, it was essential to include gestational age as a confounding factor for all statistical analyses performed on the cohort covering the first trimester. We also recorded the time (minutes) between pregnancy termination and tissue cryo-preservation, i.e. processing time. This is important, because tissue exposure to ambient oxygen after pregnancy termination may affect the outcomes analyzed in this study. For all these analyses, we used a statistical MVLR model to adjust for the *a priori* defined confounders, i.e., gestational age and tissue processing time.

We also have to acknowledge some apparent limitations to this study. The preservation methods used in this study, i.e., snap freezing and formalin-fixation followed by paraffin embedding, made a direct measurement of placental oxidative stress or ROS content impossible also because of the very short half-life of ROS. Also, the half-time of ROS is very short. We could only measure indirect readouts of oxidative stress. Therefore, we cannot fully rule out oxidative stress as principle cause of obesity related CTB DNA damage.

A main limitation was the lack of protein data for antioxidants, stress signaling genes and most DNA damage repair transducers. Furthermore, the effect of obesity-induced stress on placental tissue is rather diverse and requires a broad range of experiments on a tissue, which is limited in size. Therefore, the study design chosen was a compromise as not all experiments can be conducted. Nonetheless, the large sample size for gene expression analysis and trophoblast specific *in situ* analysis is a major strength. As the syncytiotrophoblast is in contact with maternal blood and, therefore, directly affected by maternal metabolic changes, trophoblast specific *in situ* analysis with fluorescent quantification of DNA damage, proliferation and apoptosis is crucial to understand changes of biological importance. Here, a further trophoblast specific analysis of senescence markers is missing.

In the present study all *in vitro* experiments with human first trimester placental tissue were conducted in a physiological, i.e., low, oxygen environment. This is a major strength and

avoids potential hyperoxic effects of ambient oxygen (21% O_2), which by itself may overwhelm antioxidative defense systems and induce oxidative stress. We used TNF-α as the cytokine most prominently associated with the pro-inflammatory environment of obesity (Pendeloski et al., 2017). However, concentration and time-dependent effects of TNF-α or other pro-inflammatory cytokines cannot be ruled out. An important limitation of the *in vitro* experiments is their short-term nature, different from the *in vivo* situation. *In vivo*, placental tissue is exposed to the obesity-associated environment for several weeks, a condition difficult to mimic in an *in vitro* setting. Hence, the short-term exposure might not have been long enough to induce changes seen as the result of long-term tissue exposure to the obesity environment.

5.8. Future studies

The present study used human first trimester placental tissue after pregnancy termination for psychosocial reasons. Thus, sampling happens in a critical time period in pregnancy and the number of samples is limited. Further studies should increase sample size for obese women in early first trimester and aim to include more extremes of the morbidly obese group, i.e., with BMI ≥ 40.

Future studies should take into account that maternal BMI is easy to calculate, but it may not fully reflect the maternal metabolic status and is a poor indicator of fat mass (Dybala *et al.*, 2019; Hyun *et al.*, 2019). Obesity may be associated with different degrees of inflammation, and in a subgroup of obese pregnant women inflammation may be absent at all. This condition is described as metabolically healthy obesity, although women would be categorized as obese based on their BMI (Blüher, 2019). Hence, in future research metabolic and inflammatory characteristics of all subjects should be carefully determined. This would allow for a better categorization of the women than by BMI. Moreover, the cohort can then be stratified into subgroups on the basis of metabolic serum parameters, e.g., leptin, glucose, C-peptide and calculated insulin sensitivity, which will be biologically more relevant than using BMI.

In this study we found significantly decreased gene expression of HO-1 in placental tissue from obese pregnant women and also mRNA of key antioxidants was lower. Moreover, stress signaling pathways are likely less activated. As suggested above, this may reflect less oxidative stress in the placenta in obesity. If this were confirmed by direct measurements, then one might speculate that spiral artery remodeling is either delayed or reduced in maternal

obesity in early pregnancy. Our data are supported by findings in human (Perdu *et al.*, 2016; Castellana *et al.*, 2018; St-Germain *et al.*, 2020) and a life-long obesity rat model where a delay in spiral artery remodeling was demonstrated (Hayes *et al.*, 2014). The early human embryo and FT placenta is nourished through a histiotrophic route before onset of maternal blood flow (Hempstock *et al.*, 2004; Perdu *et al.*, 2016; St-Germain *et al.*, 2020). Thus, spiral artery remodeling as well as the composition of secretions from endometrial glands in obesity remain to be studied, since they might also entail consequences for early placental growth and development.

Future studies should snap-freeze placenta tissue immediately after the surgical procedure or, ideally, tissue obtained from chorionic villus sampling should be used. Cryo-sections would then allow determining dihydroethidium (DHE), Mito-SOX or dichloro-dihydro-fluorescein diacetate (DCFH-DA) staining as a direct measure for placental oxidative stress. Moreover, the consequences of the altered trophoblast turnover for placental function remains to be elucidated.

Already between gestational week 11 and 13 the placental transcriptome differs between male and female fetuses indicating sex-specific responses already in late first trimester of human pregnancy (Gonzalez *et al.*, 2018; Sun *et al.*, 2020). Therefore, the influence of fetal sex on FT placental DNA integrity and stress response needs to be further considered.

Including extreme cases of obesity may help to identify the cause of increased DNA damage in first trimester CTBs of obese pregnant women. So far, we seem to have ruled out oxidative stress as the main trigger. Therefore, maternal FT serum samples of obese and lean women should be analyzed using metabolomics. This may lead to characterization of metabolic derangements that underlie obesity and affect early placental development.

5.9. Conclusion

To the best of our knowledge, this is the first study assessing the influence of maternal obesity specifically on placental DNA integrity and stress response during the first trimester of pregnancy. A proposed scheme of obesity-associated effects is shown in Figure 43.

In conclusion, we found no evidence for obesity-associated oxidative placental stress by assessing various markers, signaling pathways and byproducts of oxidative stress on gene and protein level in FT placentas of lean and obese women.

Furthermore, the results of this thesis may suggest that maternal obesity in early human pregnancy alters CTB turnover by:

- inducing DNA damage specifically in CTB
- trophoblast telomere shortening
- dysregulation of DNA damage repair pathways
- induction of cell cycle arrest
- decreasing proliferation and increasing apoptosis

Components of the maternal environment and underlying mechanisms leading to these changes remain to be studied as well as specific consequences for early placental development. Overall, maternal obesity in the first trimester might alter placental development with potentially ensuing adverse consequences for maternal and fetal health.

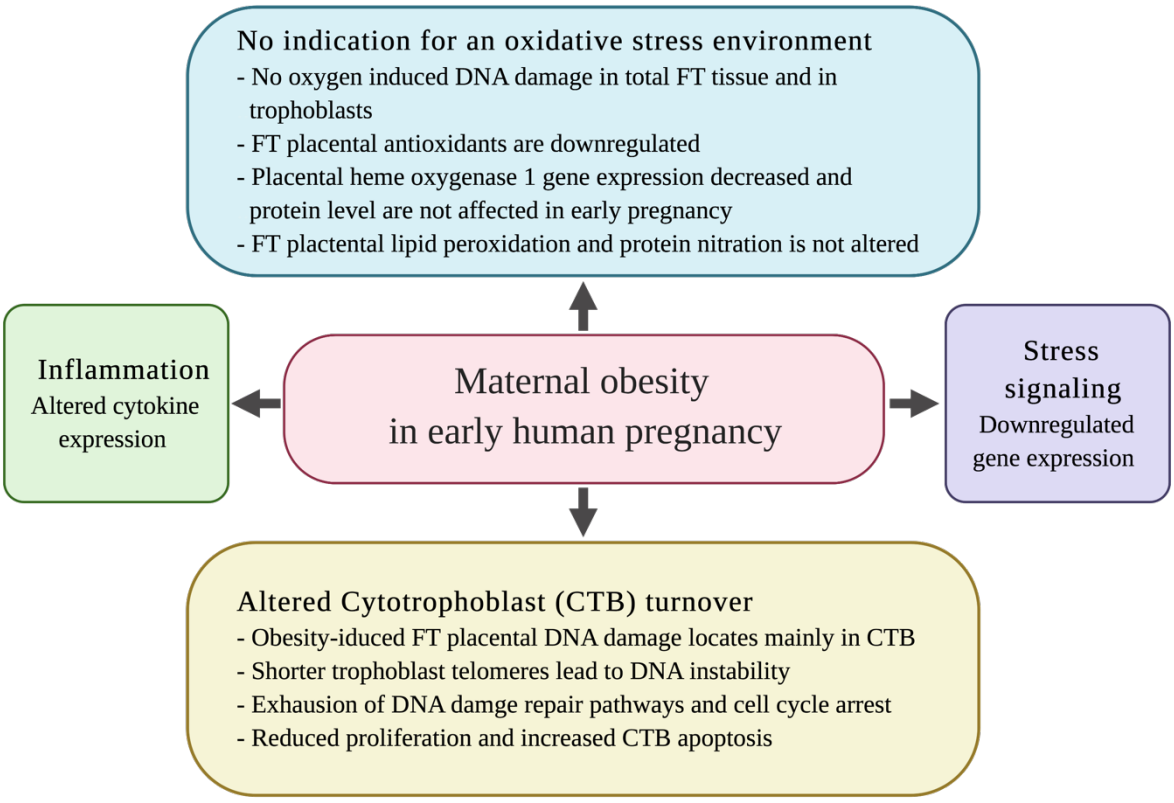

Figure 43: Proposed effect of maternal obesity on first trimester placental function. Created with BioRender.com

6. References

Abdullah, A. *et al.* (2010) 'The magnitude of association between overweight and obesity and the risk of diabetes: a meta-analysis of prospective cohort studies.', *Diabetes research and clinical practice*. Ireland, 89(3), pp. 309–319. doi: 10.1016/j.diabres.2010.04.012.

Abrahams, V. M. *et al.* (2004) 'Macrophages and apoptotic cell clearance during pregnancy.', *American journal of reproductive immunology (New York, N.Y. : 1989)*, 51(4), pp. 275–82. doi: 10.1111/j.1600-0897.2004.00156.x.

Agarwal, A. and Bolisetty, S. (2013) 'Adaptive responses to tissue injury: role of heme oxygenase-1', *Transactions of the American Clinical and Climatological Association*. American Clinical and Climatological Association, 124, pp. 111–122. Available at: https://pubmed.ncbi.nlm.nih.gov/23874015.

Ahmed, A. *et al.* (2000) 'Regulation of placental vascular endothelial growth factor (VEGF) and placenta growth factor (PIGF) and soluble Flt-1 by oxygen - A review', *Placenta*, 21(SUPPL.1), pp. 16–24. doi: 10.1053/plac.1999.0524.

Al-Aubaidy, H. A. and Jelinek, H. F. (2011) 'Oxidative DNA damage and obesity in type 2 diabetes mellitus.', *European journal of endocrinology*. England, 164(6), pp. 899–904. doi: 10.1530/EJE-11-0053.

Aldo, P. B. *et al.* (2014) 'Trophoblast induces monocyte differentiation into CD14+/CD16+ macrophages.', *American journal of reproductive immunology (New York, N.Y. : 1989)*, 72(3), pp. 270–84. doi: 10.1111/aji.12288.

Allione, A. *et al.* (2013) 'Inter-individual variation in nucleotide excision repair pathway is modulated by non-synonymous polymorphisms in ERCC4 and MBD4 genes', *Mutation Research - Fundamental and Molecular Mechanisms of Mutagenesis*. Netherlands, 751–752(1), pp. 49–54. doi: 10.1016/j.mrfmmm.2013.08.005.

Alvarez, B. and Radi, R. (2003) 'Peroxynitrite reactivity with amino acids and proteins', *Amino Acids*, 25(3–4), pp. 295–311. doi: 10.1007/s00726-003-0018-8.

Anderson, D. *et al.* (1998) 'An examination of DNA strand breakage in the comet assay and antioxidant capacity in diabetic patients.', *Mutation research*. Netherlands, 398(1–2), pp. 151–161.

Aplin, J. D. (2010) 'Developmental cell biology of human villous trophoblast: current research problems', *The International Journal of Developmental Biology*, 54(2–3), pp. 323–329. doi: 10.1387/ijdb.082759ja.

Awasthi, P. *et al.* (2016) 'ATM and ATR signaling at a glance CELL SCIENCE AT A GLANCE ATM and ATR signaling at a glance', pp. 4255–4262. doi: 10.1242/jcs.188631.

Aye, I. L. M. H. *et al.* (2014) 'Increasing maternal body mass index is associated with systemic inflammation in the mother and the activation of distinct placental inflammatory pathways.', *Biology of reproduction*, 90(6), p. 129. doi: 10.1095/biolreprod.113.116186.

Baczyk, D. *et al.* (2004) 'Complex patterns of GCM1 mRNA and protein in villous and extravillous trophoblast cells of the human placenta.', *Placenta*, 25(6), pp. 553–9. doi:

10.1016/j.placenta.2003.12.004.

Baczyk, D. *et al.* (2006) 'Bi-potential behaviour of cytotrophoblasts in first trimester chorionic villi.', *Placenta*, 27(4–5), pp. 367–74. doi: 10.1016/j.placenta.2005.03.006.

Bandres-Meriz, J. *et al.* (2020) 'Maternal Obesity Affects the Glucose-Insulin Axis During the First Trimester of Human Pregnancy', *Frontiers in Endocrinology*, 11(October). doi: 10.3389/fendo.2020.566673.

Baptiste Auguie (2017) 'gridExtra: Miscellaneous Functions for "Grid" Graphics', *R package version 2.3*. Available at: https://cran.r-project.org/package=gridExtra.

Barnes, R. P., Fouquerel, E. and Opresko, P. L. (2019) 'The impact of oxidative DNA damage and stress on telomere homeostasis', *Mechanisms of Ageing and Development*, 177(3), pp. 37–45. doi: 10.1016/j.mad.2018.03.013.

Barzilai, A. and Yamamoto, K. I. (2004) 'DNA damage responses to oxidative stress', *DNA Repair*, 3(8–9), pp. 1109–1115. doi: 10.1016/j.dnarep.2004.03.002.

Basu, S. *et al.* (2011) 'Pregravid Obesity Associates With Increased Maternal Endotoxemia and Metabolic Inflammation', *Obesity*, 19(3), pp. 476–482. doi: 10.1038/oby.2010.215.

Bauer, S. *et al.* (2004) 'Tumor necrosis factor-alpha inhibits trophoblast migration through elevation of plasminogen activator inhibitor-1 in first-trimester villous explant cultures.', *The Journal of clinical endocrinology and metabolism*. United States, 89(2), pp. 812–822. doi: 10.1210/jc.2003-031351.

Bausenwein, J. *et al.* (2010) 'Elevated levels of oxidized low-density lipoprotein and of catalase activity in follicular fluid of obese women.', *Molecular human reproduction*. England, 16(2), pp. 117–124. doi: 10.1093/molehr/gap078.

Bautista-Castaño, I. *et al.* (2013) 'Maternal obesity in early pregnancy and risk of adverse outcomes.', *PloS one*, 8(11), p. e80410. doi: 10.1371/journal.pone.0080410.

Bellver, J. *et al.* (2011) 'Endometrial gene expression in the window of implantation is altered in obese women especially in association with polycystic ovary syndrome.', *Fertility and sterility*. United States, 95(7), pp. 2335–41, 2341.e1–8. doi: 10.1016/j.fertnstert.2011.03.021.

Bellver, J. *et al.* (2013) 'Obesity reduces uterine receptivity: clinical experience from 9,587 first cycles of ovum donation with normal weight donors.', *Fertility and sterility*. United States, 100(4), pp. 1050–1058. doi: 10.1016/j.fertnstert.2013.06.001.

Benirschke, K. *et al.* (2000) 'Early Development of the Human Placenta', in *Pathology of the Human Placenta*. New York, NY: Springer New York, pp. 42–49. doi: 10.1007/978-1-4757-4199-5_5.

Bennett, W. A. *et al.* (1997) 'Expression and production of interleukin-10 by human trophoblast: relationship to pregnancy immunotolerance.', *Early pregnancy : biology and medicine : the official journal of the Society for the Investigation of Early Pregnancy*. United States, 3(3), pp. 190–198.

Benowitz, N. L. *et al.* (2009) 'Optimal serum cotinine levels for distinguishing cigarette smokers and nonsmokers within different racial/ethnic groups in the United States between 1999 and 2004', *American Journal of Epidemiology*, 169(2), pp. 236–248. doi: 10.1093/aje/kwn301.

Berger, M. *et al.* (1983) '[The value of education of diabetics in the therapy of type 1 diabetes].', *Deutsche medizinische Wochenschrift (1946)*. Germany, 108(11), pp. 424–430. doi: 10.1055/s-2008-1069573.

Berghöfer, A. *et al.* (2008) 'Obesity prevalence from a European perspective: a systematic review.', *BMC public health*, 8, p. 200. doi: 10.1186/1471-2458-8-200.

Biron-Shental, T. *et al.* (2010) 'Telomeres are shorter in placental trophoblasts of pregnancies complicated with intrauterine growth restriction (IUGR)', *Early Human Development*. Elsevier Ltd, 86(7), pp. 451–456. doi: 10.1016/j.earlhumdev.2010.06.002.

Black, S. *et al.* (2004) 'Syncytial fusion of human trophoblast depends on caspase 8', *Cell Death & Differentiation*, 11(1), pp. 90–98. doi: 10.1038/sj.cdd.4401307.

Blaschitz, A. *et al.* (2015) 'Adhering maternal platelets can contribute to the cytokine and chemokine cocktail released by human first trimester villous placenta.', *Placenta*. Elsevier Ltd, 36(11), pp. 1333–6. doi: 10.1016/j.placenta.2015.09.002.

Blasiak, J. *et al.* (2004) 'DNA damage and repair in type 2 diabetes mellitus.', *Mutation research*. Netherlands, 554(1–2), pp. 297–304. doi: 10.1016/j.mrfmmm.2004.05.011.

Blüher, M. (2019) 'Obesity: global epidemiology and pathogenesis', *Nature Reviews Endocrinology*. England, 15(5), pp. 288–298. doi: 10.1038/s41574-019-0176-8.

Boots, C. and Stephenson, M. D. (2011) 'Does obesity increase the risk of miscarriage in spontaneous conception: a systematic review.', *Seminars in reproductive medicine*. United States, 29(6), pp. 507–513. doi: 10.1055/s-0031-1293204.

Brieger, K. *et al.* (2012) 'Reactive oxygen species: From health to disease', *Swiss Medical Weekly*, 142(August), pp. 1–14. doi: 10.4414/smw.2012.13659.

Bruun, J. M. *et al.* (2005) 'Monocyte chemoattractant protein-1 release is higher in visceral than subcutaneous human adipose tissue (AT): implication of macrophages resident in the AT.', *The Journal of clinical endocrinology and metabolism*. United States, 90(4), pp. 2282–2289. doi: 10.1210/jc.2004-1696.

Buettner, G. R. (1993) 'The pecking order of free radicals and antioxidants: lipid peroxidation, alpha-tocopherol, and ascorbate.', *Archives of biochemistry and biophysics*, pp. 535–43. doi: 10.1006/abbi.1993.1074.

Burton, G. J. (2009) 'Oxygen, the Janus gas; its effects on human placental development and function', *Journal of Anatomy*, 215(1), pp. 27–35. doi: 10.1111/j.1469-7580.2008.00978.x.

Burton, G. J. and Fowden, A. L. (2015) 'The placenta: A multifaceted, transient organ', *Philosophical Transactions of the Royal Society B: Biological Sciences*. doi: 10.1098/rstb.2014.0066.

Burton, G. J., Hempstock, J. and Jauniaux, E. (2003) 'Oxygen, early embryonic metabolism and free radical-mediated embryopathies', *Reproductive BioMedicine Online*, 6(1), pp. 84–96. doi: 10.1016/S1472-6483(10)62060-3.

Burton, G. J., Jauniaux, E. and Charnock-Jones, D Sephen (2010) 'The influence of the intrauterine environment on human placental development', *The International Journal of Developmental Biology*, 54(2–3), pp. 303–312. doi: 10.1387/ijdb.082764gb.

Burton, G. J., Jauniaux, E. and Charnock-Jones, D. Sephen (2010) 'The influence of the intrauterine environment on human placental development', *The International Journal of Developmental Biology*, 54(2–3), pp. 303–312. doi: 10.1387/ijdb.082764gb.

Caniggia, I. *et al.* (2000) 'Oxygen and placental development during the first trimester: Implications for the pathophysiology of pre-eclampsia', *Placenta*, 21(SUPPL.1), pp. 25–30. doi: 10.1053/plac.1999.0522.

Cartier, A. *et al.* (2008) 'Visceral obesity and plasma glucose-insulin homeostasis: contributions of interleukin-6 and tumor necrosis factor-alpha in men.', *The Journal of clinical endocrinology and metabolism*. United States, 93(5), pp. 1931–1938. doi: 10.1210/jc.2007-2191.

Castellana, B. *et al.* (2018) 'Maternal obesity alters uterine NK activity through a functional KIR2DL1/S1 imbalance', *Immunology and Cell Biology*, 96(8), pp. 805–819. doi: 10.1111/imcb.12041.

Castellucci, M. *et al.* (2000) 'Villous sprouting: fundamental mechanisms of human placental development.', *Human reproduction update*. England, 6(5), pp. 485–494. doi: 10.1093/humupd/6.5.485.

Catalano, P. M. *et al.* (2009) 'Fetuses of obese mothers develop insulin resistance in utero.', *Diabetes care*, 32(6), pp. 1076–80. doi: 10.2337/dc08-2077.

Catalano, P. M., Drago, N. M. and Amini, S. B. (1995) 'Maternal carbohydrate metabolism and its relationship to fetal growth and body composition.', *American journal of obstetrics and gynecology*. United States, 172(5), pp. 1464–1470. doi: 10.1016/0002-9378(95)90479-4.

Caulín, C., Salvesen, G. S. and Oshima, R. G. (1997) 'Caspase cleavage of keratin 18 and reorganization of intermediate filaments during epithelial cell apoptosis', *Journal of Cell Biology*, 138(6), pp. 1379–1394. doi: 10.1083/jcb.138.6.1379.

Cawthon, R. M. (2009) 'Telomere length measurement by a novel monochrome multiplex quantitative PCR method', *Nucleic Acids Research*, 37(3), pp. 1–7. doi: 10.1093/nar/gkn1027.

Challier, J. C. *et al.* (2008a) 'Obesity in Pregnancy Stimulates Macrophage Accumulation and Inflammation in the Placenta', *Placenta*, 29(3), pp. 274–281. doi: 10.1016/j.placenta.2007.12.010.

Challier, J. C. *et al.* (2008b) 'Obesity in Pregnancy Stimulates Macrophage Accumulation and Inflammation in the Placenta', *Placenta*, 29(3), pp. 274–281. doi:

10.1016/j.placenta.2007.12.010.

Chan, A. C. (1993) 'Partners in defense, vitamin E and vitamin C.', *Canadian journal of physiology and pharmacology*. Canada, 71(9), pp. 725–731.

Chan, C. C. W., Lao, T. T. and Cheung, A. N. Y. (1999) 'Apoptotic and Proliferative Activities in First Trimester Placentae', *Placenta*, 20(2–3), pp. 223–227. doi: 10.1053/plac.1998.0375.

Chen, S.-U. *et al.* (2010) 'Lysophosphatidic acid up-regulates expression of growth-regulated oncogene-alpha, interleukin-8, and monocyte chemoattractant protein-1 in human first-trimester trophoblasts: possible roles in angiogenesis and immune regulation.', *Endocrinology*, 151(1), pp. 369–79. doi: 10.1210/en.2009-0779.

Chou, S.-Y., Grossman, M. and Saffer, H. (2004) 'An economic analysis of adult obesity: results from the Behavioral Risk Factor Surveillance System.', *Journal of health economics*. Netherlands, 23(3), pp. 565–587. doi: 10.1016/j.jhealeco.2003.10.003.

Cimprich, K. A. and Cortez, D. (2008) 'ATR: an essential regulator of genome integrity', *Nature Reviews Molecular Cell Biology*, 9(8), pp. 616–627. doi: 10.1038/nrm2450.

Cindrova-Davies, T. *et al.* (2014) 'Energy status and HIF signalling in chorionic villi show no evidence of hypoxic stress during human early placental development', *Molecular Human Reproduction*, 21(3), pp. 296–308. doi: 10.1093/molehr/gau105.

Cindrova-Davies, T. *et al.* (2018) 'Evidence of oxidative stress-induced senescence in mature, post-mature and pathological human placentas', *Placenta*, 68, pp. 15–22. doi: 10.1016/j.placenta.2018.06.307.

Colomiere, M. *et al.* (2009) 'Defective insulin signaling in placenta from pregnancies complicated by gestational diabetes mellitus.', *European journal of endocrinology*. England, 160(4), pp. 567–578. doi: 10.1530/EJE-09-0031.

Colomiere, M., Permezel, M. and Lappas, M. (2010) 'Diabetes and obesity during pregnancy alter insulin signalling and glucose transporter expression in maternal skeletal muscle and subcutaneous adipose tissue.', *Journal of molecular endocrinology*, 44(4), pp. 213–23. doi: 10.1677/JME-09-0091.

Conway, B. and Rene, A. (2004) 'Obesity as a disease: no lightweight matter.', *Obesity reviews : an official journal of the International Association for the Study of Obesity*, 5(3), pp. 145–51. doi: 10.1111/j.1467-789X.2004.00144.x.

Cooke, M. S. *et al.* (2000) 'Urinary 8-oxo-2'-deoxyguanosine--source, significance and supplements.', *Free radical research*. England, 32(5), pp. 381–397. doi: 10.1080/10715760000300391.

Cox, B. D. and Whichelow, M. J. (1996) 'Ratio of waist circumference to height is better predictor of death than body mass index Consensus statement on management of hypothyroidism and hyperthyroidism', *British Medical Journal*, 313(December), p. 1996.

Cox, L. S. and Redman, C. (2017) 'The role of cellular senescence in ageing of the placenta', *Placenta*, 52, pp. 139–145. doi: 10.1016/j.placenta.2017.01.116.

Daugaard, M., Rohde, M. and Jäättelä, M. (2007) 'The heat shock protein 70 family: Highly homologous proteins with overlapping and distinct functions', *FEBS Letters*. England, 581(19), pp. 3702–3710. doi: 10.1016/j.febslet.2007.05.039.

Dekel, N. *et al.* (2010) 'Inflammation and implantation.', *American journal of reproductive immunology (New York, N.Y. : 1989)*, 63(1), pp. 17–21. doi: 10.1111/j.1600-0897.2009.00792.x.

Delidaki, M. *et al.* (2011) 'Interplay of cAMP and MAPK pathways in hCG secretion and fusogenic gene expression in a trophoblast cell line.', *Molecular and cellular endocrinology*. Ireland, 332(1–2), pp. 213–220. doi: 10.1016/j.mce.2010.10.013.

Demissie, S. *et al.* (2006) 'Insulin resistance, oxidative stress, hypertension, and leukocyte telomere length in men from the Framingham Heart Study', *Aging Cell*, 5(4), pp. 325–330. doi: 10.1111/j.1474-9726.2006.00224.x.

Dempsey, J. C. *et al.* (2005) 'Maternal pre-pregnancy overweight status and obesity as risk factors for cesarean delivery.', *The journal of maternal-fetal & neonatal medicine : the official journal of the European Association of Perinatal Medicine, the Federation of Asia and Oceania Perinatal Societies, the International Society of Perinatal Obstetricians*. England, 17(3), pp. 179–185. doi: 10.1080/14767050500073456.

Deng, C. X. (2006) 'BRCA1: Cell cycle checkpoint, genetic instability, DNA damage response and cancer evolution', *Nucleic Acids Research*, 34(5), pp. 1416–1426. doi: 10.1093/nar/gkl010.

Denison, F. C. *et al.* (2010) 'Obesity, pregnancy, inflammation, and vascular function', *Reproduction*, 140(3), pp. 373–385. doi: 10.1530/REP-10-0074.

Desoye, G. (2018) 'The Human Placenta in Diabetes and Obesity: Friend or Foe? The 2017 Norbert Freinkel Award Lecture', *Diabetes Care*, 41(7), pp. 1362–1369. doi: 10.2337/dci17-0045.

Dietz, P. M. *et al.* (2005) 'Population-based assessment of the risk of primary cesarean delivery due to excess prepregnancy weight among nulliparous women delivering term infants.', *Maternal and child health journal*. United States, 9(3), pp. 237–244. doi: 10.1007/s10995-005-0003-9.

Du, M.-R., Wang, S.-C. and Li, D.-J. (2014) 'The integrative roles of chemokines at the maternal-fetal interface in early pregnancy.', *Cellular & molecular immunology*, 11(5), pp. 438–48. doi: 10.1038/cmi.2014.68.

Dybala, M. P. *et al.* (2019) 'Pancreatic beta cell/islet mass and body mass index.', *Islets*, 11(1), pp. 1–9. doi: 10.1080/19382014.2018.1557486.

Esterbauer, H., Schaur, R. J. and Zollner, H. (1991) 'Chemistry and biochemistry of 4-hydroxynonenal, malonaldehyde and related aldehydes', *Free Radical Biology and Medicine*, 11(1), pp. 81–128. doi: 10.1016/0891-5849(91)90192-6.

Fernandez-Capetillo, O. *et al.* (2003) 'H2AX regulates meiotic telomere clustering', *Journal of Cell Biology*, 163(1), pp. 15–20. doi: 10.1083/jcb.200305124.

Fernandez, M., Gonzalez, R. and Subirats, A. (1988) 'The Tutor's Role in Teaching Practice in Initial Teacher Training', *European Journal of Teacher Education*, 11(2), pp. 123–130. doi: 10.1172/JCI117936.

Fontes, F. L. *et al.* (2015) 'Role of DNA repair in host immune response and inflammation', *Mutation Research - Reviews in Mutation Research*, pp. 246–257. doi: 10.1016/j.mrrev.2014.11.004.

Forbes, K. and Westwood, M. (2010) 'Maternal growth factor regulation of human placental development and fetal growth', *Journal of Endocrinology*, 207(1), pp. 1–16. doi: 10.1677/JOE-10-0174.

Frias, A. E. *et al.* (2011) 'Maternal high-fat diet disturbs uteroplacental hemodynamics and increases the frequency of stillbirth in a nonhuman primate model of excess nutrition.', *Endocrinology*, 152(6), pp. 2456–2464. doi: 10.1210/en.2010-1332.

Fröhlich, J. D. *et al.* (2012) 'Oxygen modulates the response of first-trimester trophoblasts to hyperglycemia', *American Journal of Pathology*, 180(1), pp. 153–164. doi: 10.1016/j.ajpath.2011.09.012.

Garcia-Lloret, M. I. *et al.* (1994) 'Demonstration of Functional Cytokine-Placental Interactions: CSF-1 and GM-CSF Stimulate Human Cytotrophoblast Differentiation and Peptide Hormone Secretion', *Experimental Cell Research*, 214(1), pp. 46–54. doi: 10.1006/excr.1994.1232.

Gardner, J. P. *et al.* (2005) 'Rise in insulin resistance is associated with escalated telomere attrition', *Circulation*, 111(17), pp. 2171–2177. doi: 10.1161/01.CIR.0000163550.70487.0B.

Gardosi, J. *et al.* (2013) 'Maternal and fetal risk factors for stillbirth: population based study', *BMJ*, 346(jan24 3), pp. f108–f108. doi: 10.1136/bmj.f108.

Gauster, M. *et al.* (2017) 'Maternal Type 1 diabetes activates stress response in early placenta', *Placenta*. Elsevier Ltd, 50, pp. 110–116. doi: 10.1016/j.placenta.2017.01.118.

Genbacev, O. (1997) 'Regulation of Human Placental Development by Oxygen Tension', *Science*, 277(5332), pp. 1669–1672. doi: 10.1126/science.277.5332.1669.

Godfrey, K. M., Inskip, H. M. and Hanson, M. A. (2011) 'The long-term effects of prenatal development on growth and metabolism', *Seminars in Reproductive Medicine*, 29(1526-4564 (Electronic)), pp. 257–265. doi: 10.1055/s-0031-1275518.The.

Gonzalez-Hunt, C. P., Wadhwa, M. and Sanders, L. H. (2018) 'DNA damage by oxidative stress: Measurement strategies for two genomes', *Current Opinion in Toxicology*. Elsevier Ltd, 7, pp. 87–94. doi: 10.1016/j.cotox.2017.11.001.

Gonzalez, T. L. *et al.* (2018) 'Sex differences in the late first trimester human placenta transcriptome', *Biology of Sex Differences*. Biology of Sex Differences, 9(1), pp. 1–23. doi: 10.1186/s13293-018-0165-y.

Greider, C. W. and Blackburn, E. H. (1985) 'Identification of a specific telomere terminal transferase activity in Tetrahymena extracts.', *Cell*. United States, 43(2 Pt 1), pp. 405–

413. doi: 10.1016/0092-8674(85)90170-9.

Gude, N. M. *et al.* (2004a) 'Growth and function of the normal human placenta', *Thrombosis Research*, 114(5–6), pp. 397–407. doi: 10.1016/j.thromres.2004.06.038.

Gude, N. M. *et al.* (2004b) 'Growth and function of the normal human placenta', *Thrombosis Research*, 114(5-6 SPEC. ISS.), pp. 397–407. doi: 10.1016/j.thromres.2004.06.038.

Hayes, E. K. *et al.* (2014) 'Trophoblast invasion and blood vessel remodeling are altered in a rat model of lifelong maternal obesity.', *Reproductive sciences (Thousand Oaks, Calif.)*, 21(5), pp. 648–57. doi: 10.1177/1933719113508815.

Hempstock, J. *et al.* (2004) 'Endometrial glands as a source of nutrients, growth factors and cytokines during the first trimester of human pregnancy: a morphological and immunohistochemical study.', *Reproductive biology and endocrinology : RB&E*, 2(1), p. 58. doi: 10.1186/1477-7827-2-58.

Herskind, A. M. *et al.* (1996) 'Untangling genetic influences on smoking, body mass index and longevity: a multivariate study of 2464 Danish twins followed for 28 years.', *Human genetics*. Germany, 98(4), pp. 467–475. doi: 10.1007/s004390050241.

Hertig, A. T., Rock, J. and Adams, E. C. (1956) 'A description of 34 human ova within the first 17 days of development', *American Journal of Anatomy*, 98(3), pp. 435–493. doi: 10.1002/aja.1000980306.

Heslehurst, N. *et al.* (2010) 'A nationally representative study of maternal obesity in England, UK: trends in incidence and demographic inequalities in 619 323 births, 1989-2007.', *International journal of obesity (2005)*. England, 34(3), pp. 420–428. doi: 10.1038/ijo.2009.250.

Hirata, I. *et al.* (2009) 'Heat-Shock Protein 70-Overexpressing Gastric Epithelial Cells Are Resistant to Indomethacin-Induced Apoptosis', *Digestion*, 79(4), pp. 243–250. doi: 10.1159/000215352.

Hjort, L. *et al.* (2018) 'Gestational diabetes and maternal obesity are associated with epigenome-wide methylation changes in children', *JCI insight*, 3(17), pp. 1–14. doi: 10.1172/jci.insight.122572.

Hoch, D. *et al.* (2019) 'Diabesity-associated oxidative and inflammatory stress signalling in the early human placenta', *Molecular Aspects of Medicine*. Elsevier, 66(November 2018), pp. 21–30. doi: 10.1016/j.mam.2018.11.002.

Hoch, D., Bachbauer, M., *et al.* (2020) 'Maternal Obesity Alters Placental Cell Cycle Regulators in the First Trimester of Human Pregnancy: New Insights for BRCA1', *International journal of molecular sciences*, 21(2), pp. 1–18. doi: 10.3390/ijms21020468.

Hoch, D., Novakovic, B., *et al.* (2020) 'Sex matters: XIST and DDX3Y gene expression as a tool to determine fetal sex in human first trimester placenta', *Placenta*. Elsevier Ltd, 97, pp. 68–70. doi: 10.1016/j.placenta.2020.06.016.

Hoshina, M., Boothby, M. and Boime, I. (1982) 'Cytological localization of chorionic

gonadotropin alpha and placental lactogen mRNAs during development of the human placenta.', *The Journal of cell biology*, 93(1), pp. 190–8. doi: 10.1083/jcb.93.1.190.

Hotamisligil, G. S. (2006) 'Inflammation and metabolic disorders', *Nature*, 444(7121), pp. 860–867. doi: 10.1038/nature05485.

Huppertz, B. *et al.* (1999) 'Apoptosis cascade progresses during turnover of human trophoblast: analysis of villous cytotrophoblast and syncytial fragments in vitro.', *Laboratory investigation; a journal of technical methods and pathology*. United States, 79(12), pp. 1687–702. Available at: http://www.ncbi.nlm.nih.gov/pubmed/10616217.

Huppertz, B. (2008) 'The anatomy of the normal placenta', *Journal of Clinical Pathology*, 61(12), pp. 1296–1302. doi: 10.1136/jcp.2008.055277.

Huppertz, B. *et al.* (2009) 'Oxygen as modulator of trophoblast invasion', *Journal of Anatomy*, 215(1), pp. 14–20. doi: 10.1111/j.1469-7580.2008.01036.x.

Huppertz, B., Kaufmann, P. and Kingdom, J. (2002) 'Trophoblast turnover in health and disease', *Fetal and Maternal Medicine Review*, 13(02), pp. 103–118. doi: 10.1017/S0965539502000220.

Hustin, J. and Schaaps, J. P. (1987) 'Echographic [corrected] and anatomic studies of the maternotrophoblastic border during the first trimester of pregnancy.', *American journal of obstetrics and gynecology*. United States, 157(1), pp. 162–168.

Hyun, Y. Y. *et al.* (2019) 'Body Mass Index, waist circumference, and health-related quality of life in adults with chronic kidney disease.', *Quality of life research : an international journal of quality of life aspects of treatment, care and rehabilitation*. Netherlands, 28(4), pp. 1075–1083. doi: 10.1007/s11136-018-2084-0.

Jaffe, R. and Woods, J. R. J. (1993) 'Color Doppler imaging and in vivo assessment of the anatomy and physiology of the early uteroplacental circulation.', *Fertility and sterility*. United States, 60(2), pp. 293–297.

James, P. T. (2004) 'Obesity: the worldwide epidemic.', *Clinics in dermatology*. United States, 22(4), pp. 276–80. doi: 10.1016/j.clindermatol.2004.01.010.

Jauniaux, E. *et al.* (2000) 'Onset of maternal arterial blood flow and placental oxidative stress: A possible factor in human early pregnancy failure', *American Journal of Pathology*, 157(6), pp. 2111–2122. doi: 10.1016/S0002-9440(10)64849-3.

Jauniaux, E., Greenwold, N., *et al.* (2003) 'Comparison of ultrasonographic and Doppler mapping of the intervillous circulation in normal and abnormal early pregnancies.', *Fertility and sterility*. United States, 79(1), pp. 100–106. doi: 10.1016/s0015-0282(02)04568-5.

Jauniaux, E., Hempstock, J., *et al.* (2003) 'Trophoblastic Oxidative Stress in Relation to Temporal and Regional Differences in Maternal Placental Blood Flow in Normal and Abnormal Early Pregnancies', *The American Journal of Pathology*, 162(1), pp. 115–125. doi: 10.1016/S0002-9440(10)63803-5.

Jauniaux, E., Gulbis, B. and Burton, G. J. (2003) 'The human first trimester gestational sac limits rather than facilitates oxygen transfer to the foetus - A review', *Placenta*, 24(SUPPL.

A), pp. 86–93. doi: 10.1053/plac.2002.0932.

Jauniaux, E., Watson, A. and Burton, G. (2001) 'Evaluation of respiratory gases and acid-base gradients in human fetal fluids and uteroplacental tissue between 7 and 16 weeks' gestation', *American Journal of Obstetrics and Gynecology*, 184(5), pp. 998–1003. doi: 10.1067/mob.2001.111935.

Jena, N. R. (2012) 'DNA damage by reactive species: Mechanisms, mutation and repair', *Journal of Biosciences*, 37(3), pp. 503–517. doi: 10.1007/s12038-012-9218-2.

Jeyabalan, A. (2013) 'Epidemiology of preeclampsia: impact of obesity.', *Nutrition reviews*, 71 Suppl 1(SUPPL1), pp. S18-25. doi: 10.1111/nure.12055.

Jokhi, P. P. *et al.* (1994) 'Demonstration of the low affinity alpha subunit of the granulocyte-macrophage colony-stimulating factor receptor (GM-CSF-R alpha) on human trophoblast and uterine cells.', *Journal of reproductive immunology*. Ireland, 26(2), pp. 147–64. doi: 10.1016/0165-0378(94)90037-x.

Jones, C. J. P. and Fox, H. (1991) 'Ultrastructure of the normal human placenta.', *Electron microscopy reviews*, 4(1), pp. 129–78. doi: 10.1016/0892-0354(91)90019-9.

Juge-Aubry, C. E. *et al.* (2003) 'Adipose tissue is a major source of interleukin-1 receptor antagonist: upregulation in obesity and inflammation.', *Diabetes*, 52(5), pp. 1104–10. doi: 10.2337/diabetes.52.5.1104.

Jung, U. J. and Choi, M. S. (2014) 'Obesity and its metabolic complications: The role of adipokines and the relationship between obesity, inflammation, insulin resistance, dyslipidemia and nonalcoholic fatty liver disease', *International Journal of Molecular Sciences*, 15(4), pp. 6184–6223. doi: 10.3390/ijms15046184.

Kahn, S. E., Hull, R. L. and Utzschneider, K. M. (2006) 'Mechanisms linking obesity to insulin resistance and type 2 diabetes.', *Nature*, 444(7121), pp. 840–6. doi: 10.1038/nature05482.

Kar, M., Ghosh, D. and Sengupta, J. (2007) 'Histochemical and morphological examination of proliferation and apoptosis in human first trimester villous trophoblast', *Human Reproduction*, 22(11), pp. 2814–2823. doi: 10.1093/humrep/dem284.

Kastan, M. B. and Bartek, J. (2004) 'Cell-cycle checkpoints and cancer.', *Nature*. England, 432(7015), pp. 316–323. doi: 10.1038/nature03097.

Keaney, J. F. *et al.* (2003) 'Obesity and systemic oxidative stress: Clinical correlates of oxidative stress in the Framingham study', *Arteriosclerosis, Thrombosis, and Vascular Biology*, 23(3), pp. 434–439. doi: 10.1161/01.ATV.0000058402.34138.11.

Kim, D. W. *et al.* (2014) 'Obesity during pregnancy disrupts placental morphology, cell proliferation, and inflammation in a sex-specific manner across gestation in the mouse', *Biology of Reproduction*, 90(6), pp. 1–11. doi: 10.1095/biolreprod.113.117259.

Kim, S. *et al.* (2009) 'Obesity and weight gain in adulthood and telomere length', *Cancer Epidemiology Biomarkers and Prevention*, 18(3), pp. 816–820. doi: 10.1158/1055-9965.EPI-08-0935.

Knöfler, M. (2010) 'Critical growth factors and signalling pathways controlling human trophoblast invasion', *International Journal of Developmental Biology*, 54(2–3), pp. 269–280. doi: 10.1387/ijdb.082769mk.

Knöfler, M. and Pollheimer, J. (2013) 'Human placental trophoblast invasion and differentiation: a particular focus on Wnt signaling', *Frontiers in Genetics*, 4(SEP), pp. 1–14. doi: 10.3389/fgene.2013.00190.

Korgun, E. T. *et al.* (2006) 'Location of cell cycle regulators cyclin B1, cyclin A, PCNA, Ki67 and cell cycle inhibitors p21, p27 and p57 in human first trimester placenta and deciduas', *Histochemistry and Cell Biology*, 125(6), pp. 615–624. doi: 10.1007/s00418-006-0160-y.

Krieger, K. L. *et al.* (2019) 'Functional impacts of the brca1-mtorc2 interaction in breast cancer', *International Journal of Molecular Sciences*, 20(23). doi: 10.3390/ijms20235876.

Kyriakis, J. M. and Avruch, J. (2001) 'Mammalian mitogen-activated protein kinase signal transduction pathways activated by stress and inflammation.', *Physiological reviews*. United States, 81(2), pp. 807–869. doi: 10.1152/physrev.2001.81.2.807.

Laresgoiti-Servitje, E. and Gomez-Lopez, N. (2012) 'The pathophysiology of preeclampsia involves altered levels of angiogenic factors promoted by hypoxia and autoantibody-mediated mechanisms.', *Biology of reproduction*. United States, 87(2), p. 36. doi: 10.1095/biolreprod.112.099861.

Lash, G. E. *et al.* (2005) 'Inhibition of trophoblast cell invasion by TGFB1, 2, and 3 is associated with a decrease in active proteases.', *Biology of reproduction*. United States, 73(2), pp. 374–381. doi: 10.1095/biolreprod.105.040337.

Lassance, L., Haghiac, M., Leahy, P., *et al.* (2015) 'Identification of early transcriptome signatures in placenta exposed to insulin and obesity', *American Journal of Obstetrics and Gynecology*. Elsevier Inc., 212(5), pp. 647.e1-647.e11. doi: 10.1016/j.ajog.2015.02.026.

Lassance, L., Haghiac, M., Minium, J., *et al.* (2015) 'Obesity-induced down-regulation of the mitochondrial translocator protein (TSPO) impairs placental steroid production.', *The Journal of clinical endocrinology and metabolism*, 100(1), pp. E11-8. doi: 10.1210/jc.2014-2792.

Lavin, M. F. (2008) 'Ataxia-telangiectasia: from a rare disorder to a paradigm for cell signalling and cancer.', *Nature reviews. Molecular cell biology*. England, 9(10), pp. 759–769. doi: 10.1038/nrm2514.

Leese, H. J. (2002) 'Quiet please, do not disturb: A hypothesis of embryo metabolism and viability', *BioEssays*, 24(9), pp. 845–849. doi: 10.1002/bies.10137.

Levy, A. P., Levy, N. S. and Goldberg, M. A. (1996) 'Post-transcriptional regulation of vascular endothelial growth factor by hypoxia', *J Biol.Chem.*, 271(5), pp. 2746–2753. Available at: http://www.ncbi.nlm.nih.gov/pubmed/8576250.

Levytska, K. *et al.* (2013) 'Heme oxygenase-1 in placental development and pathology', *Placenta*. Elsevier Ltd, 34(4), pp. 291–298. doi: 10.1016/j.placenta.2013.01.004.

Liu, C. *et al.* (2017) 'Protein O-fucosyltransferase 1 promotes trophoblast cell

proliferation through activation of MAPK and PI3K/Akt signaling pathways', *Biomedicine & pharmacotherapy = Biomedecine & pharmacotherapie*, 88, p. 95—101. doi: 10.1016/j.biopha.2017.01.026.

Lopez-Jaramillo, P. *et al.* (2018) 'Obesity and Preeclampsia: Common Pathophysiological Mechanisms', *Frontiers in Physiology*, 9(December), pp. 1–10. doi: 10.3389/fphys.2018.01838.

Majali-Martinez, A. *et al.* (2017) 'Endothelin-1 down-regulates matrix metalloproteinase 14 and 15 expression in human first trimester trophoblasts via endothelin receptor type B', *Human reproduction (Oxford, England)*. 2016/11/17. Oxford University Press, 32(1), pp. 46–54. doi: 10.1093/humrep/dew295.

Maksimovic, J., Gordon, L. and Oshlack, A. (2012) 'SWAN: Subset-quantile within array normalization for illumina infinium HumanMethylation450 BeadChips.', *Genome biology*, 13(6), pp. 1–12. doi: 10.1186/gb-2012-13-6-r44.

Malti-Boudilmi, N. *et al.* (2010) 'Oxidative stress biomarkers in obese mothers and their appropriate for gestational age newborns', *Journal of Clinical and Diagnostic Research*, 4(2), pp. 2237–2245.

Manna, S., McCarthy, C. and McCarthy, F. P. (2019) 'Placental ageing in adverse pregnancy outcomes: Telomere shortening, cell senescence, and mitochondrial dysfunction', *Oxidative Medicine and Cellular Longevity*, 2019. doi: 10.1155/2019/3095383.

Maréchal, A. and Zou, L. (2013) 'DNA damage sensing by the ATM and ATR kinases', *Cold Spring Harbor Perspectives in Biology*, 5(9), pp. 1–17. doi: 10.1101/cshperspect.a012716.

Martens, D. S. *et al.* (2016) 'Maternal pre-pregnancy body mass index and newborn telomere length', *BMC Medicine*. BMC Medicine, 14(1), pp. 1–10. doi: 10.1186/s12916-016-0689-0.

Martin, C. L. *et al.* (2019) 'Maternal pre-pregnancy obesity, offspring cord blood DNA methylation, and offspring cardiometabolic health in early childhood: an epigenome-wide association study.', *Epigenetics*. Taylor & Francis, 14(4), pp. 325–340. doi: 10.1080/15592294.2019.1581594.

Martino, J. *et al.* (2016) 'Maternal Body Weight and Gestational Diabetes Differentially Influence Placental and Pregnancy Outcomes', *The Journal of Clinical Endocrinology & Metabolism*, 101(1), pp. 59–68. doi: 10.1210/jc.2015-2590.

Maury, E. and Brichard, S. M. (2010) 'Adipokine dysregulation, adipose tissue inflammation and metabolic syndrome.', *Molecular and cellular endocrinology*. Ireland, 314(1), pp. 1–16. doi: 10.1016/j.mce.2009.07.031.

Mayhew, T. M. (2001) 'Villous trophoblast of human placenta: a coherent view of its turnover, repair and contributions to villous development and maturation.', *Histology and histopathology*, 16(4), pp. 1213–24. doi: 10.14670/HH-16.1213.

Meisser, A. *et al.* (1999) 'Effects of tumour necrosis factor-α, interleukin-1 α,

macrophage colony stimulating factor and transforming growth factor β on trophoblastic matrix metalloproteinases', *Molecular Human Reproduction*, 5(3), pp. 252–260. doi: 10.1093/molehr/5.3.252.

Meller, M. *et al.* (2005) 'Evaluation of housekeeping genes in placental comparative expression studies.', *Placenta*. Netherlands, 26(8–9), pp. 601–607. doi: 10.1016/j.placenta.2004.09.009.

Mendis, S., Davis, S. and Norrving, B. (2015) 'Organizational update: the world health organization global status report on noncommunicable diseases 2014; one more landmark step in the combat against stroke and vascular disease.', *Stroke*. United States, 46(5), pp. e121-2. doi: 10.1161/STROKEAHA.115.008097.

Molania, R. *et al.* (2019) 'A new normalization for Nanostring nCounter gene expression data', *Nucleic Acids Research*. Oxford University Press, 47(12), pp. 6073–6083. doi: 10.1093/nar/gkz433.

Mor, G. *et al.* (2011) 'Inflammation and pregnancy: the role of the immune system at the implantation site.', *Annals of the New York Academy of Sciences*, 1221(1), pp. 80–7. doi: 10.1111/j.1749-6632.2010.05938.x.

Moreli, J. B. *et al.* (2014) 'DNA damage and its cellular response in mother and fetus exposed to hyperglycemic environment', *BioMed Research International*, 2014. doi: 10.1155/2014/676758.

Myatt, L. and Maloyan, A. (2016) 'Obesity and Placental Function', *Seminars in Reproductive Medicine*, 34(1), pp. 42–49. doi: 10.1055/s-0035-1570027.

Nagel, Z. D., Chaim, I. A. and Samson, L. D. (2014) 'Inter-individual variation in DNA repair capacity: A need for multi-pathway functional assays to promote translational DNA repair research', *DNA Repair*, 19, pp. 199–213. doi: 10.1016/j.dnarep.2014.03.009.

Ndisang, J. F. (2010) 'Role of heme oxygenase in inflammation, insulin-signalling, diabetes and obesity', *Mediators of inflammation*. 2010/05/18. Hindawi Publishing Corporation, 2010, p. 359732. doi: 10.1155/2010/359732.

Nishino, E. *et al.* (1990) 'Trophoblast-derived interleukin-6 (IL6) regulates human chorionic gonadotropin release through IL6 receptor on human trophoblasts.', *The Journal of clinical endocrinology and metabolism*. United States, 71(2), pp. 436–441. doi: 10.1210/jcem-71-2-436.

Nogues, P. *et al.* (2019) 'Maternal obesity influences expression and DNA methylation of the adiponectin and leptin systems in human third-trimester placenta.', *Clinical epigenetics*. Clinical Epigenetics, 11(1), p. 20. doi: 10.1186/s13148-019-0612-6.

Norwitz, E. R., Schust, D. J. and Fisher, S. J. (2001) 'Implantation and the survival of early pregnancy', *New England Journal of Medicine*, 345(19), pp. 1400–1408. doi: 10.1056/NEJMra000763.

O'Tierney-Ginn, P. *et al.* (2015) 'Placental growth response to maternal insulin in early pregnancy.', *The Journal of clinical endocrinology and metabolism*, 100(1), pp. 159–65. doi:

10.1210/jc.2014-3281.

Okada, S. and Ouchi, T. (2003) 'Cell cycle differences in DNA damage-induced BRCA1 phosphorylation affect its subcellular localization', *Journal of Biological Chemistry*. United States, 278(3), pp. 2015–2020. doi: 10.1074/jbc.M208685200.

Olivares-Corichi, I. M. *et al.* (2011) 'Oxidative stress present in the blood from obese patients modifies the structure and function of insulin', *Hormone and Metabolic Research*, 43(11), pp. 748–753. doi: 10.1055/s-0031-1286305.

Ottosen, L. D. M. *et al.* (2006) 'Observations on intrauterine oxygen tension measured by fibre-optic microsensors', *Reproductive BioMedicine Online*. Reproductive Healthcare Ltd, Duck End Farm, Dry Drayton, Cambridge CB23 8DB, UK, 13(3), pp. 380–385. doi: 10.1016/S1472-6483(10)61443-5.

Ouchi, T. (2006) 'BRCA1 phosphorylation: biological consequences.', *Cancer biology & therapy*. United States, 5(5), pp. 470–475. doi: 10.4161/cbt.5.5.2845.

Pácal, L. *et al.* (2011) 'Parameters of oxidative stress, DNA damage and DNA repair in type 1 and type 2 diabetes mellitus.', *Archives of physiology and biochemistry*. England, 117(4), pp. 222–230. doi: 10.3109/13813455.2010.551135.

Pendeloski, K. P. T. *et al.* (2017) 'Maternal obesity and inflammatory mediators: A controversial association.', *American journal of reproductive immunology (New York, N.Y. : 1989)*. Denmark, 77(5). doi: 10.1111/aji.12674.

Pennarun, G. *et al.* (2010) 'ATR contributes to telomere maintenance in human cells', *Nucleic Acids Research*, 38(9), pp. 2955–2963. doi: 10.1093/nar/gkp1248.

Perdu, S. *et al.* (2016) 'Maternal obesity drives functional alterations in uterine NK cells', *JCI Insight*, 1(11), pp. 1–21. doi: 10.1172/jci.insight.85560.

Peter Stein, T. *et al.* (2008) 'Oxidative stress early in pregnancy and pregnancy outcome', *Free Radic Res*, 42(10), pp. 841–848. doi: 10.1080/10715760802510069.

Peters, T. J. *et al.* (2000) 'Placental lactogen-I gene activation in differentiating trophoblast cells: extrinsic and intrinsic regulation involving mitogen-activated protein kinase signaling pathways.', *The Journal of endocrinology*. England, 165(2), pp. 443–456. doi: 10.1677/joe.0.1650443.

Phipson, B., Maksimovic, J. and Oshlack, A. (2016) 'MissMethyl: An R package for analyzing data from Illumina's HumanMethylation450 platform', *Bioinformatics*, 32(2), pp. 286–288. doi: 10.1093/bioinformatics/btv560.

Pijnenborg, R. *et al.* (1980) 'Trophoblastic invasion of human decidua from 8 to 18 weeks of pregnancy', *Placenta*, 1(1), pp. 3–19. doi: 10.1016/S0143-4004(80)80012-9.

Pijnenborg, R. *et al.* (1981) 'The pattern of interstitial trophoblasticinvasion of the myometrium in early human pregnancy', *Placenta*, 2(4), pp. 303–315. doi: 10.1016/S0143-4004(81)80027-6.

Plesca, D., Mazumder, S. and Almasan, A. (2008) 'DNA damage response and

apoptosis.', *Methods in Enzymology*, 446(08), pp. 107–122. doi: 10.1016/S0076-6879(08)01606-6.

Plotly Technologies Inc. (2015) 'Collaborative data science'. Available at: https://plot.ly.

PrabhuDas, M. *et al.* (2015) 'Immune mechanisms at the maternal-fetal interface: perspectives and challenges', *Nature Immunology*, 16(4), pp. 328–334. doi: 10.1038/ni.3131.

Qanungo, S., Sen, A. and Mukherjea, M. (1999) 'Antioxidant status and lipid peroxidation in human fete-placental unit', *Clinica Chimica Acta*, 285(1–2), pp. 1–12.

Radons, J. (2016) 'The human HSP70 family of chaperones: where do we stand?', *Cell Stress and Chaperones*, 21(3), pp. 379–404. doi: 10.1007/s12192-016-0676-6.

Rama, S. and Rao, A. J. (2003) 'Regulation of growth and function of the human placenta.', *Molecular and cellular biochemistry*, 253(1–2), pp. 263–8. doi: 10.1023/a:1026076219126.

Ramhorst, R. *et al.* (2012) 'Modulation and recruitment of inducible regulatory T cells by first trimester trophoblast cells.', *American journal of reproductive immunology (New York, N.Y. : 1989)*, 67(1), pp. 17–27. doi: 10.1111/j.1600-0897.2011.01056.x.

Red-Horse, K. *et al.* (2004) 'Trophoblast differentiation during embryo implantation and formation of the maternal-fetal interface', *Journal of Clinical Investigation*, 114(6), pp. 744–754. doi: 10.1172/jci22991.

Redman, C. W. G. and Sargent, I. L. (2007) 'Microparticles and immunomodulation in pregnancy and pre-eclampsia', *Journal of Reproductive Immunology*, 76(1–2), pp. 61–67. doi: 10.1016/j.jri.2007.03.008.

Reeg, S. *et al.* (2016) 'The molecular chaperone Hsp70 promotes the proteolytic removal of oxidatively damaged proteins by the proteasome', *Free Radical Biology and Medicine*. Elsevier, 99, pp. 153–166. doi: 10.1016/j.freeradbiomed.2016.08.002.

Roberts, K. A. *et al.* (2011) 'Placental structure and inflammation in pregnancies associated with obesity', *Placenta*, 32(3), pp. 247–254. doi: 10.1016/j.placenta.2010.12.023.

Roberts, V. H. J. *et al.* (2009a) 'Effect of Increasing Maternal Body Mass Index on Oxidative and Nitrative Stress in The Human Placenta', *Placenta*, 30(2), pp. 169–175. doi: 10.1016/j.placenta.2008.11.019.

Roberts, V. H. J. *et al.* (2009b) 'Effect of Increasing Maternal Body Mass Index on Oxidative and Nitrative Stress in The Human Placenta', *Placenta*, 30(2), pp. 169–175. doi: 10.1016/j.placenta.2008.11.019.

Rode, L. *et al.* (2005) 'Obesity-related complications in Danish single cephalic term pregnancies.', *Obstetrics and gynecology*. United States, 105(3), pp. 537–542. doi: 10.1097/01.AOG.0000152304.39492.1c.

Rodesch, F. *et al.* (1992) 'Oxygen measurements in endometrial and trophoblastic tissues during early pregnancy.', *Obstetrics and gynecology*. United States, 80(2), pp. 283–5.

Available at: http://www.ncbi.nlm.nih.gov/pubmed/1635745.

Saben, J. *et al.* (2014) 'Maternal obesity is associated with a lipotoxic placental environment', *Placenta*. Elsevier Ltd, 35(3), pp. 171–177. doi: 10.1016/j.placenta.2014.01.003.

Sacks, G. P. *et al.* (2004) 'Maternal C-reactive protein levels are raised at 4 weeks gestation.', *Human reproduction (Oxford, England)*. England, 19(4), pp. 1025–1030. doi: 10.1093/humrep/deh179.

Saldivar, J. C., Cortez, D. and Cimprich, K. A. (2017) 'The essential kinase ATR: ensuring faithful duplication of a challenging genome', *Nature Reviews Molecular Cell Biology*, 18(10), pp. 622–636. doi: 10.1038/nrm.2017.67.

Santos-Rosendo, C. *et al.* (2020) 'Placental adaptive changes to protect function and decrease oxidative damage in metabolically healthy maternal obesity', *Antioxidants*, 9(9), pp. 1–16. doi: 10.3390/antiox9090794.

Savage, K. I. *et al.* (2014) 'Identification of a BRCA1-mRNA Splicing Complex Required for Efficient DNA Repair and Maintenance of Genomic Stability', *Molecular Cell*, 54(3), pp. 445–459. doi: 10.1016/j.molcel.2014.03.021.

Scifres, C. M. *et al.* (2011) 'Fatty acid binding protein 4 regulates intracellular lipid accumulation in human trophoblasts.', *The Journal of clinical endocrinology and metabolism*, 96(7), pp. E1083-91. doi: 10.1210/jc.2010-2084.

Shin, J. S. *et al.* (2006) 'The role of telomeres and telomerase in the pathology of human cancer and aging', *Pathology*. England, 38(2), pp. 103–113. doi: 10.1080/00313020600580468.

Shoelson, S. E., Herrero, L. and Naaz, A. (2007) 'Obesity, Inflammation, and Insulin Resistance', *Gastroenterology*, 132(6), pp. 2169–2180. doi: 10.1053/j.gastro.2007.03.059.

Singh, V. P., McKinney, S. and Gerton, J. L. (2020) 'Persistent DNA Damage and Senescence in the Placenta Impacts Developmental Outcomes of Embryos', *Developmental Cell*. Elsevier Inc., 54(3), pp. 333-347.e7. doi: 10.1016/j.devcel.2020.05.025.

Siwetz, M. *et al.* (2016a) 'TNF-α alters the inflammatory secretion profile of human first trimester placenta.', *Laboratory investigation; a journal of technical methods and pathology*. Nature Publishing Group, 96(4), pp. 428–38. doi: 10.1038/labinvest.2015.159.

Siwetz, M. *et al.* (2016b) 'TNF-α alters the inflammatory secretion profile of human first trimester placenta', *Laboratory Investigation*, 96(4), pp. 428–438. doi: 10.1038/labinvest.2015.159.

Smith, S. A., Hulsey, T. and Goodnight, W. (2008) 'Effects of obesity on pregnancy', *JOGNN - Journal of Obstetric, Gynecologic, and Neonatal Nursing*, 37(2), pp. 176–184. doi: 10.1111/j.1552-6909.2008.00222.x.

Smith, S. C. *et al.* (2000) 'Apoptosis is a rare event in first-trimester placental tissue', *American Journal of Obstetrics and Gynecology*, 183(3), pp. 697–699. doi: 10.1067/mob.2000.106555.

Smith, S. C., Baker, P. N. and Symonds, E. M. (1997) 'Placental apoptosis in normal

human pregnancy', *American Journal of Obstetrics and Gynecology*, 177(1), pp. 57–65. doi: 10.1016/S0002-9378(97)70438-1.

St-Germain, L. E. *et al.* (2020) 'Maternal obesity and the uterine immune cell landscape: The shaping role of inflammation', *International Journal of Molecular Sciences*, 21(11). doi: 10.3390/ijms21113776.

Stavri, G. T. *et al.* (1995) 'Basic Fibroblast Growth Factor Upregulates the Expression of Vascular Endothelial Growth Factor in Vascular Smooth Muscle Cells', *Circulation*, 92(1), pp. 11 LP – 14. Available at: http://circ.ahajournals.org/content/92/1/11.abstract.

Stone, R. A. *et al.* (2014) 'Increasing Body Mass Index Exacerbates Inflammation in Obese Gravidas', *Obstetrics & Gynecology*, 123(5), p. 81S. doi: 10.1097/01.AOG.0000447406.31798.d3.

Straczkowski, M. *et al.* (2002) 'Plasma interleukin-8 concentrations are increased in obese subjects and related to fat mass and tumor necrosis factor-alpha system.', *The Journal of clinical endocrinology and metabolism*. United States, 87(10), pp. 4602–4606. doi: 10.1210/jc.2002-020135.

Sun, T. *et al.* (2020) 'Sexually Dimorphic Crosstalk at the Maternal-Fetal Interface.', *The Journal of clinical endocrinology and metabolism*, 105(12). doi: 10.1210/clinem/dgaa503.

Takeda, K. *et al.* (2008) 'Apoptosis signal-regulating kinase 1 in stress and immune response.', *Annual review of pharmacology and toxicology*. United States, 48, pp. 199–225. doi: 10.1146/annurev.pharmtox.48.113006.094606.

Team, R. C. (2019) 'R: A Language and Environment for Statistical Computing', *Vienna, Austria*.

Tzanavari, T., Giannogonas, P. and Karalis, K. P. (2010) 'TNF-alpha and obesity.', *Current directions in autoimmunity*. Switzerland, 11, pp. 145–156. doi: 10.1159/000289203.

Tzanetakou, I. P. *et al.* (2012) '" Is obesity linked to aging?". Adipose tissue and the role of telomeres.', *Ageing Research Reviews*. Elsevier B.V., 11(2), pp. 220–229. doi: 10.1016/j.arr.2011.12.003.

Uchida, K. (2003) '4-Hydroxy-2-nonenal: A product and mediator of oxidative stress', *Progress in Lipid Research*, 42(4), pp. 318–343. doi: 10.1016/S0163-7827(03)00014-6.

Varastehpour, A. *et al.* (2006) 'Activation of phospholipase A2 is associated with generation of placental lipid signals and fetal obesity', *Journal of Clinical Endocrinology and Metabolism*, 91(1), pp. 248–255. doi: 10.1210/jc.2005-0873.

Varol, U. *et al.* (2018) 'BRCA genes: BRCA 1 and BRCA 2', *Journal of B.U.ON.* Greece, 23(4), pp. 862–866.

Velicky, P. *et al.* (2018) 'Genome amplification and cellular senescence are hallmarks of human placenta development', *PLoS Genetics*, 14(10), pp. 1–25. doi: 10.1371/journal.pgen.1007698.

La Vignera, S. *et al.* (2011) 'Obesity is associated with a higher level of pro-

inflammatory cytokines in follicular fluid of women undergoing medically assisted procreation (PMA) programs.', *European review for medical and pharmacological sciences*, 15(3), pp. 267–73. Available at: http://www.ncbi.nlm.nih.gov/pubmed/21528772.

Watanabe, M. *et al.* (2002) 'The pros and cons of apoptosis assays for use in the study of cells, tissues, and organs', *Microscopy and Microanalysis*, 8(5), pp. 375–391. doi: 10.1017/S1431927602010346.

Watson, A. L. *et al.* (1997) 'Variations in expression of Copper/Zinc superoxide dismutase in villous trophoblast of the human placenta with gestational age', *Placenta*, 18(4), pp. 295–299. doi: 10.1016/S0143-4004(97)80064-1.

Watson, A. L. *et al.* (1998) 'Susceptibility of human placental syncytiotrophoblastic mitochondria to oxygen-mediated damage in relation to gestational age', *Journal of Clinical Endocrinology and Metabolism*, 83(5), pp. 1697–1705. doi: 10.1210/jc.83.5.1697.

Wegiel, B. *et al.* (2014) 'Heme oxygenase-1: A metabolic nike', *Antioxidants and Redox Signaling*, 20(11), pp. 1709–1722. doi: 10.1089/ars.2013.5667.

Wheeler, T., Elcock, C. L. and Anthony, F. W. (1995) 'Angiogenesis and the placental environment', *Placenta*, 16(3), pp. 289–296. doi: 10.1016/0143-4004(95)90115-9.

Whitley, G. S. J. and Cartwright, J. E. (2010) 'Cellular and Molecular Regulation of Spiral Artery Remodelling: Lessons from the Cardiovascular Field', *Placenta*. Elsevier Ltd, 31(6), pp. 465–474. doi: 10.1016/j.placenta.2010.03.002.

Wickham, H. (2009) *ggplot2 Elegant Graphics for Data Analysis*. New York, NY: Springer New York. doi: 10.1007/978-0-387-98141-3.

Włodarczyk, M. *et al.* (2018) 'Anthropometric and Dietary Factors as Predictors of DNA Damage in Obese Women.', *Nutrients*, 10(5). doi: 10.3390/nu10050578.

Wolfe, H. M. *et al.* (1990) 'Maternal obesity: a potential source of error in sonographic prenatal diagnosis.', *Obstetrics and gynecology*. United States, 76(3 Pt 1), pp. 339–342.

World Health Organization (WHO) (2018) *Obesity and Overweight. Fact Sheet 311*. Available at: http://www.who.int/news-room/fact- sheets/detail/obesity-and-overweight (Accessed: 25 October 2020).

Wu, J., Lu, L.-Y. and Yu, X. (2010) 'The role of BRCA1 in DNA damage response', *Protein & Cell*, 1(2), pp. 117–123. doi: 10.1007/s13238-010-0010-5.

Wu, W. L. and Papagiannakopoulos, T. (2020) 'The Pleiotropic Role of the KEAP1/NRF2 Pathway in Cancer', *Annual Review of Cancer Biology*, 4, pp. 413–435. doi: 10.1146/annurev-cancerbio-030518-055627.

Xiao, W. and Loscalzo, J. (2019) 'Metabolic Responses to Reductive Stress', *Antioxidants & Redox Signaling*, 00(00), p. ars.2019.7803. doi: 10.1089/ars.2019.7803.

Xu, H. *et al.* (2003) 'Chronic inflammation in fat plays a crucial role in the development of obesity-related insulin resistance.', *The Journal of clinical investigation*, 112(12), pp. 1821–1830. doi: 10.1172/JCI19451.

Yasuda, M. *et al.* (1995) 'Apoptotic cells in the human endometrium and placental villi: pitfalls in applying the TUNEL method.', *Archives of histology and cytology*. Japan, 58(2), pp. 185–190. doi: 10.1679/aohc.58.185.

Yedwab, G. A. *et al.* (1976) 'The temperature, pH, and partial pressure of oxygen in the cervix and uterus of women and uterus of rats during the cycle', *Fertility and Sterility*. Elsevier Masson SAS, 27(3), pp. 304–309. doi: 10.1016/S0015-0282(16)41722-X.

Yu, Z. *et al.* (2013) 'Pre-pregnancy body mass index in relation to infant birth weight and offspring overweight/obesity: a systematic review and meta-analysis.', *PloS one*, 8(4), p. e61627. doi: 10.1371/journal.pone.0061627.

Von Zglinicki, T. (2002) 'Oxidative stress shortens telomeres', *Trends in Biochemical Sciences*, 27(7), pp. 339–344. doi: 10.1016/S0968-0004(02)02110-2.

Zhang, E. G. *et al.* (2001) 'The regulation and localization of angiopoietin-1, -2, and their receptor Tie2 in normal and pathologic human placentae.', *Molecular medicine (Cambridge, Mass.)*, 7(9), pp. 624–35.

Zhao, H. *et al.* (2015) 'Heme oxygenase-1 in pregnancy and cancer: similarities in cellular invasion, cytoprotection, angiogenesis, and immunomodulation', *Frontiers in Pharmacology*, 5(January), pp. 1–10. doi: 10.3389/fphar.2014.00295.

Zhu, H. *et al.* (2013) 'Downregulation of antioxidants and phase 2 proteins', *Molecular Basis of Oxidative Stress: Chemistry, Mechanisms, and Disease Pathogenesis*, pp. 113–121. doi: 10.1002/9781118355886.ch5.

Zou, L., Liu, D. and Elledge, S. J. (2003) 'Replication protein A-mediated recruitment and activation of Rad17 complexes.', *Proceedings of the National Academy of Sciences of the United States of America*, 100(24), pp. 13827–32. doi: 10.1073/pnas.2336100100.

7. Appendix

App.Table 1: nCounter PlexSet Design Details. Genes and Target Sequences. HK = Housekeeper.

Report Date: 22-Jan-19							
Name	**Accession**	**Position**	**Target Sequence**	**A Tm**	**B Tm**	**Flag**	**Species**
HPRT-1	NM_000194.1	241-340	TGTGATGAAGGAGATGGGAGGCCATCACATTGTAGCCCTCTGTGTGCTCAAGGGGGGCTATAAATTCTTTGCTGACCTGCTGGATTACATCAAAGCACTG	87	80	HK	Homo sapiens
TBP	NM_001172085.1	588-687	ACAGTGAATCTTGGTTGTAAACTTGACCTAAAGACCATTGCACTTCGTGCCCGAAACGCCGAATATAATCCCAAGCGGTTTGCTGCGGTAATCATGAGGA	79	82	HK	Homo sapiens
WDR45L	NM_019613.3	1331-1430	CTGCCCAGGGACCTTGGTCTCGAAGCCATACGTGGTTGTCTGCTTTCCTAAGGACTCCCATTTCCAGTATTAAAGAGAGAATCATCATCAAGGCACCGTA	84	80	HK	Homo sapiens

ATM	NM_138292.3	1324-1423	TGAAGATAAAGAACTTCAGTGGACCTTCATAATGCTGACCTACCTGAATAACACACTGGTAGAAGATTGTGTCAAAGTTCGATCAGCAGCTGTTACCTGT	82	81		Homo sapiens
ATR	NM_001184.2	566-665	AAGACTTGGTTTACCTCCATAGAAGAAATGTGATGGGTCATGCTGTGGAATGGCCAGTGGTCATGAGCCGATTTTAAGTCAATTAGATGAACACATGGG	76	76		Homo sapiens
PRKDC	NM_006904.6	12751-12850	GCAAGTTAGTGAAACAGCTGTCTCCGTAAATGGAGGAAATGTGGGGAAGCCTTGGAATGCCCTTCTGGTTCTGGCACATTGGAAAGCACACTCAGAAGGC	78	82		Homo sapiens
HDAC1	NM_004964.2	786-885	CAAGCCGGTCATGTCCAAAGTAATGGAGATGTTCCAGCCTAGTGCGGTGGTCTTACAGTGTGGCTCAGACTCCCTATCTGGGGATCGGTTAGGTTGCTTC	81	82		Homo sapiens
HDAC8	NM_018486.2	388-487	CCGGTTTATATCTATAGTCCCGAGTATGTCAGTATGTGTGACTCCCTGGCCAAGATCCCCAAACGGGCCAGTATGGTGCATTCTTTGATTGAAGCATATG	79	80		Homo sapiens
ATRIP	NM_130384.1	467-566	GCGAGACTCACTACATCAGACGGAATCCGTTCTAGAGGAACAGAGAAGATCACATTTTCTTCTTGAGCAAGAGAAAACCCAAGCACTCAGTGACAAGGAA	85	81	X	Homo sapiens
NEIL1	NM_024608.3	518-617	CCCCGAGCTGCACCTGGCCAGCCAGTTTGTGAATGAGGCCTGCAGGGCGCTGGTGTTCGGCGGCTGCGTGGAGAAGTCCTCTGTCAGCCGCAACCCTGAG	91	91		Homo sapiens
BRCA1	NM_007305.2	1276-1375	CATTAGATGATAGGTGGTACATGCACAGTTGCTCTGGGAGTCTTCAGAATAGAAACTACCCATCTCAAGAGGAGCTCATTAAGGTTGTTGATGTGGAGGA	81	84		Homo sapiens
H2AFX	NM_002105.2	1393-1492	CCGCCCCATTTCCCTTCCAGCAAACTCAACTCGGCAATCCAAGCACCTAGATACCAGCACAAGTCGGTTAATCCCTGTCTGGACTGAGCCTCCGTTGGCT	79	81		Homo sapiens
PARP1	NM_001618.3	3017-3116	AAGGTTTGGGCAAAACTACCCCTGATCCTTCAGCTAACATTAGTCTGGATGGTGTAGACGTTCCTCTTGGGACCGGGATTTCATCTGGTGTGAATGACAC	82	83		Homo sapiens
TP53	NM_000546.2	1331-1430	GGGGAGCAGGGCTCACTCCAGCCACCTGAAGTCCAAAAAGGGTCAGTCTACCTCCCGCCATAAAAAACTCATGTTCAAGACAGAAGGGCCTGACTCAGAC	81	79		Homo sapiens
OGG1	NM_002542.5	260-359	CCTTGTCTGGGCGGGGTCTTTGGGCGTCGACGAGGCCTGGTTCTGGGTAGGCGGGGCTACTACGGGGCGGTGCCTGCTGTGGAAATGCCTGCCCGCGCGC	88	92		Homo sapiens
XPA	NM_000380.3	679-778	AAGAGGTCTCTTGAAGTTTGGGGTAGTCAAGAAGCATTAGAAGAAGCAAAGGAAGTCCGACAGGAAAACCGAGAAAAAATGAAACAGAAGAAATTTGATA	81	82		Homo sapiens
APEX1	NM_001641.2	728-827	CCTGCTTTCCCGCCAGTGCCCACTCAAAGTTTCTTACGGCATAGGCGATGAGGAGCATGATCAGGAAGGCCGGGTGATTGTGGCTGAATTTGACTCGTTT	83	84		Homo sapiens
FEN1	NM_004111.4	426-525	CCGGGAGAATGACATCAAGAGCTACTTTGGCCGTAAGGTGGCCATTGATGCCTCTATGAGCATTTATCAGTTCCTGATTGCTGTTCGCCAGGGTGGGGAT	82	81		Homo sapiens

LIG1	NM_000234.1	2165-2264	TCCGGGAGAACTTTGTGGAGACAGAGGGCGAGTTTGTCTTCGCCACCTCCCTGGACACCAAGGACATCGAGCAGATCGCCGAGTTCCTGGAGCAGTCAGT	83	84		Homo sapiens
UNG	NM_003362.3	1314-1413	TTGACCAAATGTCTTTCTCTGCAACATGGCTTCGGCCTAAAATATGCAGAAGACAGATGAGGTCAAATACTCAGTTGGCTCTCTTTATCTCCCTTGCCTT	79	79		Homo sapiens
RAD52	NM_134424.3	491-590	GGTTCATATCATGAAGATGTTGGTTATGGTGTTAGTGAGGGCCTCAAGTCCAAGGCTTTATCTTTGGAGAAGGCAAGGAAGGAGGCGGTGACAGACGGGC	78	86		Homo sapiens
ABL1	NM_005157.3	3201-3300	CTGCGTGAGCTATGTGGATTCCATCCAGCAAATGAGGAACAAGTTTGCCTTCCGAGAGGCCATCAACAAACTGGAGAATAATCTCCGGGAGCTTCAGATC	78	81		Homo sapiens
DDIT4	NM_019058.2	86-185	CCCATTCAAGCGGCAGGACGCACTTGTCTTAGCAGTTCTCGCTGACCGCGCTAGCTGCGGCTTCTACGCTCCGGCACTCTGAGTTCATCAGCAAACGCCC	82	82		Homo sapiens
BLM	NM_000057.2	2136-2235	TGCTTGGTGAAGACTGTTTTATCCTGATGCCGACTGGAGGTGGTAAGAGTTTGTGTTACCAGCTCCCTGCCTGTGTTTCTCCTGGGGTCACTGTTGTCAT	81	81		Homo sapiens
FANCA	NM_000135.2	799-898	CTGAGAAGAACTGTGGAGCCTGAAAAAATGCCGCAGGTCACGGTTGATGTACTGCAGAGAATGCTGATTTTTGCACTTGACGCTTTGGCTGCTGGAGTAC	83	83		Homo sapiens
GADD45A	NM_001924.2	866-965	GTTACTCCCTACACTGATGCAAGGATTACAGAAACTGATGCCAAGGGGCTGAGTGAGTTCAACTACATGTTCTGGGGGCCCGGAGATAGATGACTTTGCA	81	82		Homo sapiens
MSH2	NM_000251.1	2106-2205	CGACAAACTGGGGTGATAGTACTCATGGCCCAAATTGGGTGTTTTGTGCCATGTGAGTCAGCAGAAGTGTCCATTGTGGACTGCATCTTAGCCCGAGTAG	79	83		Homo sapiens
PCNA	NM_002592.2	281-380	GGTGTTGGAGGCACTCAAGGACCTCATCAACGAGGCCTGCTGGGATATTAGCTCCAGCGGTGTAAACCTGCAGAGCATGGACTCGTCCCACGTCTCTTTG	81	83		Homo sapiens
RAD51	NM_133487.2	567-666	AGACCACCAGACCCAGCTCCTTTATCAAGCATCAGCCATGATGGTAGAATCTAGGTATGCACTGCTTATTGTAGACAGTGCCACCGCCCTTTACAGAACA	81	82		Homo sapiens
Ku70	NM_001469.3	671-770	GACTTGATGCACCTGAAGAAACCTGGGGGCTTTGACATATCCTTGTTCTACAGAGATATCATCAGCATAGCAGAGGATGAGGACCTCAGGGTTCACTTTG	83	84		Homo sapiens
POLG	NM_002693.2	3596-3695	CTGTTGACTACTTACACCTCATGCTTGTGGCCATGAAGTGGCTGTTTGAAGAGTTTGCCATAGATGGGCGCTTCTGCATCAGCATCCATGACGAGGTTCG	81	83		Homo sapiens
POLB	NM_002690.2	681-780	TCTGAATACATTGCTACAGTCTGTGGCAGTTTCAGAAGAGGTGCAGAGTCCAGTGGTGACATGGATGTTCTCCTGACCCATCCCAGCTTCACTTCAGAAT	83	83		Homo sapiens
TREX1	NM_016381.3	1487-1586	GCTCACGCCAGGCCTTTCGGCACCATCAGGCCCATGTATGGGGTCACAGCCTCTGCTAGGACCAAGCCAAGACCATCTGCTGTCACAACCACTGCACACC	84	86	X	Homo sapiens

BCL2	NM_000657.2	6-105	GTGAAGCAGAAGTCTGGGAATCGATCTGGAAATCCTCCTAATTTTTACTCCCTCTCCCCGCGACTCCTGATTCATTGGGAAGTTTCAAATCAGCTATAAC	78	80		Homo sapiens
BBC3	NM_014417.2	1096-1195	GCTGATGGACTCAGCATCGGAAGGTGGCGGTGACCGAGGGGGTGGGGACCTGAGCCGCCCGCCTCTGCCGCCCACCACCATCTCAGGAAAGGCTGTTGTGC	92	91		Homo sapiens
PMAIP1	NM_021127.2	689-788	CTAGTGTTTTTGCCGAAGATTACCGCTGGCCTACTGTGAAGGGAGATGACCCTGTGATTAGACTGGGCGGCTGGGGAGAAACAGTTCAGTGCATTGTTGTT	83	83		Homo sapiens
BAK1	NM_001188.2	1541-1640	ACGTGTCAGAAGCCTCCAAGCCTGCCTCCCAAGGTCCTCTCAGTTCTCTCCCTTCCTCTCTCCTTATAGACACTTGCTCCCAACCCATTCACTACAGGTG	82	80		Homo sapiens
CDKN1A	NM_000389.2	1976-2075	CATGTGTCCTGGTTCCCGTTTCTCCACCTAGACTGTAAACCTCTCGAGGGCAGGGACCACACCCTGTACTGTTCTGTGTCTTTCACAGCTCCTCCCACAA	80	82		Homo sapiens
CDKN1B	NM_004064.2	366-465	GCTTCCGAGAGGGGTTCGGGCCGCGTAGGGGCGCTTTGTTTTGTTCGGTTTTGTTTTTTGAGAGTGCGAGAGAGGCGGTCGTGCAGACCCGGGAGAAAG	82	81		Homo sapiens
CCND1	NM_053056.2	691-790	TTGAACACTTCCTCTCCAAAATGCCAGAGGCGGAGGAGAACAAACAGATCATCCGCAAACACGCGCAGACCTTCGTTGCCCTCTGTGCCACAGATGTGAA	80	83		Homo sapiens
CCNA1	NM_003914.3	1606-1705	TTGTGCCTTGCCTGAGTGAGCTTCATAAAGCGTACCTTGATATACCCCATCGACCTCAGCAAGCAATTAGGGAGAAGTACAAGGCTTCAAAGTACCTGTG	79	78		Homo sapiens
CHEK1	NM_001114121.1	2226-2325	AGGGTGATGGATTGGAGTTCAAGAGACACTTCCTGAAGATTAAAGGGAAGCTGATTGATATTGTGAGCAGCCAGAAGATTTGGCTTCCTGCCACATGATC	83	81		Homo sapiens
CCNB1	NM_031966.3	1103-1202	CAGATGGAAATGAAGATTCTAAGAGCTTTAAACTTTGGTCTGGGTCGGCCTCTACCTTTGCACTTCCTTCGGAGAGCATCTAAGATTGGAGAGGTTGATG	80	80		Homo sapiens
CHEK2	NM_001005735.1	895-994	GGAGAGGTAAAGCTGGCTTTCGAGAGGAAAACATGTAAGAAAGTAGCCATAAAGATCATCAGCAAAAGGAAGTTTGCTATTGGTTCAGCAAGAGAGGCAG	83	82		Homo sapiens
HIF1A	NM_001530.2	1986-2085	ATGGATGATGACTTCCAGTTACGTTCCTTCGATCAGTTGTCACCATTAGAAAGCAGTTCCGCAAGCCCTGAAAGCGCAAGTCCTCAAAGCACAGTTACAG	75	79		Homo sapiens
NFE2L2	NM_006164.3	996-1095	TCCCGGTCACATCGAGAGCCCAGTCTTCATTGCTACTAATCAGGCTCAGTCACCTGAAACTTCTGTTGCTCAGGTAGCCCCTGTTGATTTAGACGGTATG	84	80		Homo sapiens
HSPA1A	NM_005345.5	99-198	GCTTCCCAGAGCGAACCTGTGCGGCTGCAGGCACCGGCGCGTCGAGTTTCCGGCGTCCGGAAGGACCGAGCTCTTCTCGCGGATCCAGTGTTCCGTTTCC	86	84	X	Homo sapiens
HMOX1	NM_002133.1	1431-1530	TGTTGTTTTTATAGCAGGGTTGGGGTGGTTTTTGAGCCATGCGTGGGTGGGGAGGGAGGTGTTTAACGGCACTGTGGCCTTGGTCTAACTTTTGTGTGAA	78	79		Homo sapiens

JNK 1	NM_002750.2	946-1045	TCTCTGTAGATGAAGCTCTCCAACACCCGTACATCAATGTCTGGTATGATCCTTCTGAAGCAGAAGCTCCACCACCAAAGATCCCTGACAAGCAGTTAGA	78	81		Homo sapiens
JNK2	XM_005265940.1	164-263	GAGCGACAGTAAATGTGACAGTCAGTTTTATAGTGTGCAAGTGGCAGACTCAACCTTCACTGTCCTAAAACGTTACCAGCAGCTGAAACCAATTGGCTCT	81	83		Homo sapiens
NFKB1	NM_003998.2	1676-1775	AGGGTATAGCTTCCCACACTATGGATTTCCTACTTATGGTGGGATTACTTTCCATCCTGGAACTACTAAATCTAATGCTGGGATGAAGCATGGAACCATG	79	79		Homo sapiens
NFKB2	NM_001077493.1	1062-1161	TGTGTTCCGGACACCCCCCTATCACAAGATGAAGATTGAGCGGCCTGTAACAGTGTTTCTGCAACTGAAACGCAAGCGAGGAGGGGACGTGTCTGATTCC	83	81		Homo sapiens
CHUK	NM_001278.3	861-960	TAGAACCCATGGAAAACTGGCTACAGTTGATGTTGAATTGGGACCCTCAGCAGAGAGGAGGACCTGTTGACCTTACTTTGAAGCAGCCAAGATGTTTTGT	79	79		Homo sapiens
IKBKB	NM_001556.1	1996-2095	GTGATCTATACGCAGCTCAGTAAAACTGTGGTTTGCAAGCAGAAGGCGCTGGAACTGTTGCCCAAGGTGGAAGAGGTGGTGAGCTTAATGAATGAGGATG	79	82		Homo sapiens
ASK1	NM_005923.3	2416-2515	TTTAGGAAAAGGCACTTATGGGATAGTCTACGCAGGTCGGGACTTGAGCAACCAAGTCAGAATTGCTATTAAGGAAATCCCAGAGAGAGACAGCAGATAC	81	79		Homo sapiens
MAP3K6	NM_001297609.1	1276-1375	TTGAGGGCTCTGTGGCGCCCGATCTGTACTGCATGTGTGGCCGTATCTACAAGGACATGTTCTTCAGCTCGGGTTTCCAGGATGCTGGGCACCGGGAGCA	83	82		Homo sapiens
MAPK14	NM_001315.2	793-892	GGTGACCCATCTCATGGGGGCAGATCTGAACAACATTGTGAAATGTCAGAAGCTTACAGATGACCATGTTCAGTTCCTTATCTACCAAATTCTCCGAGGT	85	77		Homo sapiens
MAPK11	NM_002751.6	419-518	CACCCTGATGGGCGCCGACCTGAACAACATCGTCAAGTGCCAGGCGCTGAGCGACGAGCACGTTCAATTCCTGGTTTACCAGCTGCTGCGCGGGCTGAAG	84	83		Homo sapiens
MAPK12	NM_002969.3	426-525	TATTCACTCCTGATGAGACCCTGGATGACTTCACGGACTTTTACCTGGTGATGCCGTTCATGGGCACCGACCTGGGCAAGCTCATGAAACATGAGAAGCT	82	82		Homo sapiens
MAPK13	NM_002754.3	1051-1150	CGGAGGCCCAGCAGCCGTTTGATGATTCCTTAGAACACGAGAAACTCACAGTGGATGAATGGAAGCAGCACATCTACAAGGAGATTGTGAACTTCAGCCC	81	82		Homo sapiens
ATF6	NM_007348.2	111-210	TTAGCCCGGGACTCTTTCACAGGCTGGATGAAGATTGGGATTCTGCTCTCTTTGCTGAACTCGGTTATTTCACAGACACTGATGAGCTGCAATTGGAAGC	84	81		Homo sapiens
ERN1	NM_001433.2	436-535	TACATGGGTAAAAAGCAGGACATCTGGTATGTTATTGACCTCCTGACCGGAGAGAAGCAGCAGACTTTGTCATCGGCCTTTGCAGATAGTCTCTGCCCAT	79	83		Homo sapiens
CDKN2A	NM_000077.4	560-659	CTGCCCGGGAGGGCTTCCTGGACACGCTGGTGGTGCTGCACCGGGCCGGGGCGCGGCTGGACGTGCGCGATGCCTGGGGCCGTCTGCCCGTGGACCTGGC	92	92	X	Homo sapiens

SIRT1	NM_012238.4	841-940	GGGTGTCTGTTTCATGTGGAATACCTGACTTCAGGTCAAGGGATGGTATTTATGCTCGCCTTGCTGTAGACTTCCCAGATCTTCCAGATCCTCAAGCGAT	78	81	Homo sapiens
GPX1	NM_000581.2	746-845	GGTTTTCATCTATGAGGGTGTTTCCTCTAAACCTACGAGGGAGGAACACCTGATCTTACAGAAAATACCACCTCGAGATGGGTGCTGGTCCTGTTGATCC	79	81	Homo sapiens
GPX2	NM_002083.2	831-930	CCTCTGGTTGGTGATTCAACTTGGGCTCCAAGACTTGGGTAAGCTCTGGGCCTTCACAGAATGATGGCACCTTCCTAAACCCTCATGGGTGGTGTCTGAG	83	82	Homo sapiens
GPX3	NM_002084.3	1297-1396	GTCCAATTGTTCTGCTCTAACTGATACCTCAACCTTGGGGCCAGCATCTCCCACTGCCTCCAAATATTAGTAACTATGACTGACGTCCCCAGAAGTTTCT	84	80	Homo sapiens
GSTP1	NM_000852.2	416-515	TTTTGAGACCCTGCTGTCCCAGAACCAGGGAGGCAAGACCTTCATTGTGGGAGACCAGATCTCCTTCGCTGACTACAACCTGCTGGACTTGCTGCTGATC	81	81	Homo sapiens
GSS	NM_000178.2	1511-1610	CAACCAGGCCACGGGACCTTCTATCCTCTGTATTTGTCATTCCTCTCCTAGCCCTCCTGAGGGGTATCCTCCTAAAGACCTCCAAAGTTTTTATGGAAGG	80	84	Homo sapiens
PRDX3	NM_014098.3	964-1063	CATGGTTAGTTGCTAGTACAAGGAATCCTTTATTGGTAACATCTTGGTGGCTGGCTAGCTAGTTTCTACAGAACATAATTTGCCTCTATAGAAGGCTATT	75	77	Homo sapiens
CAT	NM_001752.2	1131-1230	ATGCTTCAGGGCCGCCTTTTTGCCTATCCTGACACTCACCGCCATCGCCTGGGACCCAATTATCTTCATATACCTGTGAACTGTCCCTACCGTGCTCGAG	82	80	Homo sapiens
CYBB	NM_000397.3	2687-2786	TTTGAAGCATGAAAAAAGAGGGTTGGAGGTGGAGAATTAACCTCCTGCCATGACTCTGGCTCATCTAGTCCTGCTCCTTGTGCTATAAAATAAATGCAGA	85	82	Homo sapiens
CYGB	NM_134268.4	709-808	AAGCACAAGGTGGAACCGGTGTACTTCAAGATCCTCTCTGGGGTCATTCTGGAGGTGGTCGCCGAGGAATTTGCCAGTGACTTCCCACCTGAGACGCAGA	83	83	Homo sapiens
MGST3	NM_004528.2	196-295	CAAAGTGGAGTATCCTATCATGTACAGCACGGACCCTGAAAATGGGCACATCTTCAACTGCATTCAGCGAGCCCACCAGAACACGTTGGAAGTGTATCCT	81	80	Homo sapiens
NOX1	NM_007052.4	456-555	TCATTTTGCAGCCGCACACTGAGAAAGCAATTGGATCACAACCTCACCTTCCACAAGCTGGTGGCCTATATGATCTGCCTACATACAGCTATTCACATCA	78	83	Homo sapiens
GSR	NM_000637.2	1526-1625	ATGCAGGGACTTGGGTGTGATGAAATGCTGCAGGGTTTTGCTGTTGCAGTGAAGATGGGAGCAACGAAGGCAGACTTTGACAACACAGTCGCCATTCACC	82	81	Homo sapiens
SOD1	NM_000454.4	36-135	GCCTATAAAGTAGTCGCGGAGACGGGGTGCTGGTTTGCGTCGTAGTCTCCTGCAGCGTCTGGGGTTTCCGTTGCAGTCCTCGGAACCAGGACCTCGGCGT	83	82	Homo sapiens
SOD2	NM_000636.2	202-301	TTTGGGGTATCTGGGCTCCAGGCAGAAGCACAGCCTCCCCGACCTGCCCTACGACTACGGCGCCCTGGAACCTCACATCAACGCGCAGATCATGCAGCTG	93	92	Homo sapiens

SOD3	NM_003102.2	140-239	GGTGCAGCTCTCTTTTCAGGAGAGAAAGCTCTCTTGGAGGAGCTGGAAAGGTGCCCGACTCCAGCCATGCTGGCGCTACTGTGTTCCTGCCTGCTCCTGG	84	86	Homo sapiens
SRXN1	NM_080725.1	1656-1755	AAGAGAGTGAGAGTAGAAGCTGAAAGACTTCTTGAGTTCTTGGCCTGGAACTGGGACTAGGACAGTGTCACTTCTGCTAAGTTCTTTTGGTCAGAGCAAA	83	81	Homo sapiens
TXNRD1	NM_001093771.1	1010-1109	AGTGATGATCTTTTCTCCTTGCCTTACTGCCCGGGTAAGACCCTGGTTGTTGGAGCATCCTATGTCGCTTTGGAGTGCGCTGGATTTCTTGCTGGTATTG	81	80	Homo sapiens
TXN	NM_003329.2	56-155	CAGCCAAGATGGTGAAGCAGATCGAGAGCAAGACTGCTTTTCAGGAAGCCTTGGACGCTGCAGGTGATAAACTTGTAGTAGTTGACTTCTCAGCCACGTG	81	79	Homo sapiens
GLRX	NM_002064.2	361-460	CACCAACCACACTAACGAGATTCAAGATTATTTGCAACAGCTCACGGGAGCAAGAACGGTGCCTCGAGTCTTTATTGGTAAAGATTGTATAGGCGGATGC	82	80	Homo sapiens
TXNRD2	NM_006440.3	496-595	TTTAACATCAAAGCCAGCTTTGTTGACGAGCACACGGTTTGCGGCGTTGCCAAAGGTGGGAAAGAGATTCTGCTGTCAGCCGATCACATCATCATTGCTA	79	82	Homo sapiens
INSR	NM_000208.2	526-625	CACCCGGGGTTCTGTCCGCATCGAGAAGAACAATGAGCTCTGTTACTTGGCCACTATCGACTGGTCCCGTATCCTGGATTCCGTGGAGGATAATTACATC	82	81	Homo sapiens
IRS1	NM_005544.2	6225-6324	TTGATGGTGGCATCAAACTACCGATTTAAAACTGGAAGTTGCTGGTACTCAAACCAAAAGTTCATACTCTGGCGACACGAAGGGTTTCCTTTGAGCAACG	81	81	Homo sapiens
IRS2	NM_003749.2	776-875	GCGCCGAAACGGGTGATCGCTCTCGACTGCTGCCTGAACATCAACAAGCGCGCCGACGCCAAGCACAAGTACCTGATCGCCCTCTACACCAAGGACGAGT	82	82	Homo sapiens
PPARG	NM_005037.5	346-445	CAGATCCAGTGGTTGCAGATTACAAGTATGACCTGAAACTTCAAGAGTACCAAAGTGCAATCAAAGTGGAGCCTGCATCTCCACCTTATTATTCTGAGAA	81	80	Homo sapiens
KRT7	NM_005556.3	532-631	CCGCCTCCCAGACATCTTTGAGGCCCAGATTGCTGGCCTTCGGGGTCAGCTTGAGGCACTGCAGGTGGATGGGGGCCGCCTGGAGGCGGAGCTGCGGAGC	83	86	Homo sapiens
PECAM1	NM_000442.3	1366-1465	ATCTGCACTGCAGGTATTGACAAAGTGGTCAAGAAAAGCAACACAGTCCAGATAGTCGTATGTGAAATGCTCTCCCAGCCCAGGATTTCTTATGATGCCC	83	81	Homo sapiens
ACTA2	NM_001613.1	646-745	ATTCCTTCGTTACTACTGCTGAGCGTGAGATTGTCCGGGACATCAAGGAGAAACTGTGTTATGTAGCTCTGGACTTTGAAAATGAGATGGCCACTGCCGC	81	78	Homo sapiens
DLK1	NM_003836.4	1329-1428	AGATTCTTGGAGTTCCGCAGAGCTTACTATACGCGGTCTGTCCTAATCTTTGTGGTGTTCGCTATCTCTTGTGTCAAATCTGGTGAACGCTACGCTTACA	78	78	Homo sapiens
PDGFRB	NM_002609.3	266-365	CCCCTTCCTCCATCCCTCTGTTCTCCTGAGCCTTCAGGAGCCTGCACCAGTCCTGCCTGTCCTTCTACTCAGCTGTTACCCACTCTGGGACCAGCAGTCT	85	85	Homo sapiens

IL6	NM_000600.3	19-118	CCCAATAAATATAGGACTGGAGATGTCTGAGGCTCATTCTGCCCTCGAGCCCACCGGGAACGAAAGAGAAGCTCTATCTCCCCTCCAGGAGCCCAGCTAT	86	93	Homo sapiens
PLA2G7	NM_001168357.1	433-532	TCCATCCCAAGATAATGATCGCCTTGACACCCTTTGGATCCCAAATAAAGAATATTTTTGGGGTCTTAGCAAATTTCTTGGAACACACTGGCTTATGGGC	81	76	Homo sapiens
AGTR1	NM_000685.3	1826-1925	AGAGGAGCAACAGGAGATGAGAGTTCCAGATTGTTCTGTCCAGTTTCCAAAGGGCAGTAAAGTTTTCGTGCCGGTTTTCAGCTATTAGCAACTGTGCTAC	79	75	Homo sapiens

App. Table 2: Significant associations between maternal BMI and genes involved in DNA damage repair, antioxidant signaling, cell cycle regulation and cellular stress.

		Unstandardized Coefficients		Standardized Coefficients		
Gene	Exposure	B	Std. Error	Beta	t	Sig.
BLM	BMI (categorical)	-10.282	2.061	-0.459	-4.990	<0.001
BCL2	BMI (categorical)	-29.728	6.329	-0.392	-4.697	<0.001
MAP3K6	BMI (categorical)	-13.640	3.038	-0.402	-4.491	<0.001
HDAC1	BMI (categorical)	-64.367	16.487	-0.373	-3.904	<0.001
HDAC8	BMI (categorical)	27.000	8.250	0.318	3.273	0.001
PARP1	BMI (categorical)	-139.666	43.452	-0.303	-3.214	0.002
ATF6	BMI (categorical)	-36.939	12.769	-0.284	-2.893	0.005
Ku70	BMI (categorical)	-95.259	34.306	-0.277	-2.777	0.007
p57	BMI (categorical)	-805.228	294.563	-0.268	-2.734	0.007
PCNA	BMI (categorical)	-32.980	12.571	-0.260	-2.623	0.010
PMAIP1	BMI (categorical)	-31.193	11.966	-0.246	-2.607	0.011
HMOX1	BMI (categorical)	-90.374	35.139	-0.245	-2.572	0.012
FEN1	BMI (categorical)	-23.085	8.984	-0.256	-2.570	0.012
MGST3	BMI (categorical)	-172.571	69.183	-0.241	-2.494	0.014
MAPK13	BMI (categorical)	-20.798	8.486	-0.242	-2.451	0.016
MAPK12	BMI (categorical)	-5.623	2.299	-0.236	-2.445	0.016
SOD3	BMI (categorical)	-25.233	10.415	-0.199	-2.423	0.017
GSTP1	BMI (categorical)	-48.850	20.811	-0.223	-2.347	0.021
TBP	BMI (categorical)	8.014	3.510	0.221	2.283	0.025
JNK 1	BMI (categorical)	-6.176	2.774	-0.203	-2.226	0.028
CDKN1B	BMI (categorical)	-16.798	7.661	-0.221	-2.193	0.031
GLRX	BMI (categorical)	-334.134	156.636	-0.215	-2.133	0.035
BAK1	BMI (categorical)	-9.220	4.421	-0.200	-2.086	0.040
ASK1	BMI (categorical)	24.924	12.105	0.192	2.059	0.042

TXNRD1	BMI (categorical)	-37.285	18.253	-0.203	-2.043	0.044
MAPK11	BMI (categorical)	2.877	1.437	0.195	2.003	0.048

Multivariate linear regression analysis adjusted for gestational age and processing time, n = 101.

App. Table 3: Nanostring gene expression subanalysis of DNA damage repair genes in gestational week 7.

		Unstandardized Coefficients		Standardized Coefficients	t	Sig.
Gene	Exposure	B	Std. Error	Beta		
BLM	**BMI (categorical)**	**-18.060**	**4.752**	**-0.929**	**-3.801**	**0.002**
POLG	**BMI (categorical)**	**-55.793**	**22.447**	**-0.744**	**-2.486**	**0.026**
PARP1	**BMI (categorical)**	**-294.057**	**131.640**	**-0.706**	**-2.234**	**0.042**
HDAC1	BMI (categorical)	-96.015	50.147	-0.589	-1.915	0.076
XPA	BMI (categorical)	-31.608	19.760	-0.517	-1.600	0.132
GADD45A	BMI (categorical)	-33.536	23.113	-0.462	-1.451	0.169
Ku70	BMI (categorical)	-160.925	132.801	-0.403	-1.212	0.246
OGG1	BMI (categorical)	-10.165	8.684	-0.383	-1.171	0.261
FANCA	BMI (categorical)	17.048	15.078	0.387	1.131	0.277
ATM	BMI (categorical)	-70.953	64.013	-0.376	-1.108	0.286
FEN1	BMI (categorical)	-27.908	28.259	-0.332	-0.988	0.340
PCNA	BMI (categorical)	-41.943	44.143	-0.335	-0.950	0.358
RAD52	BMI (categorical)	-13.913	14.878	-0.325	-0.935	0.366
BRCA1	BMI (categorical)	-13.705	14.977	-0.310	-0.915	0.376
ATR	BMI (categorical)	-46.144	66.144	-0.239	-0.698	0.497
RAD51	BMI (categorical)	8.798	13.089	0.242	0.672	0.512
PRKDC	BMI (categorical)	-109.891	186.152	-0.207	-0.590	0.564
LIG1	BMI (categorical)	-9.637	17.734	-0.198	-0.543	0.595
UNG	BMI (categorical)	-15.460	29.129	-0.184	-0.531	0.604
NEIL1	BMI (categorical)	-3.188	6.249	-0.173	-0.510	0.618
MSH2	BMI (categorical)	-14.042	30.342	-0.162	-0.463	0.651
ATRIP	BMI (categorical)	-10.970	23.913	-0.163	-0.459	0.653
HDAC8	BMI (categorical)	-8.251	19.177	-0.157	-0.430	0.674
TP53	BMI (categorical)	-5.341	15.032	-0.126	-0.355	0.728
POLB	BMI (categorical)	-5.223	16.426	-0.113	-0.318	0.755
H2AFX	BMI (categorical)	-12.929	47.730	-0.098	-0.271	0.790
APEX	BMI (categorical)	4.918	26.612	0.063	0.185	0.856
ABL1	BMI (categorical)	4.222	29.852	0.051	0.141	0.890
DDIT4	BMI (categorical)	-0.572	21.342	-0.009	-0.027	0.979

Multivariate linear regression analysis adjusted for gestational age and processing time, n = 101

App. Table 4: Multivariate linear regression analysis of ATR, ATM and ATM/ATR substrate phosphorylation. BMI was groups according to lean (BMI < 25) and obese (BMI > 30) samples. n = 54.

Exposure	Unstandardized Coefficients		Standardized Coefficients	t	Sig.
	B	Std. Error	Beta		
(Constant)	-0.079	0.119		-0.666	0.510
BMI (categorical)	**0.225**	**0.024**	**0.837**	**9.586**	**0.000**
Gestational age (days)	0.000	0.001	-0.011	-0.127	0.899
Preparation time (min)	0.000	0.000	-0.075	-0.843	0.405

Dependent variable: ATR protein

Exposure	Unstandardized Coefficients		Standardized Coefficients	t	Sig.
	B	Std. Error	Beta		
(Constant)	0.041	0.027		1.536	0.133
BMI (categorical)	**0.015**	**0.005**	**0.396**	**2.806**	**0.008**
Gestational age (days)	-0.001	0.000	-0.245	-1.699	0.097
Preparation time (min)	-5.682E-05	0.000	-0.163	-1.138	0.262

Dependent variable: ATM protein

Exposure	Unstandardized Coefficients		Standardized Coefficients	t	Sig.
	B	Std. Error	Beta		
(Constant)	0.298	0.373		0.799	0.429
BMI (categorical)	0.070	0.074	0.154	0.954	0.346
Gestational age (days)	-0.001	0.004	-0.047	-0.283	0.778
Preparation time (min)	4.521E-05	0.001	0.011	0.065	0.948

Dependent variable: ATM/ATR substrate phosphorylation

App. Table 5: Significant associations between maternal BMI and proteins involved in cell cycle regulation.

	Unstandardized Coefficients		Standardized Coefficients	t	Sig.
	B	Std. Error	Beta		
RAD52 Ab104	39.565	0.214	1.000	185.074	0.000
HDAC1 Ab421	23.151	2.853	0.951	8.114	0.000
Cyclin E1 Ab77	11.900	1.960	0.916	6.071	0.001
BRCA1 Ab1423	16.374	3.353	0.878	4.883	0.002
Myc Ab358	5.800	1.268	0.849	4.575	0.003

14-3-3 zeta/delta Ab232	5.678	1.249	0.857	4.547	0.003
P90RSK Ab359/363	8.611	2.010	0.850	4.283	0.004
CDC25C Ab216	8.937	2.091	0.830	4.274	0.004
Chk2 Ab68	3.440	0.857	0.834	4.013	0.005
p95 Ab343	2.067	0.516	0.834	4.003	0.005
ATRIP Ab68/72	5.807	1.480	0.816	3.925	0.006
HDAC6 Ab22	2.693	0.699	0.824	3.853	0.006
HDAC3 Ab424	1.517	0.403	0.818	3.761	0.007
HDAC8 Ab39	0.958	0.255	0.817	3.752	0.007
MDM2 Ab166	12.170	3.307	0.811	3.680	0.008
BRCA1 Phospho-Ser1423	2.289	0.636	0.747	3.598	0.009
PP2A Ab307	3.204	0.946	0.786	3.385	0.012
Chk1 Ab286	1.672	0.497	0.770	3.363	0.012
Cyclin D1 Ab286	3.154	0.944	0.780	3.341	0.012
ABL1 Ab204	15.187	4.777	0.768	3.179	0.016
BRCA1 Ab1524	1.405	0.472	0.731	2.976	0.021
Smad2 3 Ab8	0.599	0.214	0.723	2.795	0.027
E2F1 Ab433	3.691	1.324	0.725	2.788	0.027
Cyclin D1 Phospho-Thr286	2.885	1.058	0.717	2.727	0.029
Smad3 Phospho-Ser213	1.043	0.404	0.696	2.585	0.036
TGFBR2 Ab250	1.692	0.664	0.693	2.546	0.038

Multivariate linear regression analysis adjusted for processing time, n = 14.

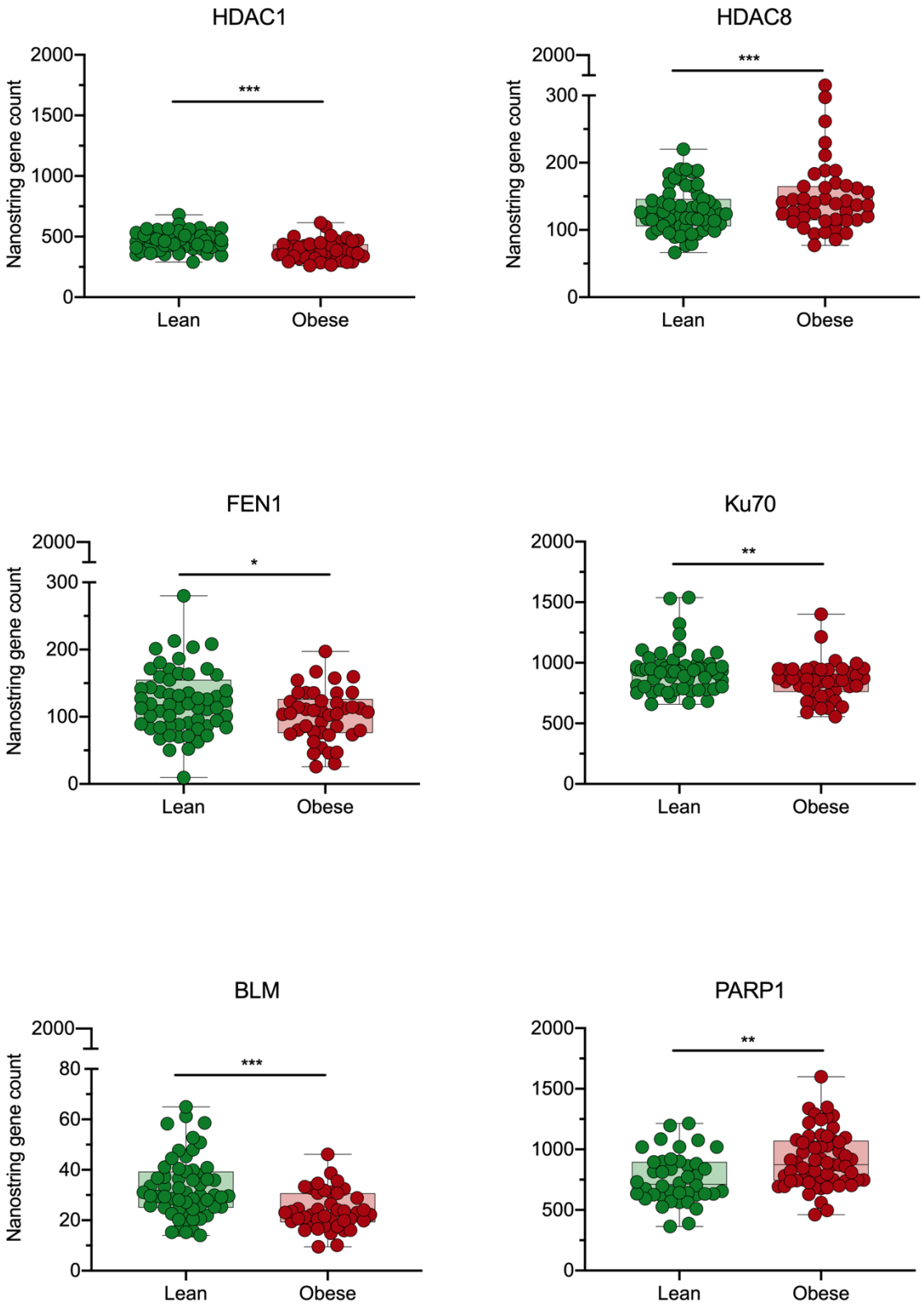

App. Figure 1: Obesity-regulated DNA damage repair genes. Gene expression was determined in first trimester placental tissue from lean (n = 59) and obese (n = 41) women by Nanostring. Gene counts were normalized to the mean of two different housekeeping (HK) genes WD repeat domain 45B (WDR45L) and TATA box binding protein (TBP). Results are presented as mean ± SD. Statistical analysis was performed using a

multivariate linear regression analysis with BMI as categorical dependent variable adjusted for gestational age and tissue processing time. HDAC1: Histone Deacetylase 1, HDAC8: Histone Deacetylase 8, FEN1: Flap Structure-Specific Endonuclease 1, Ku70: ATP-Dependent DNA Helicase 2 Subunit 1, BLM: BLM RecQ Like Helicase, PARP: Poly(ADP-Ribose) Polymerase 1.

8. Publications 2016 – 2020

First author publications

Hoch D, Novakovic B, Cvitic S, Saffery R, Desoye G, Majali-Martinez A. Sex matters: XIST and DDX3Y gene expression as a tool to determine fetal sex in human first trimester placenta. *Placenta*. 2020;97:68-70. doi:10.1016/j.placenta.2020.06.016

Hoch D, Bachbauer M, Pöchlauer C, et al. Maternal Obesity Alters Placental Cell Cycle Regulators in the First Trimester of Human Pregnancy: New Insights for BRCA1. *Int J Mol Sci*. 2020;21(2):468. Published 2020 Jan 11. doi:10.3390/ijms21020468

Hoch D, Gauster M, Hauguel-de Mouzon S, Desoye G. Diabesity-associated oxidative and inflammatory stress signalling in the early human placenta. *Mol Aspects Med*. 2019;66:21-30. doi:10.1016/j.mam.2018.11.002

Co-authorship

Juch H, Nikitina L, Reimann S, Hoch D, et al. Dendritic polyglycerol nanoparticles show charge dependent bio-distribution in early human placental explants and reduce hCG secretion. *Nanotoxicology*. 2018;12(2):90-103. doi:10.1080/17435390.2018.1425496

Majali-Martinez A, Hoch D, Tam-Amersdorfer C, et al. Matrix metalloproteinase 15 plays a pivotal role in human first trimester cytotrophoblast invasion and is not altered by maternal obesity. *FASEB J*. 2020;10.1096/fj.202000773R. doi:10.1096/fj.202000773R

Todd N, McNally R, Alqudah A, Hoch D, et al. Role of a novel angiogenesis FKBPL-CD44 pathway in preeclampsia risk stratification and mesenchymal stem cell treatment. *J Clin Endocrinol Metab*. 2020;. doi:10.1210/clinem/dgaa403

Bandres-Meriz, J, Dieberger A, Hoch, D, *et al.* (2020) 'Maternal Obesity Affects the Glucose-Insulin Axis During the First Trimester of Human Pregnancy', *Frontiers in Endocrinology*, 2020. doi: 10.3389/fendo.2020.566673.